FIRST 54 HOURS OF AFTERSHOCKS OF THE 1979 PETATLAN, MEXICO, EARTHQUAKE

A THESIS SUBMITTED TO THE GRADUATE DIVISION OF THE
UNIVERSITY OF HAWAII IN PARTIAL FULFILLMENT
OF THE REQUIREMENTS FOR THE DEGREE OF

MASTER OF SCIENCE

IN GEOLOGY AND GEOPHYSICS

DECEMBER 1983

By

David Alberto Novelo Casanova

Thesis Committee:

Eduard Berg, Chairman
Charles E. Helsley
Vindell Hsu

We certify that we have read this thesis and that in our opinion it is satisfactory in scope and quality as a thesis for the degree of Master of Science in Geology and Geophysics.

THESIS COMMITTEE

____

Chairman

____

____

ACKNOWLEDGMENTS

I would like to thank Dr. Joseph F. Gettrust for his invaluable support and academic assistance. I avail the opportunity to express my sincere thanks to Dr. Eduard Berg for many helpful discussions and suggestions during the course of this research. I also benefited from discussions with Dr. Vindell Hsu and Dr. Charles E. Helsley. I thank Dr. Vindell Hsu for allowing me to use some of his computer programs. I am indebted to Emilio Herrero for his help in the processing of the data.

I am also grateful to Carlos Mortera, Brian Iwatake, Craig Fisher, Ernestina Novelo, and Mrinal Sen for their friendship and encouragement throughout this study. This research was supported by the Consejo Nacional de Ciencia y Tecnologia de Mexico (CONACYT) and a grant from the National Science Foundation (Grant EAR82-13029).

ABSTRACT

The aftershocks following the Petatlan, Mexico earthquake of March 14, 1979 (Ms=7.6) were recorded by six stations of the portable seismic network deployed by the Hawaii Institute of Geophysics. The analysis of the aftershocks within a period of 54 hours after the main shock shows that the aftershock area was about 4800 km^2 after one day passed. This area did not expand significant during the first 54 hours and increased by only 26% during the first 36 days after the Petatlan earthquake.

The analysis of both, the foreshocks and aftershocks suggests that two asperities were broken in the rupture area. The Petatlan earthquake ruptured one of the asperities, and later the other asperity was triggered. Energy release and concentration of aftershocks there after alternate between one asperity to the other.

The b value for the rupture region is 1.49, which is higher than the b value of 1.07 obtained for the foreshocks. This result is consistent with the low state of stress of the area after the major shock.

TABLE OF CONTENTS

LIST OF TABLES

LIST OF ILLUSTRATIONS

1. INTRODUCTION

The major subduction earthquake (Ms=7.6) that took place on March 14, 1979 was located about 15 km southwest of Petatlan, Guerrero, Mexico (Gettrust et al., 1981). The "Petatlan" earthquake has been extensively studied (Zuniga et al., 1980; Gettrust et al., 1981; Hsu, 1981; Valdes et al., 1982; and Hsu et al., 1983). All these studies, have been stimulated by the fact that data was collected prior to and after the main shock, and because the earthquake ocurred at the seismo-tectonic setting at the intersection of the Orozco Fracture Zone with the Middle America Trench.

The seismic data was gathered during the Rivera Ocean Seismic Experiment (ROSE) project (Ewing and Meyer, 1982). Several institutions participated in this project. Six weeks before the main event, the Hawaii Institute of Geophysics (HIG) deployed a seismic network, by coincidence surrounding the epicentral region of the future Petatlan event (Figure 1.1). This network continued recording for one month immediately following the main shock. Therefore, this is one of the few cases of continuous recording of microearthquakes prior to and after a large earthquake.

Gettrust et al. (1981), located the epicenter of the Petatlan earthquake to be offshore of the town of Petatlan in the state of

Figure 1.1 The network of portable seismographs deployed by HIG along the coast of Guerrero, Mexico during the ROSE project. The aftershock area is the region defined by the aftershocks analized in this study. This figure is modified from Hsu (1981).

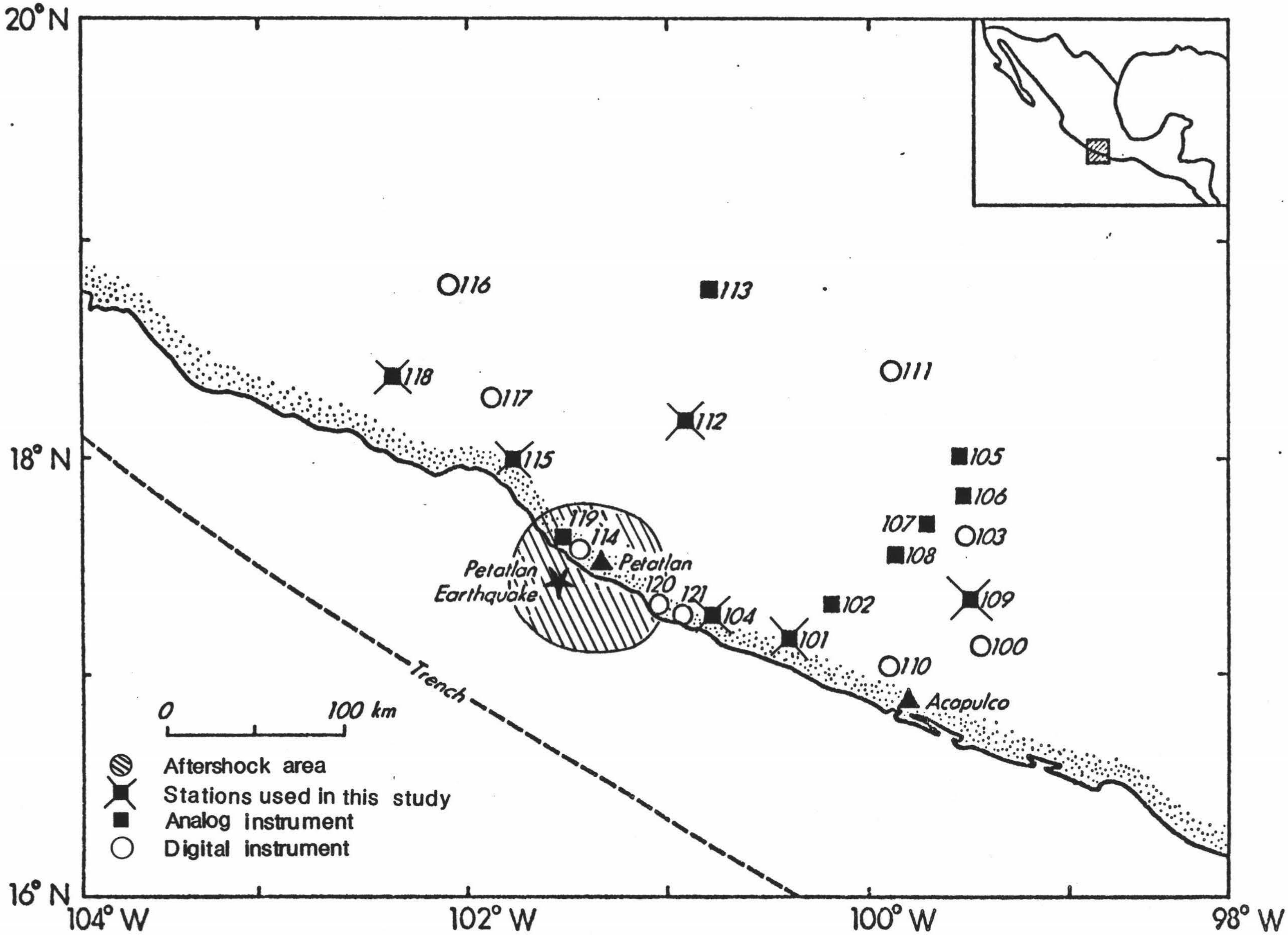
20° N
18° N
16° N
104° W
102° W
100° W
98° W
116
113
111
118
117
112
115
105
106
107
103
108
119
114
Petatlan
Petatlan Earthquake
120
121
104
102
109
101
100
110
Acapulco
Trench
0
100 km
Aftershock area
Stations used in this study
Analog instrument
Digital instrument

Guerrero, Mexico (Figure 1.1) and suggested a focal depth of 15 km. Chael and Stewart (1982), suggested a depth of 20 km based upon synthetic modeling of body and surface wave seismograms. Hsu (1981), and Hsu et al. (1983), showed that the foreshock epicenters lie within the continental block, reported several zones of concentrated seismic activity before the Petatlan event (Figure 1.2), and estimated a b-value of 1.07 for the group of foreshocks.

Valdes et al. (1982) have analyzed the aftershocks recorded by the University of Wisconsin-Madison network of portable stations having coda lengths greater than 60 seconds and which occurred between 11 hours and 36 days after the main shock. They reported 255 events, outlined an epicentral aftershock area of 6060 km^2, and suggested an asperity which contained the hypocenter of the main shock. They also calculated a stress drop of 5 bars and an average slip of 60 cm considering the entire aftershock area, and a stress drop of 15 bars and an average slip of 120 cm considering only the asperity region. They computed a rupture velocity of 2.8 km/s in the asperity. The hypocenters defined a zone 25 km thick, dipping 15° in a N 20° E direction, perpendicular to the Middle America Trench. The b-value estimated in this work was 1.6.

This thesis analyzes the aftershocks for a period of 54 hours following the Petatlan earthquake. The reason to choose this period is that Kanamori (1977) found that energy, seimic moment, strain energy

Figure 1.2 The spatial distribution of earthquakes preceding the Petatlan earthquake (Solid star). The zones of concentrated seismic activity are denoted as zones A, B, and C (Hsu, 1981).

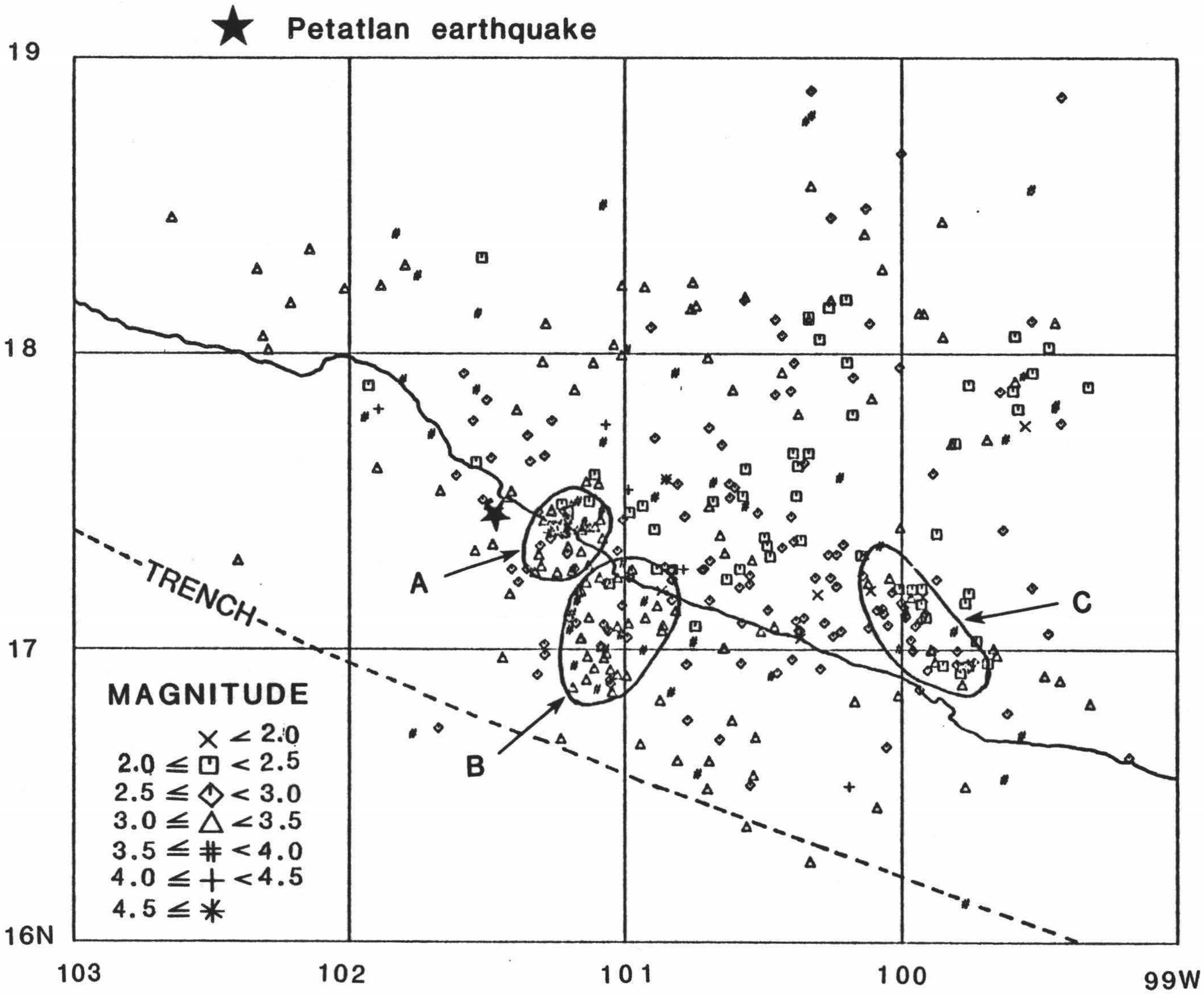
Petatlan earthquake
19
18
17
16N
103
102
101
100
99W
TRENCH
A
B
C
MAGNITUDE
× < 2.0
2.0 ≤ ◻ < 2.5
2.5 ≤ ◇ < 3.0
3.0 ≤ △ < 3.5
3.5 ≤ # < 4.0
4.0 ≤ + < 4.5
4.5 ≤ ✳

drop and rupture area for large events, can be well defined by the early (first day or two) aftershock locations. Another important reason is that our unique data set is continuous after the main shock. In most cases this kind of research is impossible because the aftershocks recording networks are usually deployed and start recording several hours (sometimes days) after the major shock.

During the first 54 hours of the aftershock sequence, it has been possible to obtain epicenter, focal depth, and magnitude for 389 aftershocks. 354 of these events, locate inside the coordinates 17^{o}N and 18^{o}N, and 101^{o}W and 102^{o}W. This study is based on the analysis of the events which lie in this region.

The objectives of this thesis are: to study the spatial distribution of the aftershocks; to compare results of this investigation with those obtained by others; to highlight the possible relationships between foreshocks and aftershocks; and finally to interpret some of the tectonic processes surrounding the Petatlan earthquake.

2. TECTONICS AND SEISMICITY

2.1 Tectonic Setting

The Petatlan earthquake was the result of the tectonic processes that take place along the Middle America Trench. The trench borders the southern Pacific coast of Mexico and Central America (Figure 2.1), is 2500 km long, and its average depth and average width are 6.7 km and 40 km, respectively (Kennett, 1982).

Molnar and Sykes (1969), and Dean and Drake (1978), using seismicity and focal mechanism solutions showed that the Middle America Trench is formed due to the subduction of the Cocos plate underneath the North American and the Caribbean plates (Figure 2.1). Molnar and Sykes (1969) found that the Cocos lithosphere descends more steeply beneath the Caribbean plate. This result was verified by Couch and Woodcock (1981), who, using gravity and magnetic measurements, concluded that the Tehuantepec Ridge (a linear range of submarine mountains on the Cocos plate oriented approximately N 40^{o} E that intersects the Middle America trench near 15.0^{o}N latitude and 95.5^{o}W longitude) marks the boundary between the two different subduction provinces. Thus the Cocos plate subducts at a more shallow angle beneath the continental margin northwest of the Tehuantepec Ridge than southeast of the ridge.

Figure 2.1 Regional map showing the relationship of the Cocos plate to the sorrounding plates. The star shows the epicenter of the Petatlan earthquake. This figure is modified from Klitgord and Mammerickx (1982).

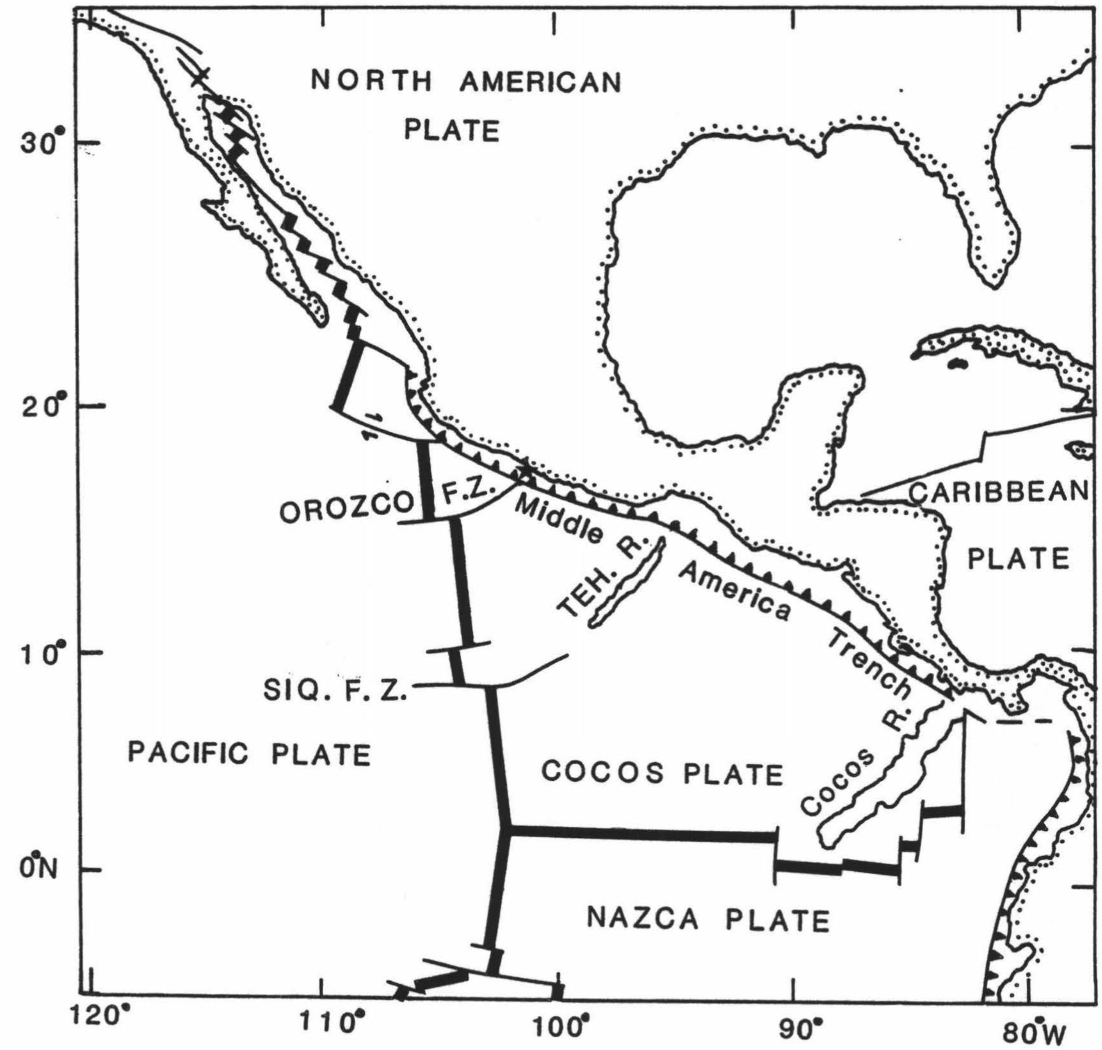

NORTH AMERICAN
PLATE
30°
20°
10°
0N
120°
110°
100°
90°
80W
OROZCO
F.Z.
Middle
America
Trench
TEH. R.
CARIBBEAN
PLATE
SIQ. F. Z.
PACIFIC PLATE
COCOS PLATE
Cocos R.
NAZCA PLATE

Minster and Jordan (1978), found an angular convergence velocity of 1.489 degrees/m.y. (corresponding to about 6 cm/year in the Petatlan area) for the Cocos-North American plates. McNutt and Batiza (1981), based on paleomagnetic latitude variations of the northern Cocos plate, calculated a linear velocity on the order of 5cm/year averaged over the past 6 m.y.

The Orozco Fracture Zone, located at the north of the Cocos plate (Figure 2.1), intersects the Middle America Trench near 17.5^{o}N latitude and 102.0^{o}W longitude. Since offshore bathymetry may affect the occurrence and mode of failure of subduction zone events (Vogt et al., 1976), it is expected that the Orozco Fracture Zone will influence the Petatlan earthquake, as well as its foreshocks and aftershocks distribution.

2.2 Seismicity

Large earthquakes (Ms $\geqslant$ 7.0) ocurr along the Middle America Trench. Because of the shallower dipping subduction zone along the Cocos-North American plate portion, a greater area of contact between the subducting oceanic crust and the overlying lithosphere is allowed; this could explain the larger and more frequent earthquakes in this zone than along the Cocos-Caribbean plate boundary (Chael and Stewart, 1982). Some segments of the subduction zone have been designated as seismic gaps, i.e., regions that have not experienced shallow earthquakes larger than magnitude 7 in the last few decades. These regions are likely places to expect large earthquakes in the next few tens of years (Kelleher et al., 1973; McCann et al., 1978). Recent large earthquakes have taken place in the gaps along the Mexican Pacific coast (Meyer et al., 1980; Singh et al., 1981). The recurrence period for large (Ms > 7.5) earthquakes in these areas are 33 to 35 years (McNally, 1981). Although this period is acceptable for the Colima, Oaxaca and Petatlan areas, the region southeast of the Petatlan zone had large events in 1907, 1909, 1911, and has not experienced another large earthquake since then.

The Petatlan area was classified by McCann et al. (1978) as a region of high seismic potential because it had a history of large earthquakes but none within the last 30 years (the zone had a large earthquake, Ms=7.5, in 1943). The Petatlan earthquake ruptured the region between 101.0^{o} and 101.7^{o}W (this study), but it did not fill the entire gap (100.0^{o}-102.5^{o}W), which is still considered an area of high seismic risk (Meyer et al. 1980).

3. DATA

3.1 Data Set and Processing

The total period of seismic data recorded by HIG on land for the Rivera Ocean Seismic Experiment lasts from February 1, 1979, to April 15, 1979. The portion studied in this thesis covers the 54 hours following the Petatlan earthquake from 1107 hr GMT March 14, to 1707 hr GMT March 16. HIG deployed 14 portable seismographs and the network occupied 22 stations (Figure 1.1). Only six stations were operating immediately following the main shock. The others stations had instrumental problems or were working at different times. The seismic stations with AM-analog-digital and 4-channel cassete-recording system (Figure 1.1), were not used because the time code signals in these instruments were inaccurate (Hsu, 1981). All six stations used in this study had three-component seismographs with nominal frequency of 1 Hz. Data were recorded on an AM analog 6-channel tape-recording system. The clock drifts were obtained by comparing the time signal from the seismograph with the time signal transmitted by WWV. A more detailed description of the station characteristics and the kind of data recorded by the HIG network have been given by Hsu (1981), in his study of foreshocks of the Petatlan earthquake.

Figure 1.1 and Table 3.1, show and list the location of the stations used in this study, respectively. Figure 3.1 shows the times of operation of the stations. It can be seen that the 54 hour period was well monitored by the seismic network. At any time during this period, at least four stations were operating, and most of the time all six stations were working. Therefore, it can be assumed that all the aftershocks large enough to be recorded by at least three stations have been detected by the network. However, for many large (M > 3.0) events during the first two hours it was not possible to obtain their seismic parameters because their record were obscured in a continuum of events immediately following the Petatlan earthquake itself.

The analog data recorded in the field were continuously digitized and stored on 9-track magnetic tapes. The digitizing procedures were developed by Hsu (1981) and are shown in figure 3.2. The three channels containing the chronometer, the vertical and one of the horizontal components of the signal were digitized. Filters were set to pass frequencies in the range of 0.4 to 20 Hz. The digitizing rate used was about 40 samples per second per channel.

Figure 3.3 shows the procedures developed by Hsu (1981) for obtaining the arrival times of seismic waves. The digitized seismic data were scanned by a program which uses an amplitude threshold to pick events. All the events detected by the program were stored into a file for later

TABLE 3.1 LOCATION OF THE STATIONS USED IN THIS STUDY

STATION	LATITUDE (N)	LONGITUDE(W)
101	17.2317	100.4272
104	17.2750	100.8117
109	17.3467	99.5817
112	18.1617	100.8767
115	18.0000	101.7917
118	18.3800	102.3317

Figure 3.1 Times of operation of the stations used in this study. The dotted area shows the two hours period when it was not possible to read all P and S arrival times (See text).

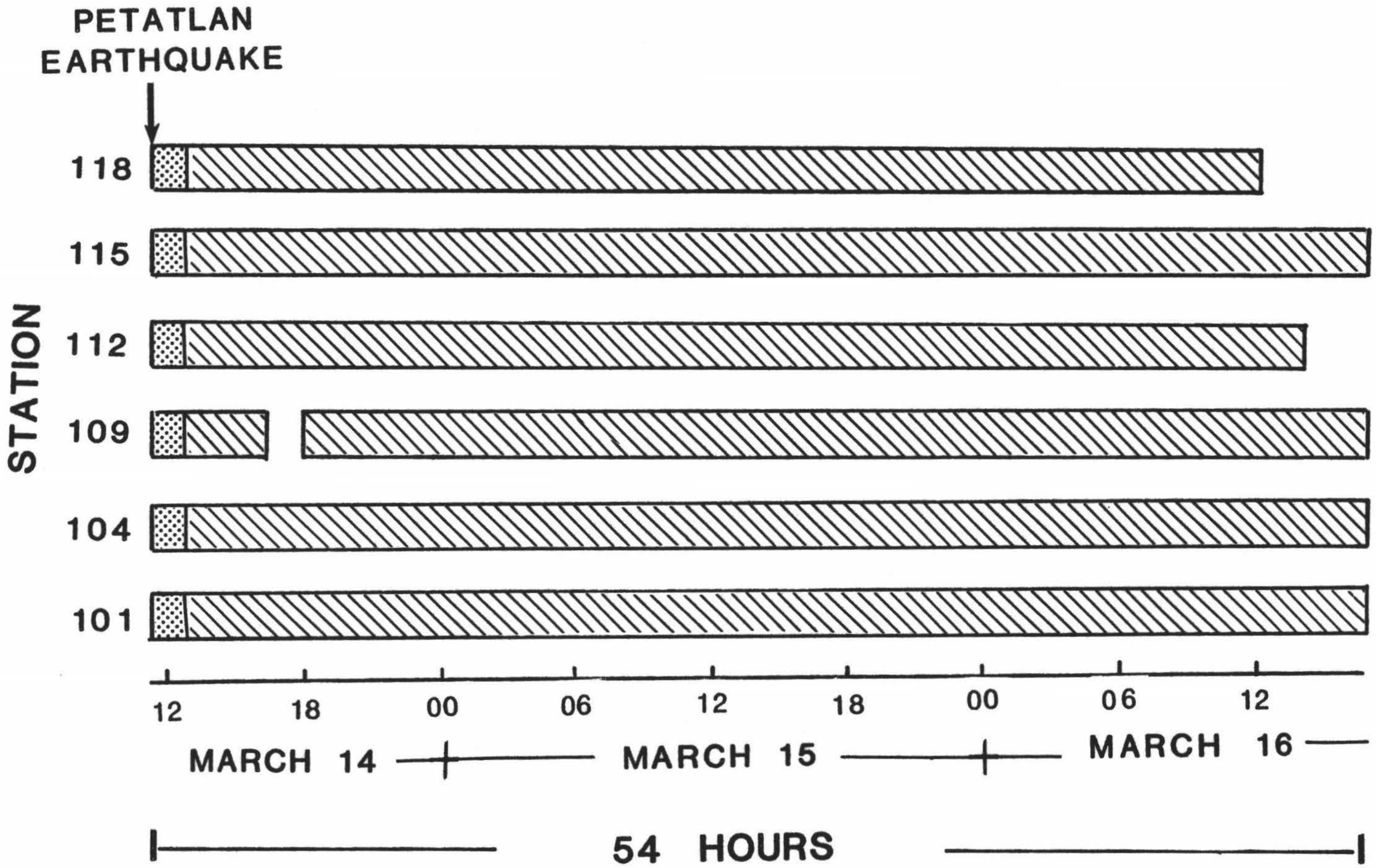
PETATLAN
EARTHQUAKE
STATION
118
115
112
109
104
101
12
18
00
06
12
18
00
06
12
MARCH 14
MARCH 15
MARCH 16
54 HOURS

Figure 3.2 Procedure for digitizing the analog seismic data (Hsu, 1981).

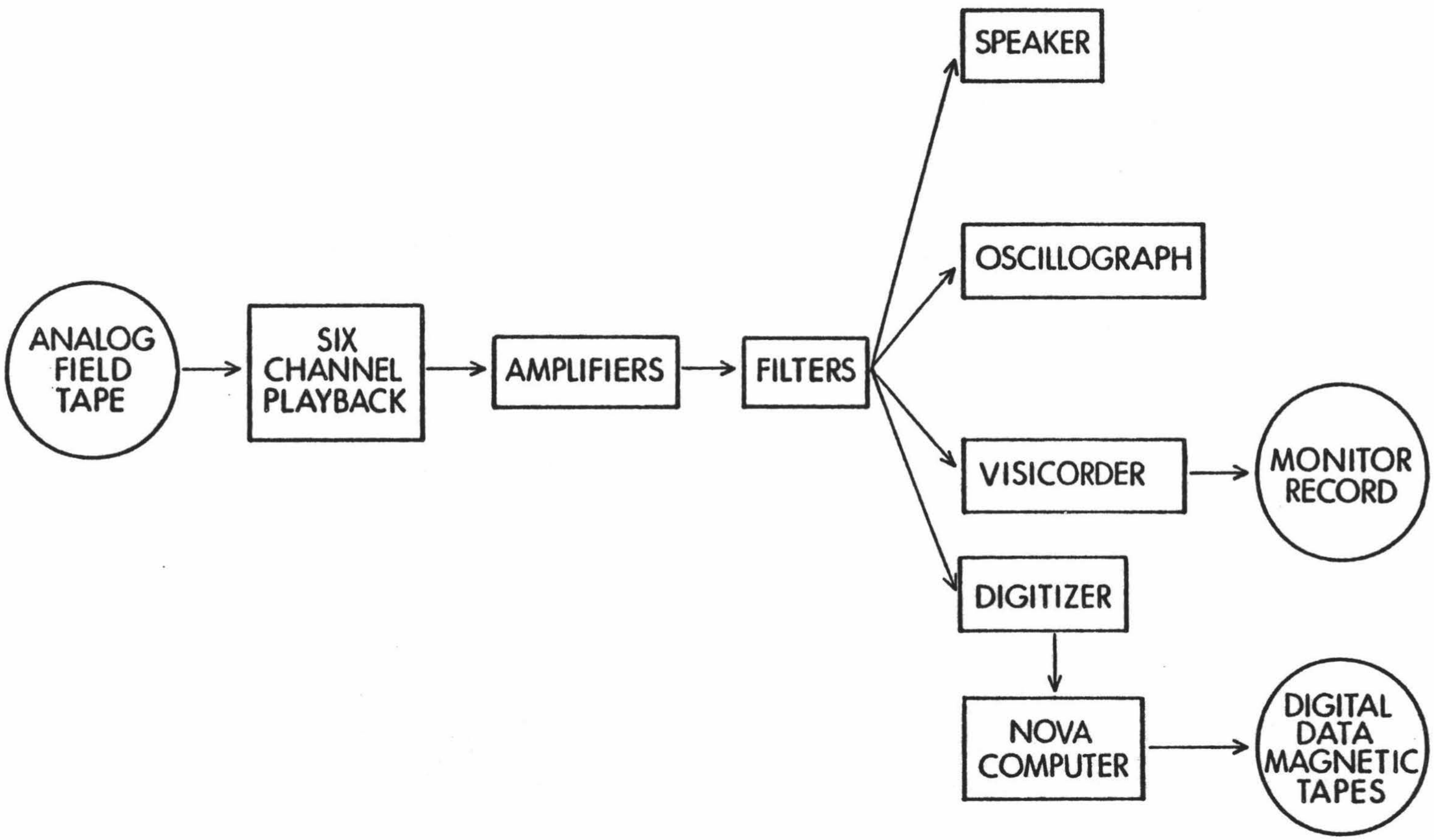
ANALOG FIELD TAPE
SIX CHANNEL PLAYBACK
AMPLIFIERS
FILTERS
SPEAKER
OSCILLOGRAPH
VISICORDER
MONITOR RECORD
DIGITIZER
NOVA COMPUTER
DIGITAL DATA MAGNETIC TAPES

Figure 3.3 Procedure for obtaining the seismic wave arrival times (Hsu 1981).

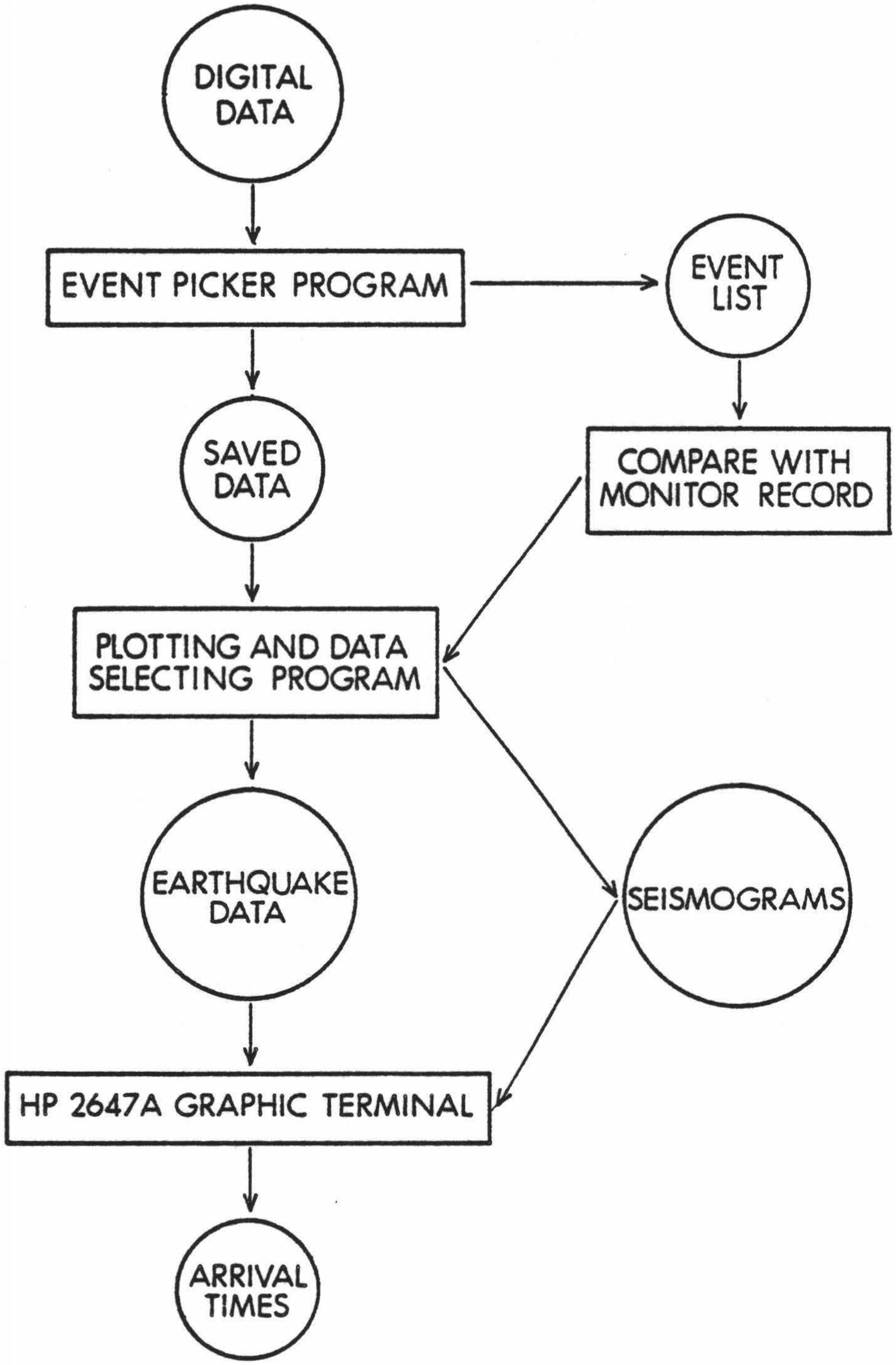
DIGITAL DATA
EVENT PICKER PROGRAM
EVENT LIST
SAVED DATA
COMPARE WITH MONITOR RECORD
PLOTTING AND DATA SELECTING PROGRAM
EARTHQUAKE DATA
SEISMOGRAMS
HP 2647A GRAPHIC TERMINAL
ARRIVAL TIMES

processing. Because sometimes the event-detecting program picked false events (noise generated by walking persons, passing vehicles, animals, etc.), the selected events were compared with the monitor record in order to choose the true events. These events were plotted to get the seismograms. The P and S times were picked by plotting the events on the screen of a HP2647A graphic terminal. With this procedures, the arrival times are considered to contain a maximum error of 0.1 and 0.5 seconds for P and S phases, respectively.

For more information about the routines and the programs used for picking the arrival times of seismic waves, the study of Hsu (1981) should be consulted.

3.2 Epicenters, Depths, and Magnitudes

Aftershocks were located using the HYPO71 program (Lee and Lahr, 1975). The velocity-depth model developed by Valdes et al. (1982) for the Petatlan region is adopted in this study. Because of the lack of gain information and instrument calibration, magnitudes were calculated using the empirical relation given by Lee et al. (1972):

$$M = -0.87 + 2.0 \log T + 0.0035 D$$

where T is coda length in seconds and D is epicentral distance in km.

Although this formula was developed for microearthquakes in California, it has been widely used for seismic events in different places.

Appendix A, lists the 389 events located during the 54 hour period. Figure 3.4 shows the 354 events located between the coordinates 17°N and 18°N latitude, and 101°W and 102°W longitude. Eighty percent of the aftershocks in this region have a root mean square (RMS) error of time residuals less than or equal to 0.5 seconds, and an error for epicentral distance (ERH) and focal depth (ERZ) less or equal to 10 km. Seventy five percent of the events have the same error limits together with a minimum of 5 readings for P and S arrival times (P and S arrival times for the same station are considered as two readings). Focal depths are shown in figure 3.5, they have been projected in a plane perpendicular to the trench axis. We observe that the aftershocks are concentrated between 5 and 25 km depth, and they are contained in the Benioff zone dipping 15° reported by Valdes et al. (1982). Most of the aftershocks have magnitudes ranging between 3 and 4.

In order to check the locations and depths obtained in this study, two tests were performed: the resolution of our seismic network, and the relocation of the aftershocks using a program different from the HYPO71.

The resolution of the seismic network was obtained using the program developed by Lienert and Frazer (1983a). This program obtains the

Figure 3.4 Epicenters locations of the 354 events located between 17^{o} N and 18^{o} N latitude, and 101^{o} W and 102^{o} W longitude. The star represents the epicenter of the Petatlan earthquake. For explanation of lines A-B, and C-D see figure 4.13 and figure 4.14. For explanation of the small squares see figure 4.20.

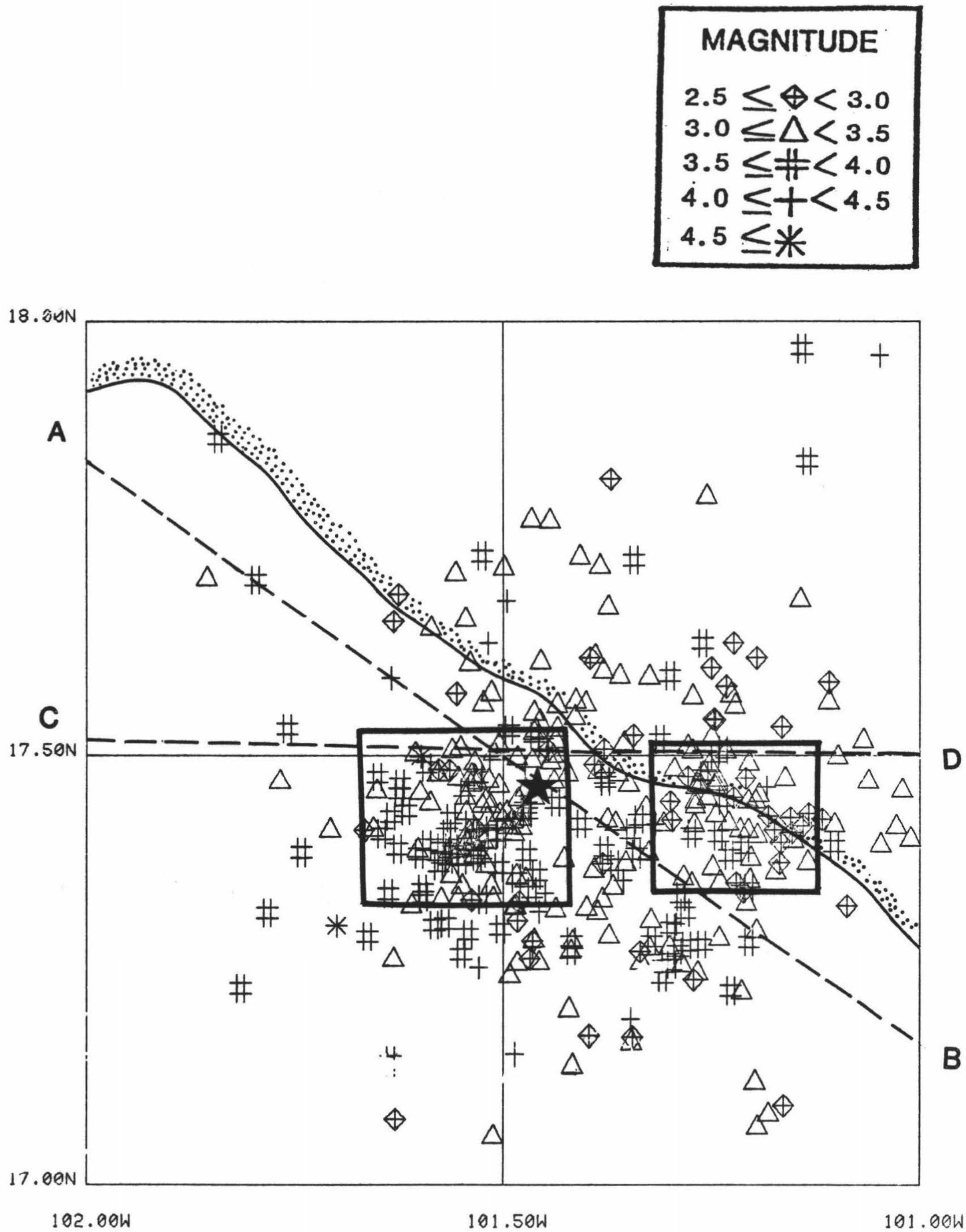

MAGNITUDE
2.5 ≤ ⊕ < 3.0
3.0 ≤ △ < 3.5
3.5 ≤ # < 4.0
4.0 ≤ + < 4.5
4.5 ≤ ✳
18.00N
17.50N
17.00N
102.00W
101.50W
101.00W
A
B
C
D

Figure 3.5 Hypocenter cross section of the aftershocks. The dashed lines represents the slab 25 km thick and dipping 15^{o} suggested by Valdes et al. (1982). The magnitude simbols are described in figure 3.4.

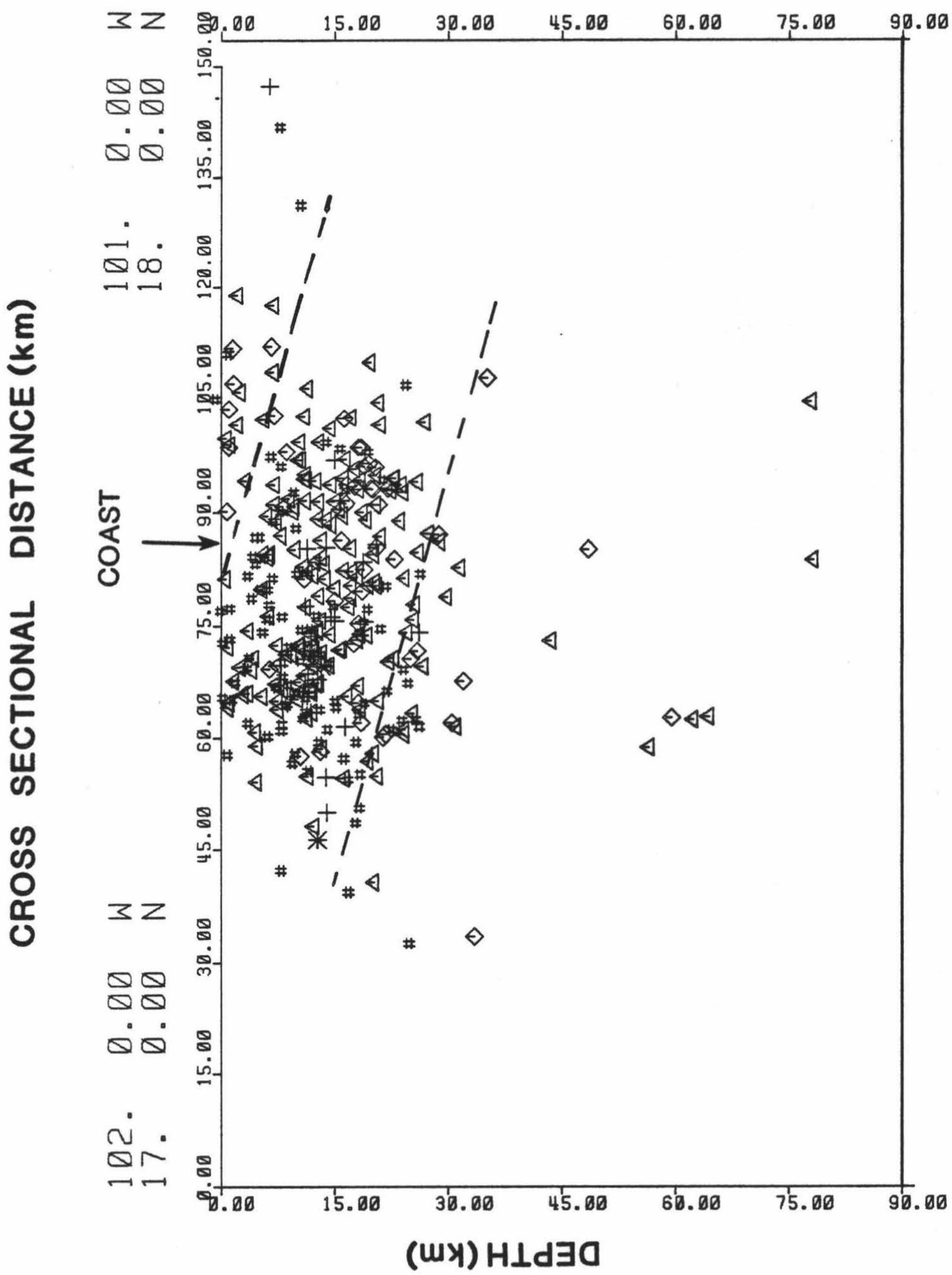
CROSS SECTIONAL DISTANCE (km)
COAST
DEPTH (km)
102. 0.00 W
17. 0.00 N
101. 0.00 W
18. 0.00 N

horizontal and vertical uncertainties for seismic arrays that use a layered velocity model for hypocenter locations. The parameters are evaluated for a specific area at any given depth and considering a certain variance (standard deviation squared) for P and S wave arrival times. Because most hypocenters are between 10 and 20 km (Figure 3.5), from all the resolution plots obtained, only the ones for 15 km depth are shown. The error considered for P and S phases were .1 and .3 seconds, respectively. Figure 3.6 shows the resolution using all six stations of our seismic network. The area of interest in this study is limited by the square in the figure. In this square there is a maximum error of 2.2 km (lower-left corner) for epicenter locations. The aftershock area (dashed circle) shows an epicentral error between 1.0 and 1.5 km, and a focal depth error between 1.0 and 1.2 km. A more extreme example is shown in figure 3.7, where the resolution using only four (badly constraining) stations shows a maximum error of 6 km for epicenter locations. However, this maximum error affects only a small portion to the north and to the east of the aftershock region, where as most of the errors are between 2.5 and 4.0 km. Similar patterns are observed for depth uncertainties shown in the upper portion of figure 3.7.

The aftershocks were relocated using the program developed by Lienert and Frazer (1983). This program combines the linearized inverse theory and the stepwise regression method (this last procedure is used by HYPO71). Figure 3.8 and figure 3.9 show the epicenter locations and a

Figure 3.6 Resolution of the HIG network using all six stations. The upper portion shows the depth uncertainty, and the lower portion shows the epicentral uncertainty. The stations are represented by the small solid squares (for identification of the stations see figure 1.1). The contours are at intervals of .2 km. The aftershock region is contained in the dashed circle.

HIG-PETATLAN ARRAY DEPTH= 15KM

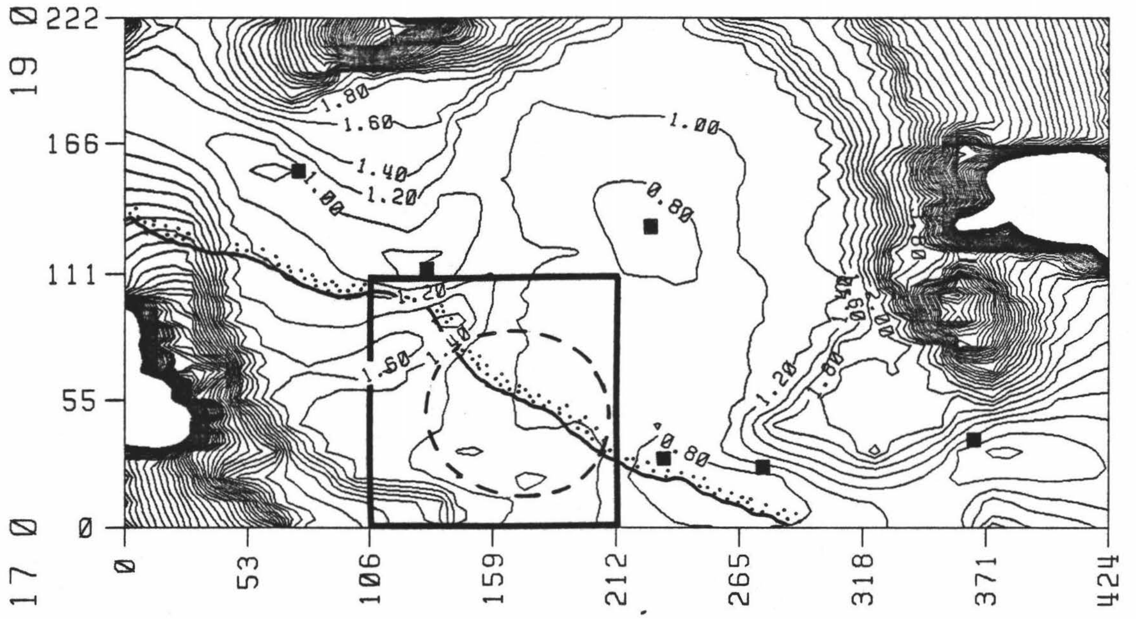

1Ø3 Ø Z UNCERTAINTY 99 Ø

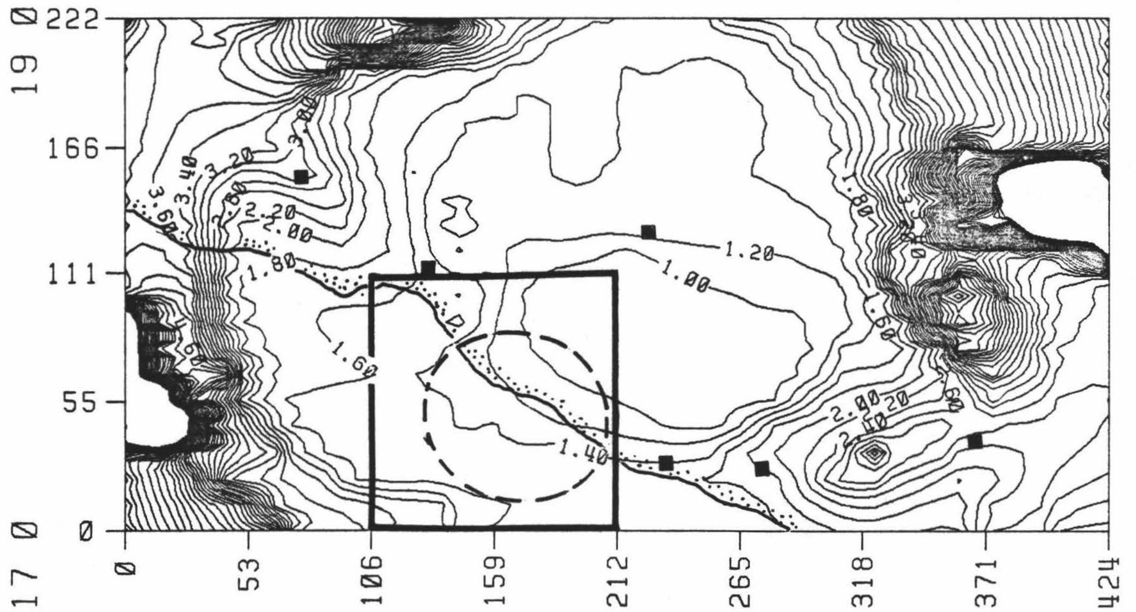

1Ø3 Ø HORIZONTAL UNCERTAINTY 99 Ø

Figure 3.7 Resolution of the HIG seismic network using four stations. The stations included are the 101, 104, 115 and 118 (See figure 1.1). The small solid squares represent the station locations. The contours are shown at intervals of 1 km. The aftershock region is contained in the dashed circle.

HIG-PETATLAN ARRAY DEPTH= 15KM

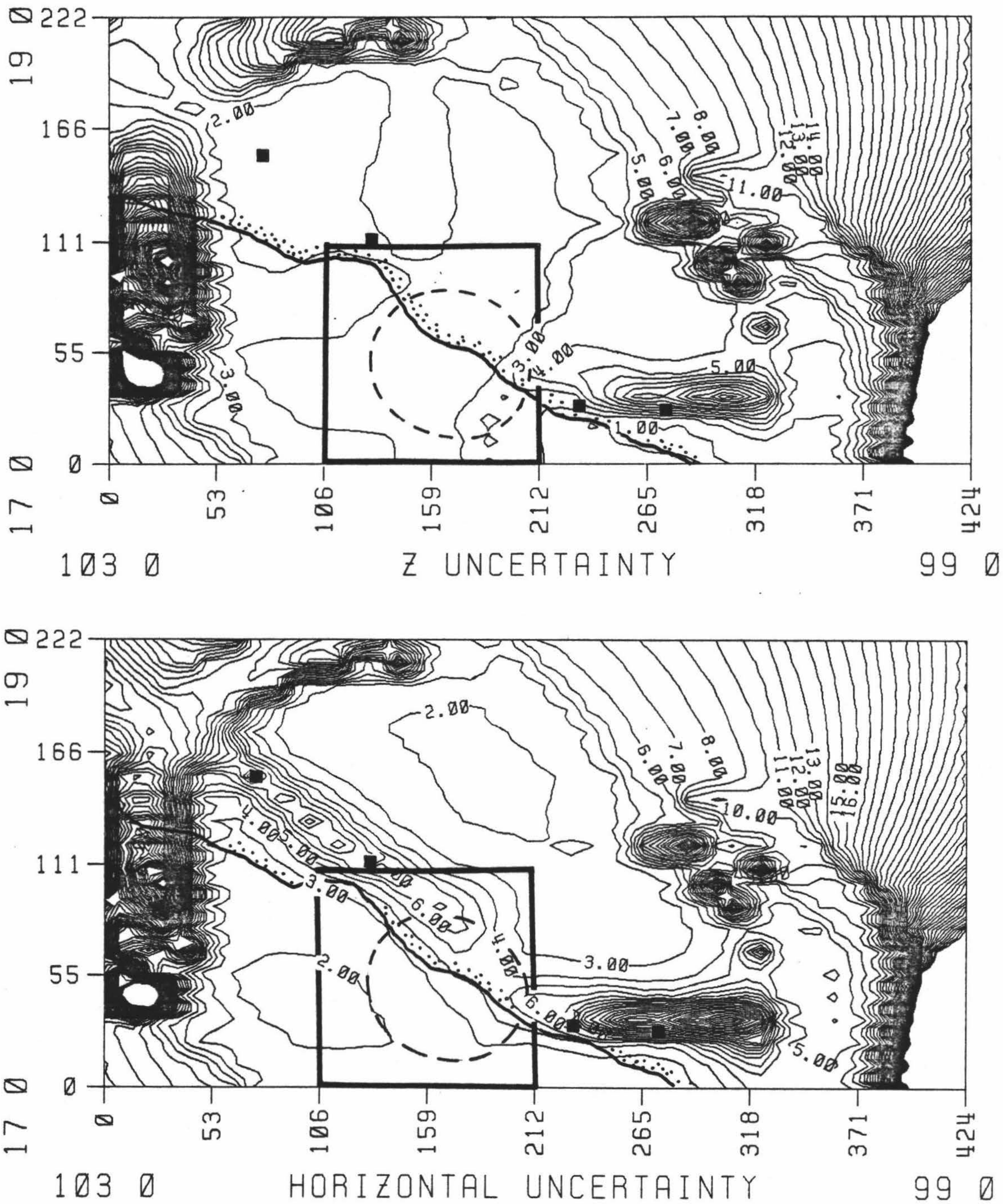

projection of the focal depths onto a plane perpendicular to the trench respectively. Comparing figure 3.4 and figure 3.8, we can see that there are no significant changes in the epicenters. The same regions of concentrated aftershocks are observed in both figures. The focal depths observed in figure 3.5 and figure 3.9 are contained in the slab 25 km thick and dipping 15° suggested by Valdes et al. (1982). However in figure 3.9, we can see inside the slab two concentrations of focal depths contained in different dipping planes. This suggests two distinct seismic zones of the Petatlan aftershocks ,this result will be discussed in the following chapter.

Since we have an acceptable resolution with our seismic network (Figure 3.6 and figure 3.7), and because we have obtained similar solutions using different methods, we can consider that our hypocenter locations are reliable, and that all our analysis based on HYPO71 solutions are well founded.

Table 3.2 compares the seismic parameters obtained by the United States Geological Survey (USGS), the University of Wisconsin-Madison (UWM, Carlos Valdes, personal communication), and this study. We observe that in general the depths given by the USGS are greater than the other two depths reported for the same event, and the USGS epicenters are shifted away from ours towards the continent (Figure 3.10). Our magnitudes are closer to the magnitudes given by the USGS than those from the UWM.

Figure 3.8 Epicenter locations using the program developed by Lienert and Frazer (1983).

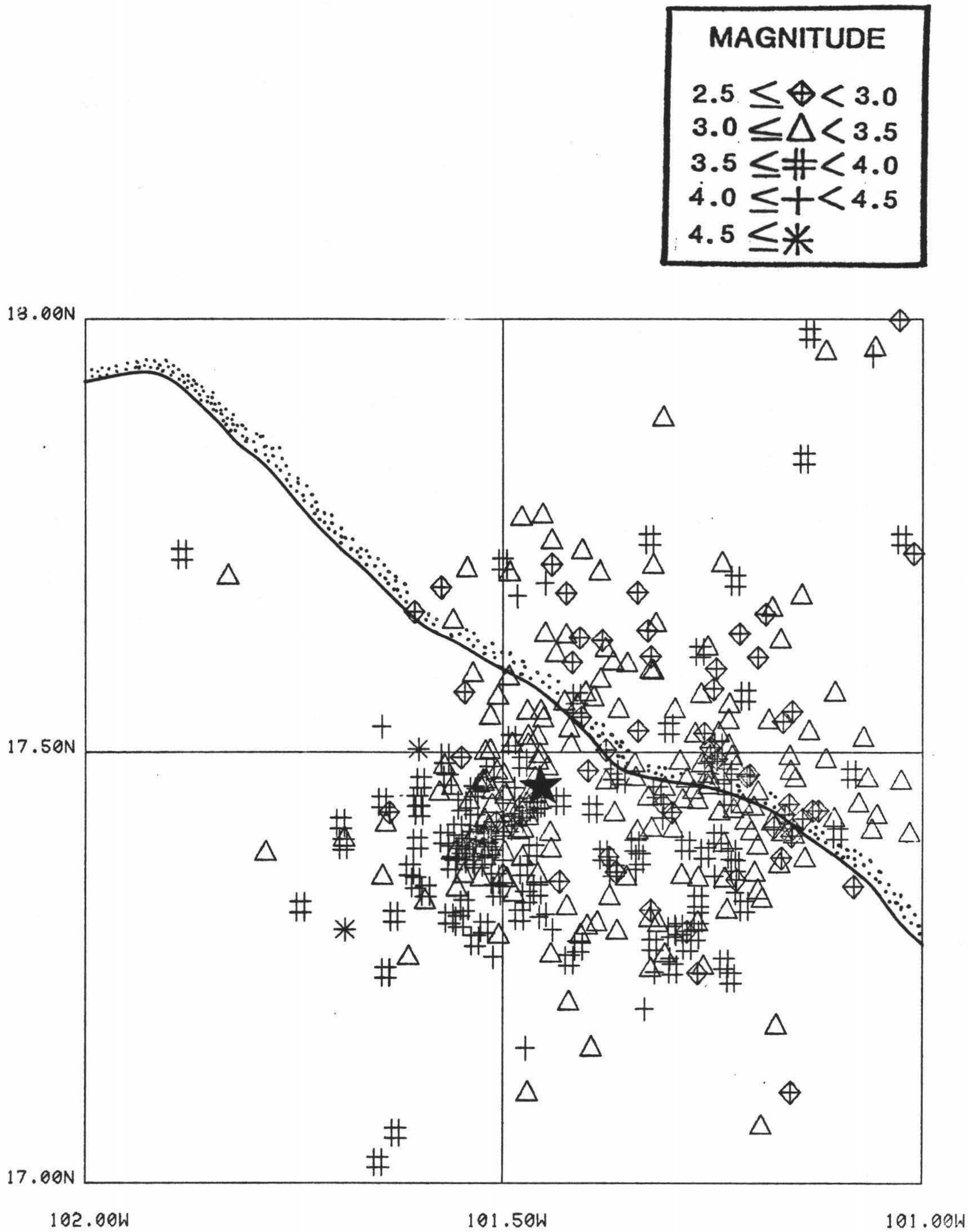

MAGNITUDE
2.5 ≤ ⊕ < 3.0
3.0 ≤ △ < 3.5
3.5 ≤ # < 4.0
4.0 ≤ + < 4.5
4.5 ≤ ✳
18.00N
17.50N
17.00N
102.00W
101.50W
101.00W

Figure 3.9 Hypocenter cross section of the aftershocks using the program developed by Lienert and Frazer (1983). Observe that there are two concentrations of focal depths contained in planes dipping different to the 15^{o} (dashed lines) suggested by Valdes et al. (1982).

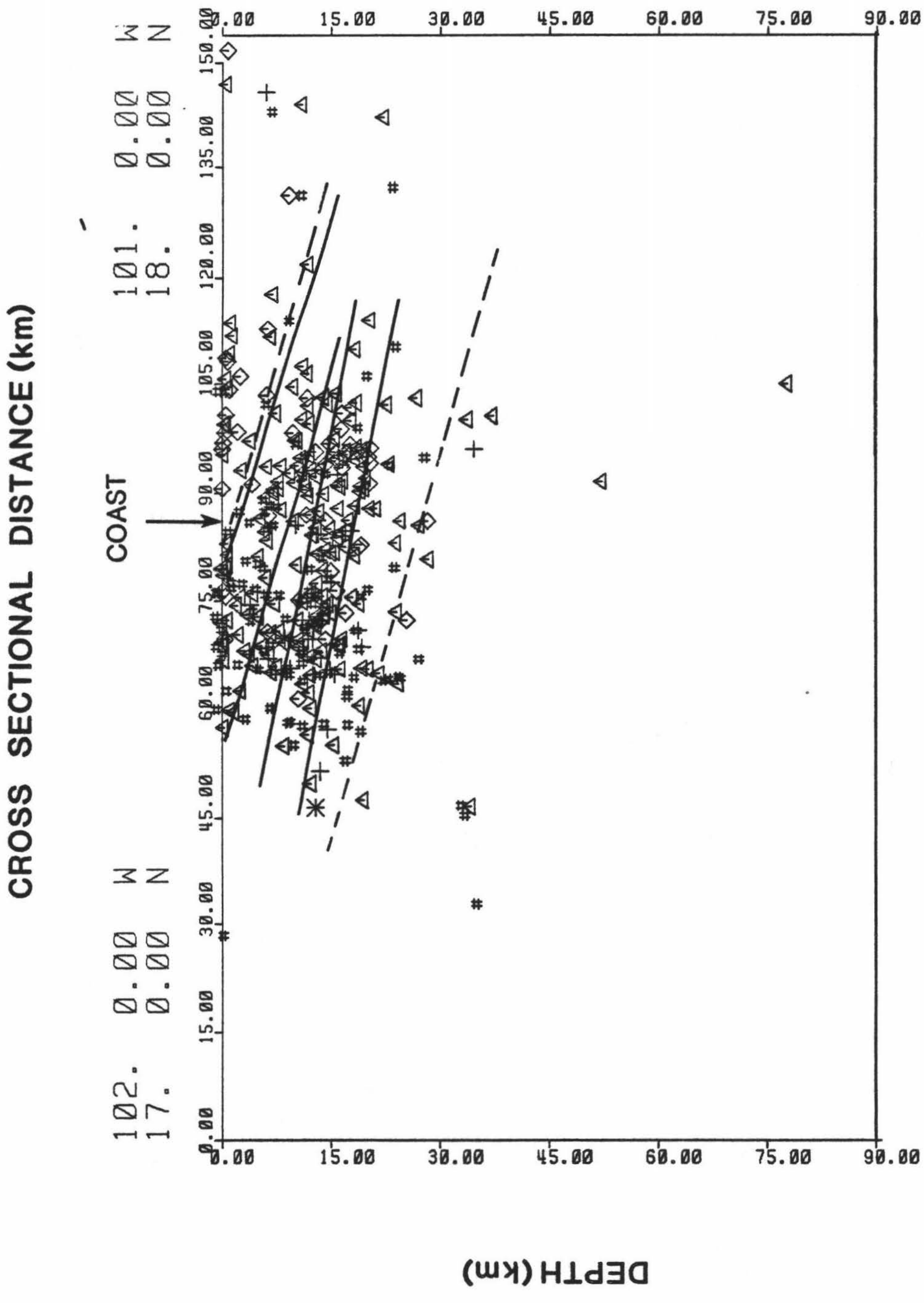
CROSS SECTIONAL DISTANCE (km)
COAST
DEPTH (km)
102. 0.00 W
17. 0.00 N
101. 0.00 W
18. 0.00 N
0.00
15.00
30.00
45.00
60.00
75.00
90.00
105.00
120.00
135.00
150.00

TABLE 3.2 AFTERSHOCKS LOCATED BY THE UNITED STATES GEOLOGICAL SURVEY, THE UNIVERSITY OF WISCONSIN-MADISON, AND THIS STUDY.

#	SOURCE	DAY	ORIGIN H/M	LATITUDE (N)	LONGITUDE (W)	DEPTH km	MB	ML
1	USGS	14	12:01	17.952	101.283	52	5.5	
	UWM			------	-------	--		---
	THIS STUDY			17.302	101.699	13		4.5
2	USGS	14	12:47	17.672	100.727	58	4.6	
	UWM			------	-------	--		---
	THIS STUDY			17.260	101.310	12		4.3
3	USGS	14	13:05	16.480	100.602	33	4.9	
	UWM			------	-------	--		---
	THIS STUDY			17.628	101.518	21		4.3
4	USGS	14	15:19	17.079	101.630	45	---	
	UWM			------	-------	--		---
	THIS STUDY			17.192	101.347	12		4.1
5	USGS	14	15:35	17.680	101.396	66	5.0	
	UWM			------	-------	--		---
	THIS STUDY			17.498	101.598	13		4.6
6	USGS	14	21:34	19.168	100.576	38	4.4	
	UWM			------	-------	--		---
	THIS STUDY			17.304	101.293	15		4.2
7	USGS	14	22:05	17.707	101.081	61	4.4	
	UWM			17.396	101.396	16		3.7
	THIS STUDY			17.340	101.450	13		4.2
8	USGS	16	10:10	17.994	101.148	33	4.4	
	UWM			17.339	101.376	25		3.6
	THIS STUDY			17.418	101.318	19		4.1

USGS: Events located by the United States Geological Survey

UWM: Events located by the University of Wisconsin-Madison

MB : Magnitudes determined using body waves

ML : Magnitudes determined using coda length

Figure 3.10 Epicenter locations reported by the USGS (asterisk), and this study (triangle). The numbers correspond to the numbers of the events in table 3.2.

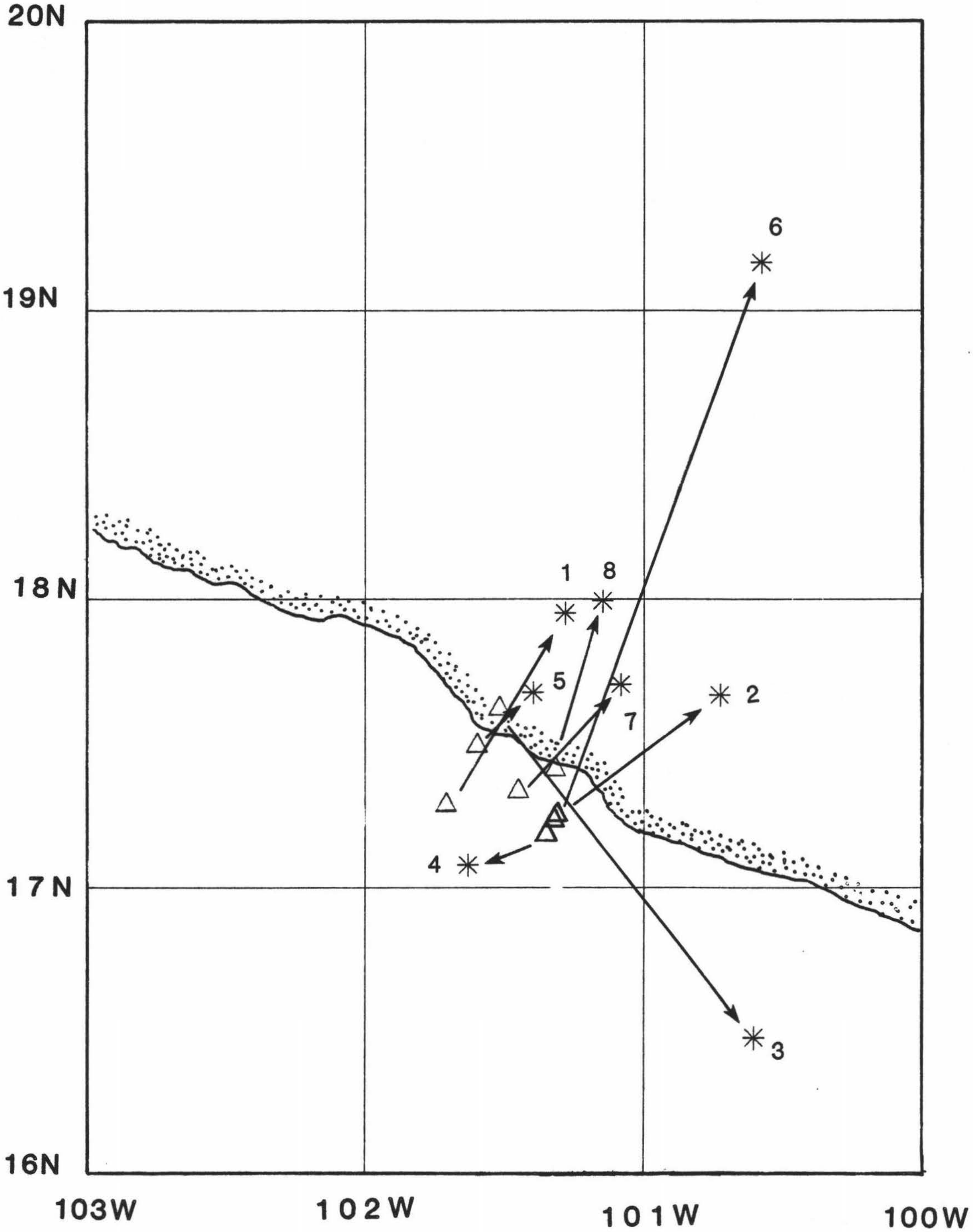
20N
19N
18N
17N
16N
103W
102W
101W
100W
1
2
3
4
5
6
7
8

Unlike the University of Wisconsin-Madison, which deployed a tight network around the main shock (figure 3.11), the University of Hawaii deployed a more spreadout network surrounding the aftershock area (Figure 1.1).

Table 3.3 lists the aftershock parameters for the events located by the University of Wisconsin-Madison (Carlos Valdes, personal communication) and this study during the first 54 hours after the Petatlan earthquake. The table also shows the results of combining data from UWM and our data. In the lower portion of figure 3.11, we observe the epicentral locations of the three data sources. The cross, triangle and asterisk represent the location given by UWM, this study, and the combined data respectively. The circles contain the epicenters for those earthquakes with variations less than 8 km. The number written close to the circles correspond to the numbers of the events in table 3.3.The average epicentral offset for these events is 4 km. The upper portion of figure 3.11 shows those events with epicentral offset greater than 8 km. The average epicentral offset between the UWM and this study is 7.7 km, and between the combined data and our data is 5.5 km.

From table 3.3, it was estimated that the depth for those events analyzed by UWM are, on the average, 11.4 km deeper than the depth found here for the same events. Unlike the aftershocks given by Valdes et al. (1982) which are concentrated between 15 and 30 kms depth, our focal depths are between 5 and 25 km (Figures 3.5 and 3.9). The average depth

Figure 3.11 Epicentral locations given by the University of Wisconsin-Madison (cross), this study (triangle), and the combination of both data sets (asterisk). The circles contain the epicenters for those events with epicentral offset less than 8 km. The upper figure shows the epicenters with offset greater than 8 km between the three source locations. The numbers correspond to the events in table 3.3. The solid squares in the figure are the station locations of the seismic network deployed by the University of Wisconsin-Madison and which were operating during the first 54 hours following the Petatlan earthquake.

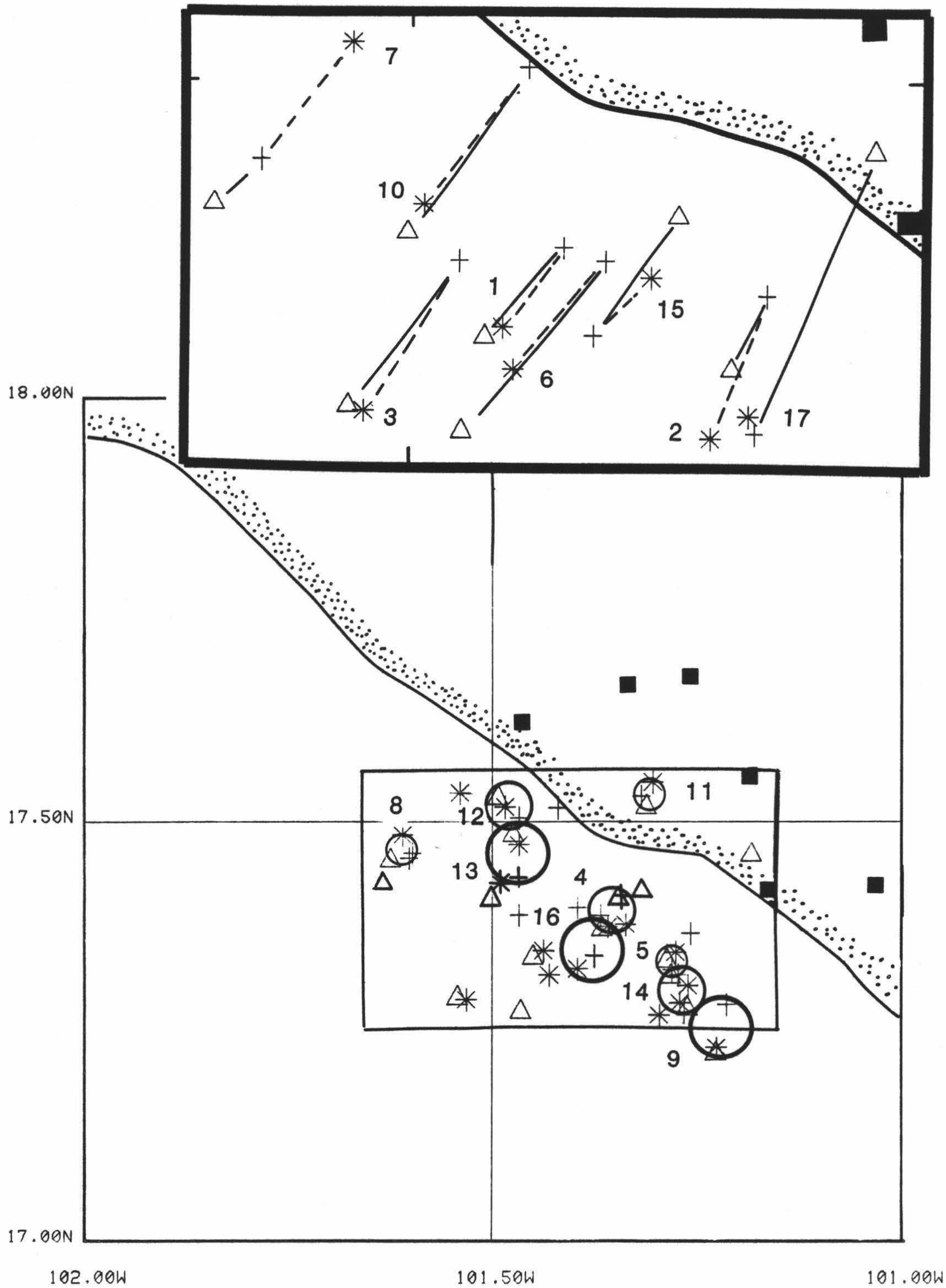
7
10
1
15
6
3
2
17
18.00N
17.50N
17.00N
8
12
11
13
4
16
5
14
9
102.00W
101.50W
101.00W

TABLE 3.3 AFTERSHOCKS OBTAINED BY THE UNIVERSITY OF WISCONSIN, THE UNIVERSITY OF HAWAII, AND BY USING THE COMBINED DATA FROM BOTH INSTITUTIONS

#	SOURCE	DAY	ORIGIN H/M	LATITUDE (N)	LONGITUDE (W)	DEPTH km	ML	N
1	UWM	14	22:05	17.3958	101.3959	15.91	3.71	5
	THIS STUDY			17.3398	101.4495	12.79	4.16	5
	UWM-TS			17.3450	101.4372	16.39	4.00	10
2	UWM	14	22:13	17.3650	101.2577	36.28	2.72	5
	THIS STUDY			17.3172	101.2823	4.95	3.72	9
	UWM-TS			17.2702	101.2960	20.56	3.56	14
3	UWM	14	22:20	17.3872	101.4668	32.62	2.91	6
	THIS STUDY			17.2927	101.5417	1.71	3.83	8
	UWM-TS			17.2887	101.5308	10.60	3.69	14
4	UWM	14	23:07	17.4103	101.3440	20.32	3.21	5
	THIS STUDY			17.4083	101.3465	7.67	3.88	8
	UWM-TS			17.3730	101.3588	17.01	3.64	13
5	UWM	14	23:21	17.3235	101.2805	18.95	3.08	6
	THIS STUDY			17.3360	101.2867	6.09	3.70	8
	UWM-TS			17.3428	101.2760	19.07	3.58	14
6	UWM	15	00:03	17.3867	101.3679	23.43	3.54	4
	THIS STUDY			17.2762	101.4648	16.40	4.11	8
	UWM-TS			17.3170	101.4300	19.42	3.92	12
7	UWM	15	01:23	17.4588	101.6013	23.29	3.00	6
	THIS STUDY			17.4277	101.6335	4.49	3.57	8
	UWM-TS			17.5333	101.5390	24.75	3.45	14
8	UWM	15	02:01	17.4625	101.5972	19.28	3.05	6
	THIS STUDY			17.4557	101.6243	15.99	3.80	8
	UWM-TS			17.4845	101.6093	19.62	3.51	14

TABLE 3.3 (Continued) AFTERSHOCKS OBTAINED BY THE UNIVERSITY OF WISCONSIN, THE UNIVERSITY OF HAWAII, AND BY USING THE COMBINED DATA FROM BOTH INSTITUTIONS

#	SOURCE	DAY	ORIGIN H/M	LATITUDE (N)	LONGITUDE (W)	DEPTH km	ML	N
9	UWM	15	06:39	17.2830	101.2142	24.18	3.17	5
	THIS STUDY			17.2253	101.2268	19.67	3.81	11
	UWM-TS			17.2312	101.2262	20.05	3.60	16
10	UWM	15	08:01	17.5162	101.4202	22.72	3.19	6
	THIS STUDY			17.4077	101.5015	9.03	3.80	8
	UWM-TS			17.4260	101.4903	17.91	3.60	14
11	UWM	15	17:50	17.5290	101.3177	20.07	3.15	5
	THIS STUDY			17.5188	101.3117	17.27	3.68	9
	UWM-TS			17.5460	101.3037	20.26	3.48	14
12	UWM	16	03:38	17.5048	101.4668	22.37	3.37	12
	THIS STUDY			17.5293	101.4927	22.64	3.95	8
	UWM-TS			17.5165	101.4842	26.18	3.72	20
13	UWM	16	06:04	17.4322	101.4668	26.65	3.75	10
	THIS STUDY			17.4867	101.4735	11.15	4.19	7
	UWM-TS			17.4725	101.4668	26.03	3.99	17
14	UWM	16	06:55	17.3168	101.2725	19.22	3.40	12
	THIS STUDY			17.2797	101.2622	20.18	3.88	10
	UWM-TS			17.3052	101.2607	21.10	3.69	22
15	UWM	16	10:10	17.3392	101.3762	25.28	3.64	11
	THIS STUDY			17.4183	101.3182	18.75	4.14	6
	UWM-TS			17.3758	101.3367	28.82	3.94	17
16	UWM	16	13:24	17.3388	101.3753	25.66	3.21	11
	THIS STUDY			17.3722	101.3660	0.81	3.68	7
	UWM-TS			17.3240	101.3963	22.17	3.45	18

TABLE 3.3 (Continued) AFTERSHOCKS OBTAINED BY THE UNIVERSITY OF WISCONSIN, THE UNIVERSITY OF HAWAII, AND BY USING THE COMBINED DATA FROM BOTH INSTITUTIONS

#	SOURCE	DAY	ORIGIN H/M	LATITUDE (N)	LONGITUDE (W)	DEPTH km	ML	N
17	UWM	16	13:52	17.2735	101.2664	21.79	3.67	10
	THIS STUDY			17.4618	101.1843	15.00	4.05	4
	UWM-TS			17.2845	101.2708	21.41	3.87	14

UWM: Hypocenter locations from the University of Wisconsin-Madison.

UWM-TS: Hypocenter locations using the combined data from the University of Wisconsin-Madison and this study.

ML : Magnitudes determined using code length.

N : Number of station readings.

obtained from the combined data is 20.7 km, which is closer to the average depth, 23.4 km, obtained using only UWM data than to our average depth of 12.0 km.

Although the same (Lee et al., 1972) formula has been used by both institutions to compute magnitudes, in figure 3.12 we can observe that in this parameter we also have differences. All our magnitudes are greater than those reported by the UWM. The average difference is over half a magnitude, and the slope of the line that fits our data is not equal to one. This may be caused by the different frequency response of the instruments used in both seismic networks. This result make our analysis of b values and energy release difficult to compare. The magnitudes of the combined data are always in between the magnitudes obtained independently by both institutions.

Figure 3.12 Magnitudes reported by the University of Wisconsin-Madison versus magnitude reported in this study.

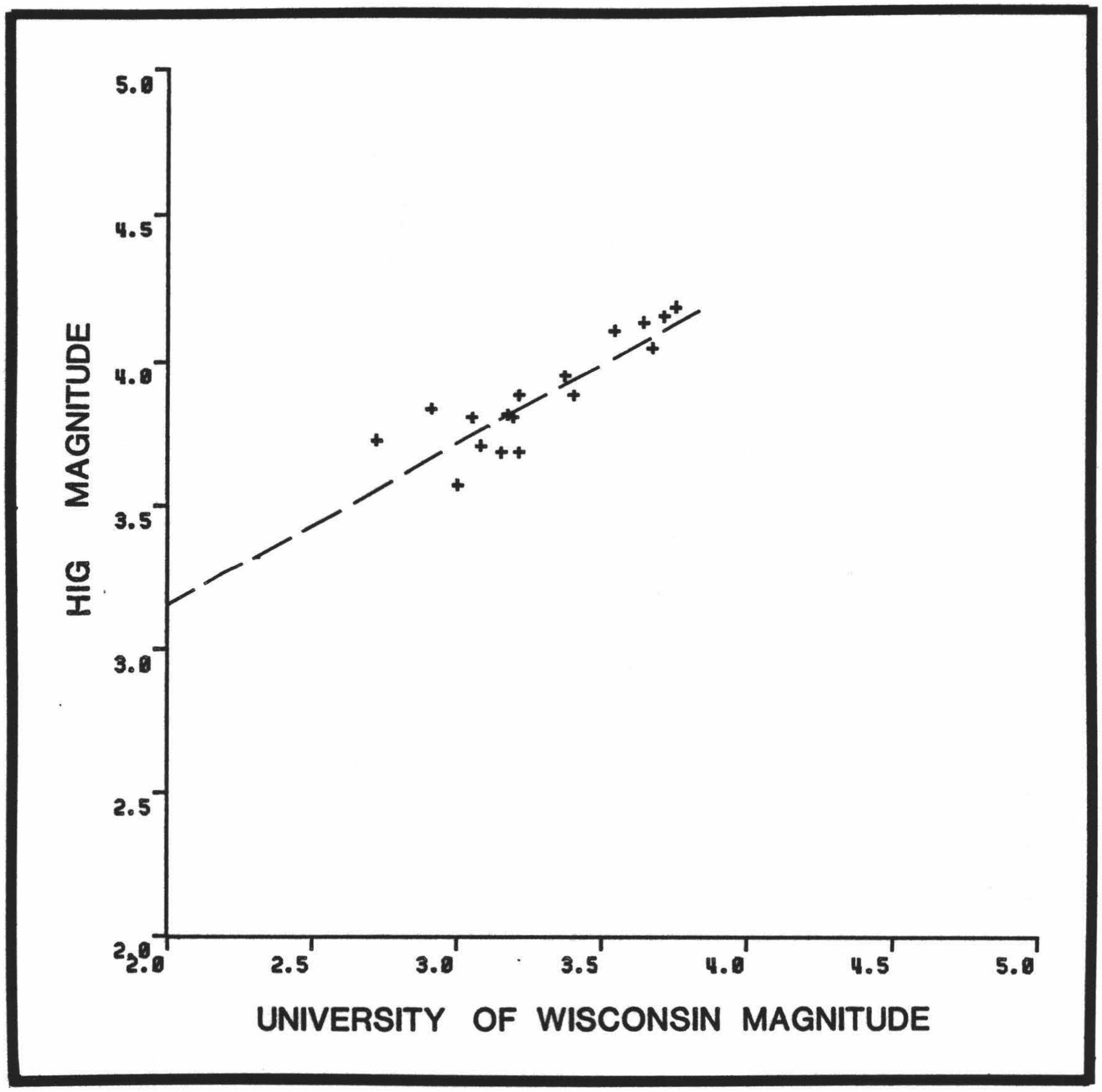

5.0
4.5
4.0
3.5
3.0
2.5
2.0
HIG MAGNITUDE
2.0
2.5
3.0
3.5
4.0
4.5
5.0
UNIVERSITY OF WISCONSIN MAGNITUDE

4 . RESULTS, DISCUSSIONS, AND CONCLUSIONS

4.1 Aftershock Area

Figures 4.1 to 4.6 show the growth of the aftershock area with time; cumulative epicentral locations have been plotted at nine hour intervals. For comparison, in each of these figures the lower portion shows the aftershock area defined by all the events where as the upper portion shows those aftershocks with a minimum of five readings for P and S arrival times, a root mean square error of time residuals less than or equal to 0.5 seconds, and an error for epicentral distance and focal depth less or equal to 10 km. It can be observed that in the first nine hours there is a dense concentration of epicenters that suggests an aftershock area of 2100 km^2(Figure 4.1). We can see a concentration of aftershocks around the epicentral area. The closest events seem to be related to the main aftershock area, but not the most distant.

Figure 4.2 shows the locations of the events in the first 18 hours. The area of concentrated aftershocks increase only 4.8% and grows to the east. By this time, there are so many aftershocks surrounding the concentrated aftershock area that a new region of more widely separated epicenters starts to emerge. This region represents the entire aftershock area and covers about 4500 km^2. The boundary between the

Figure 4.1 Epicenters during the first 9 hours following the Petatlan earthquake; the epicentral area for this period is 2100 km^2. By this time, the aftershocks around the defined aftershock area seem to be related to the rupture plane. The lower part of the figure shows all located events; the upper portion shows only those fullfilling the criteria for minimum acceptability (see text).

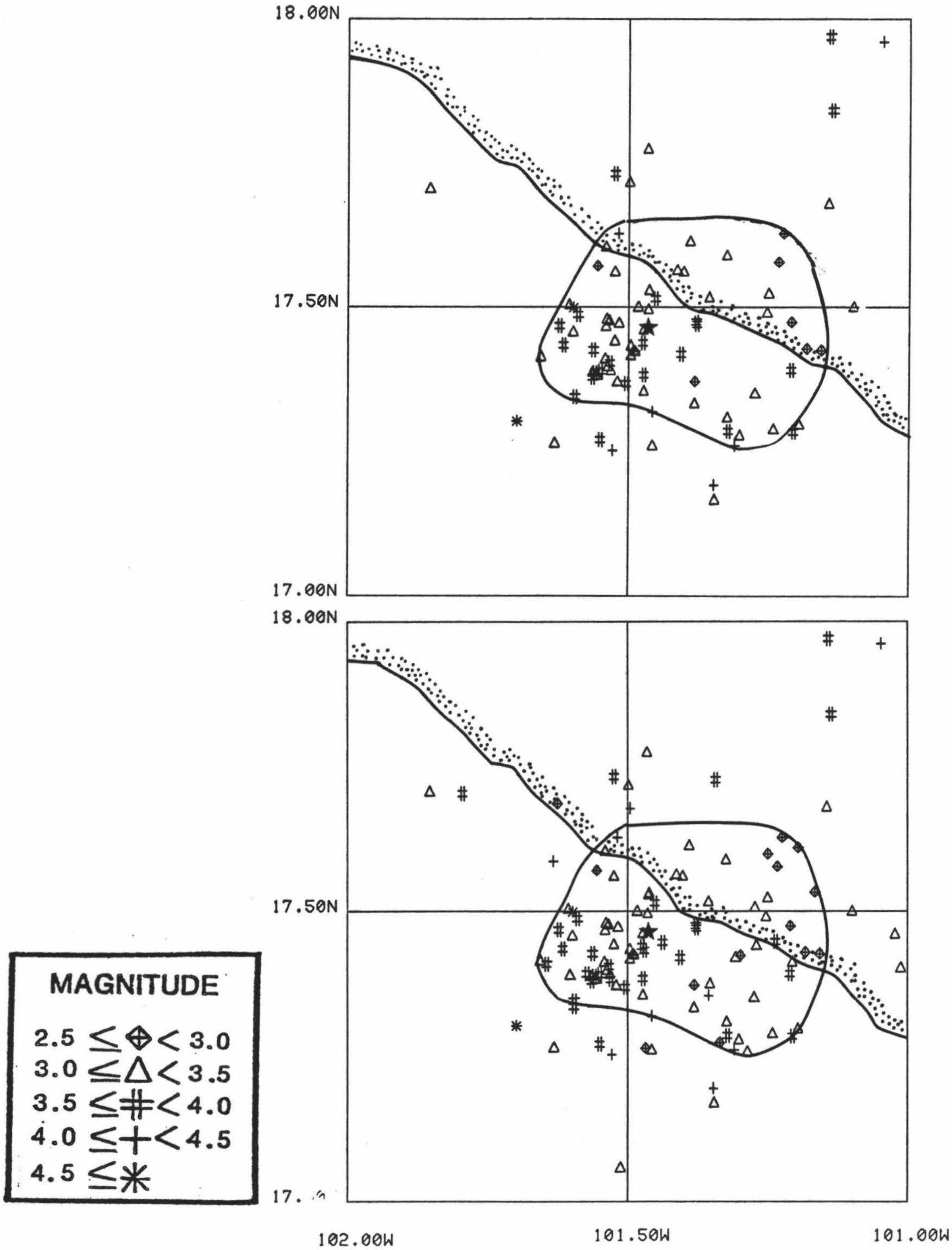
18.00N
17.50N
17.00N
18.00N
17.50N
102.00W
101.50W
101.00W
MAGNITUDE
2.5 ≤ ⊕ < 3.0
3.0 ≤ △ < 3.5
3.5 ≤ # < 4.0
4.0 ≤ + < 4.5
4.5 ≤ ✳

Figure 4.2 Events within 18 hours of the main shock; the epicentral area for the concentrated aftershocks is 2200 km^2. The area for the more dispersed epicenters is 4500 km^2. Two concentrations of epicenters inside the small area can be observed, one to the east and another to the west.

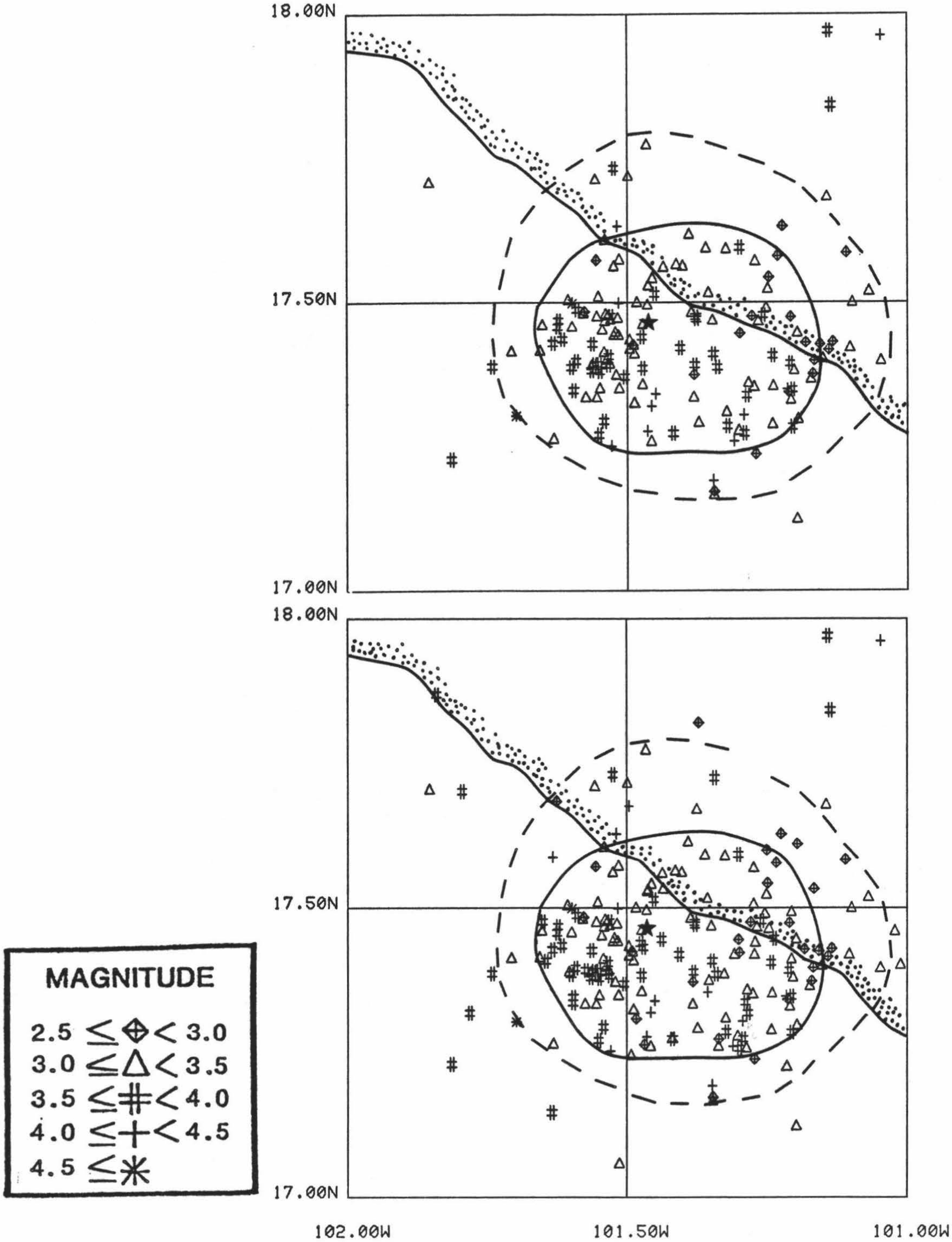
18.00N
17.50N
17.00N
18.00N
17.50N
17.00N
102.00W
101.50W
101.00W
MAGNITUDE
2.5 ≤ ⊕ < 3.0
3.0 ≤ △ < 3.5
3.5 ≤ # < 4.0
4.0 ≤ + < 4.5
4.5 ≤ ✳

region of concentrated seismic activity and the less active zone is well defined. We can observe two concentrated groups of epicenters inside the smaller area, one to the east and another to the west.

Twenty seven hours after the Petatlan earthquake (Figure 4.3), there is a slight change of shape of the entire aftershock area compared to the picture at 18 hours. The area of the zone grows to 4800 km^2, and the region of concentrated events remains about 2200 km^2. These characteristics are maintained during the following hours until the end of the 54 hour period following the Petatlan earthquake (Figures 4.4, 4.5 and 4.6). The sharp boundary between the two groups of concentrated epicenters is still preserved. This last result suggest that the two smaller areas represent two asperities (Lay and Kanamori, 1981), that is, two areas with high strength, high energy release and high concentration of aftershocks. This result will be discussed in the following section.

If we draw the epicentral aftershock area (6060 km^2) within 36 days after the main shock suggested by Valdes et al. (1982) together with our epicenters locations (figure 4.7) it can be seen that at the end of the 54 hours the rupture area as well as the area of high seismicity are well defined. Projecting both epicentral aftershock areas onto the fault plane dipping 15° (Figure 3.5), we obtain a rupture area of 4970 km^2 and 6270 km^2 respectively.

Figure 4.3 Epicentral locations for events within 27 hours of the main shock. The area for the concentrated events is 2200 km^2. The entire aftershock area is 4800 km^2.

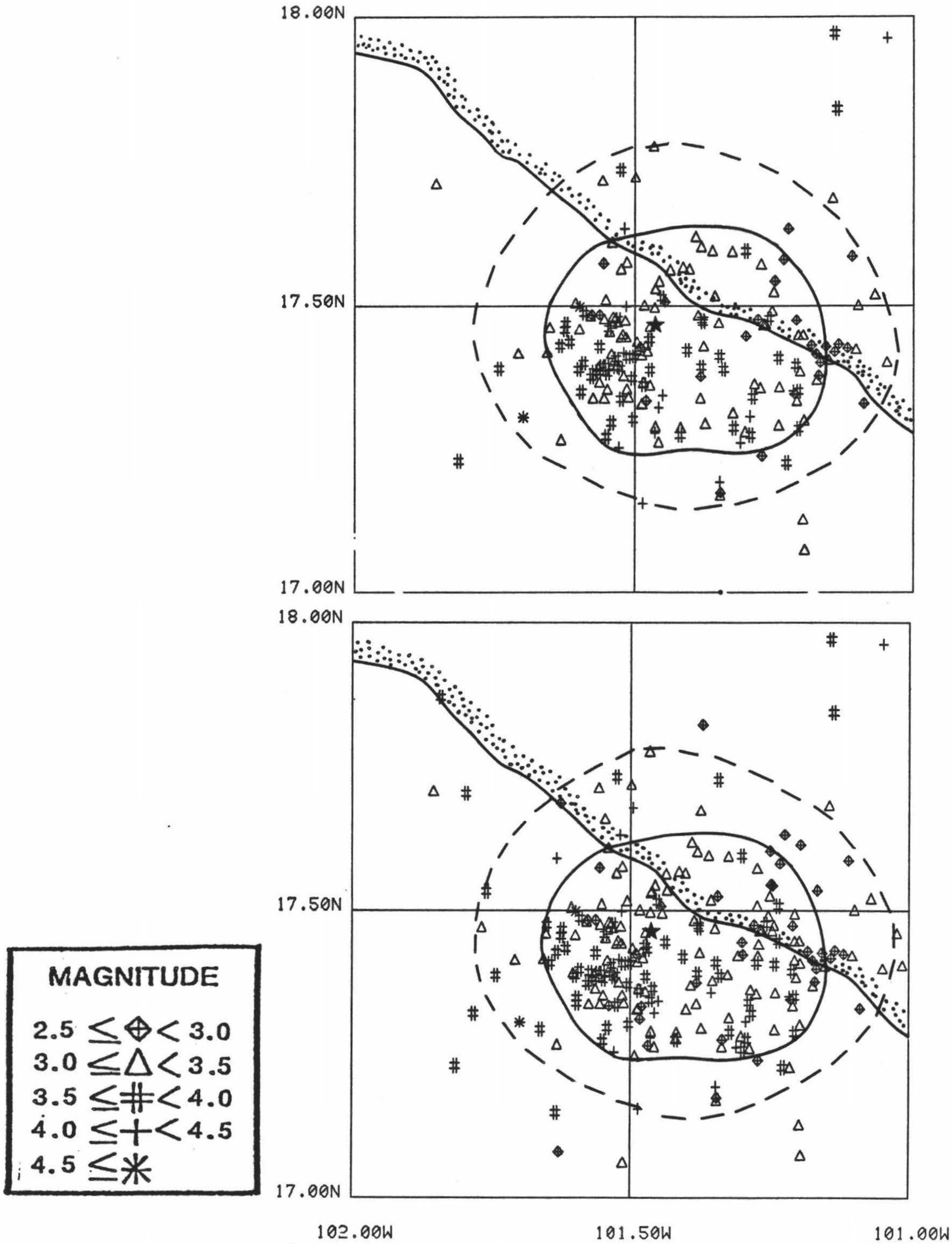
18.00N
17.50N
17.00N
18.00N
17.50N
17.00N
102.00W
101.50W
101.00W
MAGNITUDE
2.5 ≤ ⊕ < 3.0
3.0 ≤ Δ < 3.5
3.5 ≤ # < 4.0
4.0 ≤ + < 4.5
4.5 ≤ *

Figure 4.4 Events within 36 hours of the main shock. The area with the major aftershock activity is 2200 km^2, and for the entire aftershock is 4800 km^2.

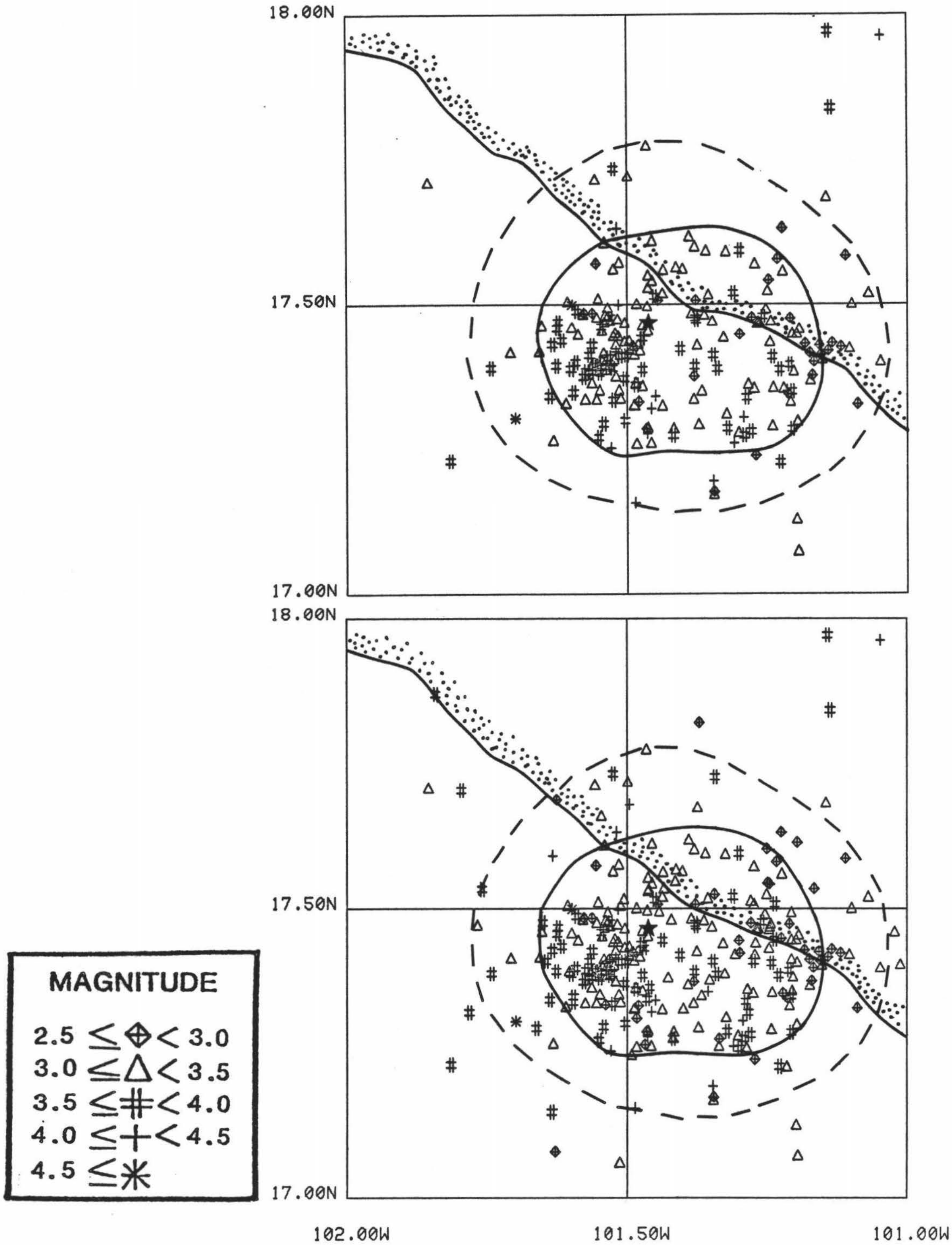
18.00N
17.50N
17.00N
18.00N
17.50N
17.00N
102.00W
101.50W
101.00W
MAGNITUDE
2.5 ≤ ◈ < 3.0
3.0 ≤ △ < 3.5
3.5 ≤ # < 4.0
4.0 ≤ + < 4.5
4.5 ≤ ✳

Figure 4.5 Epicenters of events within 45 hours of the main shock. The area where most of the events are concentrated is 2200 km^2, and for the entire aftershock area is 4800 km^2.

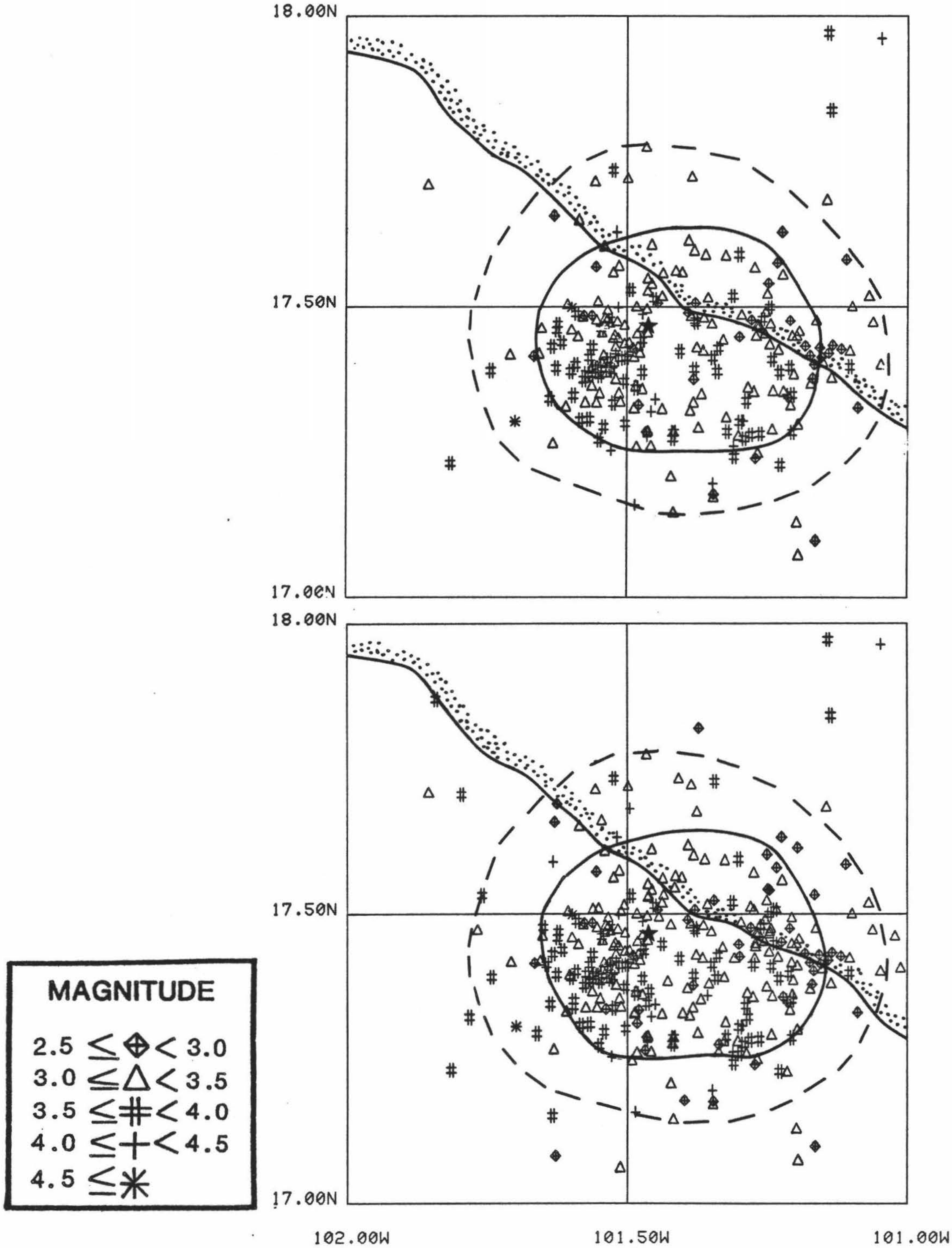
18.00N
17.50N
17.00N
18.00N
17.50N
17.00N
102.00W
101.50W
101.00W
MAGNITUDE
2.5 ≤ ⊕ < 3.0
3.0 ≤ △ < 3.5
3.5 ≤ # < 4.0
4.0 ≤ + < 4.5
4.5 ≤ ✳

Figure 4.6 Epicenters of aftershocks within 54 hours after the main shock. The area for the region of high seismicity and the entire rupture area are 2200 km^2 and 4800 km^2 respectively. By this time, the two groups of concentrated epicenters which were observed 18 hours after the main shock are still well defined. The dashed curve shows the imaginary separation between both groups.

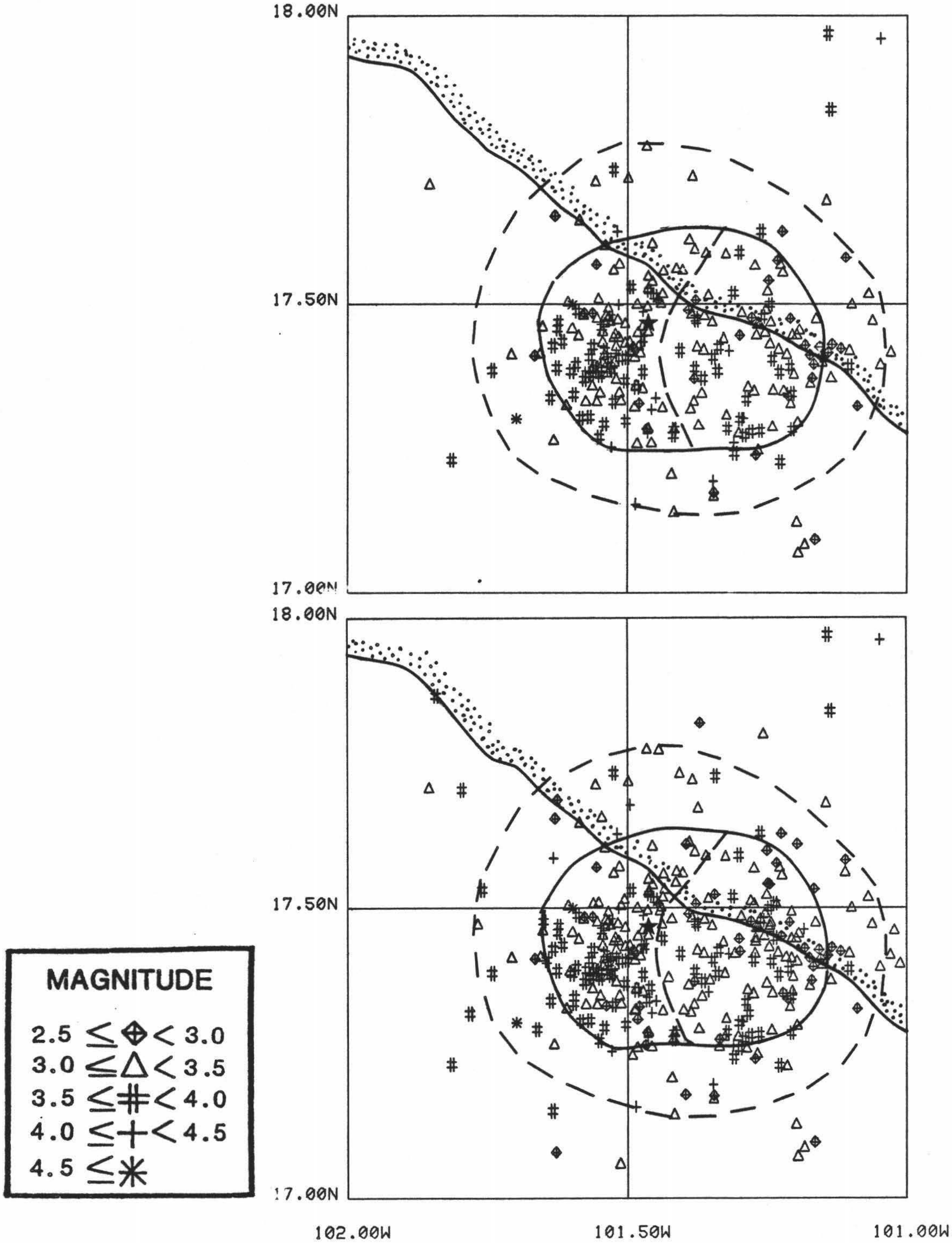
18.00N
17.50N
17.00N
18.00N
17.50N
17.00N
102.00W
101.50W
101.00W
MAGNITUDE
2.5 ≤ ⊕ < 3.0
3.0 ≤ △ < 3.5
3.5 ≤ # < 4.0
4.0 ≤ + < 4.5
4.5 ≤ ✳

Figure 4.7 Aftershock area reported by Valdes et al. (1982) within 36 days after the main shock. This area contains all the aftershocks located in the first 54 hours.

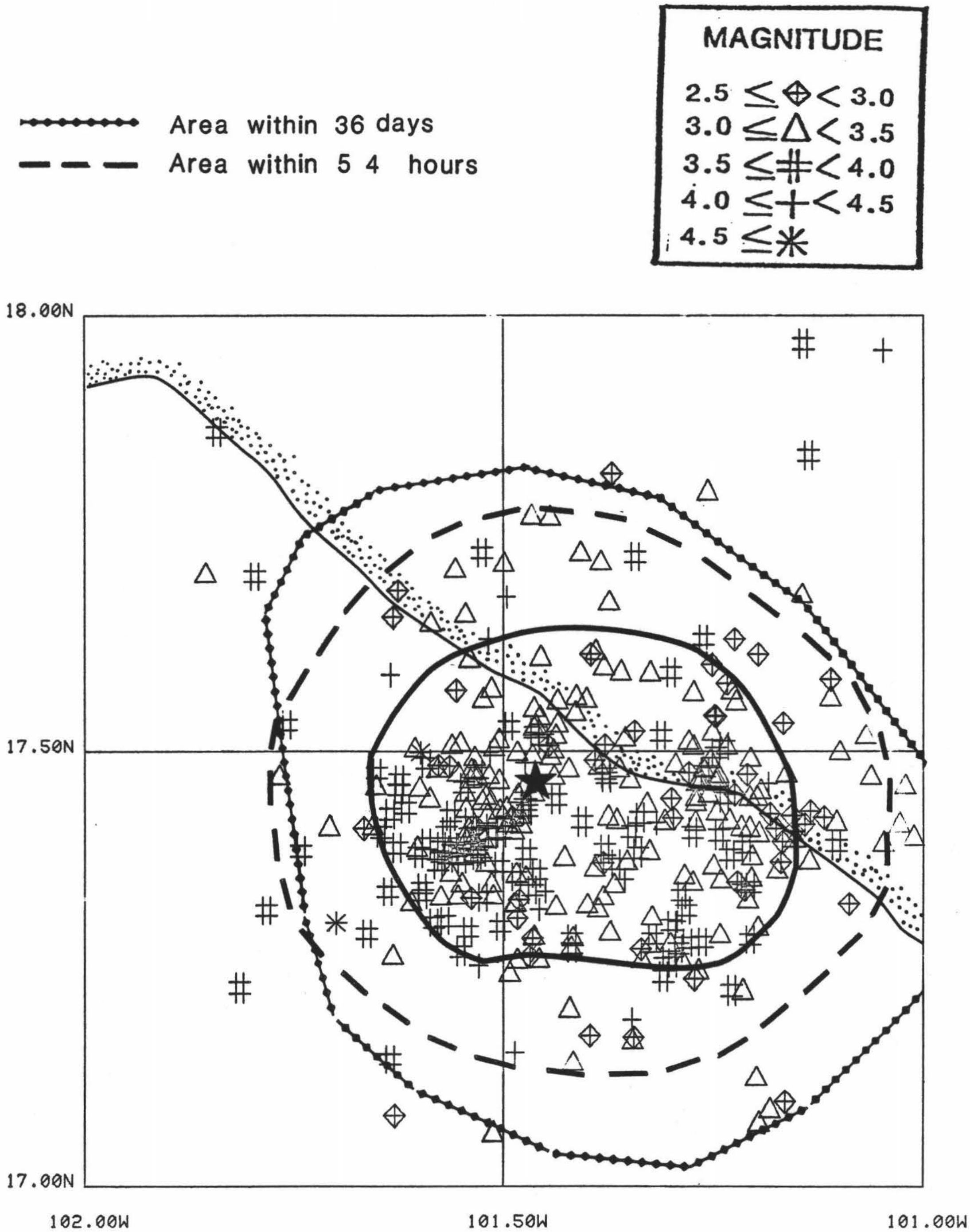
Area within 36 days
Area within 5 4 hours
MAGNITUDE
2.5 ≤ ◈ < 3.0
3.0 ≤ △ < 3.5
3.5 ≤ # < 4.0
4.0 ≤ + < 4.5
4.5 ≤ *
18.00N
17.50N
17.00N
102.00W
101.50W
101.00W

Interpreting our epicenter locations, we see that approximately one day after the main shock, the rupture region and the area of concentrated events are well defined (figure 4.3). There was no expansion in these two areas during the period between 27 and 54 hours. We find that the change between the rupture area after 27 hours and the rupture area obtained by Valdes et al. (1982) for a 36 day period is only 26%. This data suggests that there is no significant expansion in the area defined by the aftershocks after one day passed.

4.2 Two Asperities in the Rupture Area

In the last section, we have seen that two areas within the aftershock region show high concentration of aftershocks. It was suggested that these two regions may represent two asperities. To investigate this possibility further, the region between latitudes 17°N and 18°N, and longitudes 101°W and 102°W has been divided into 0.1° by 0.1° squares. The number of events and the total energy released inside of each square have been computed (the program to compute these parameters for any seismic set and any size square is given in the appendix B1, and was developed by the author). In order to compare energy release during the early aftershock sequence with the later part covered by Valdes et al. (1982), the same formula (Bath, 1979) as in Valdes et al. is used namely:

$$\log E = 1.44M + 12.25$$

where E = energy in ergs, and M = magnitude.

Figure 4.8 and figure 4.9 show the grid with the results for both, the total number of events and for those with the error limits described in section 4.1. The upper number in each 0.1^{o} by 0.1^{o} square indicates the total number of events recorded during the first 54 hours of aftershocks. The lower number indicates energy released (x 10^{17} ergs)during the same time. We can consider that these data are complete for events with magnitude larger than or equal to 3.0 and which took place after two hours following the Petatlan earhquake. In the figure we observe again two groups of concentrations, one in the east and another in the west of the aftershock area.

For a better view of these results, the value obtained in each square of figures 4.8 and 4.9 was assigned to its center. A contour map of number of events (Figure 4.10), and a 3-D plot of number of events (Figure 4.11) and energy release (Figure 4.12) were made. From these plots, we can see clearly that two areas emerge, showing a high concentration of events and high energy release. These plots confirm the existence of two asperities (Lay and Kanamori, 1981). These asperities are separated and surrounded by regions of fewer aftershocks and lower energy release.

Figure 4.8 Distribution of number of earthquakes and energy release inside each 0.1^{o} by 0.1^{o} squares between the coordinates 17^{o}N and 18^{o}N latitude, and 101^{o}W and 102^{o}W longitude. The upper number is the number of events recorded during the first 54 hours of aftershocks, the lower number is the energy release during the same time. The energy release (x 10^{17} ergs) is computed using the formula $\log E = 1.44M + 12.25$ (Bath, 1979). The regions with a high concentration of number of events and energy release are shown by squares drawn with heavy lines.

18° N	0 0.0	0 0.0	0 0.0	0 0.0	0 0.0	0 0.0	0 0.0	0 0.0	1 2.2	1 15.2
	0 0.0	1 8.9	0 0.0	0 0.0	0 0.0	0 0.0	1 0.2	0 0.0	1 7.3	0 0.0
	0 0.0	1 0.6	1 6.4	0 0.0	2 2.5	4 3.1	2 3.5	1 0.4	0 0.0	0 0.0
	0 0.0	0 0.0	0 0.0	2 0.5	4 30.1	2 13.7	3 1.0	2 2.3	0 1.0	0 0.0
	0 0.0	0 0.0	1 4.0	2 16.2	7 5.1	15 23.8	8 10.4	12 9.9	3 2.4	1 1.2
	0 0.0	0 0.0	2 1.5	9 25.1	35 143.1	23 55.7	13 42.0	29 39.4	14 19.2	5 5.0
	0 0.0	0 0.0	2 9.6	5 69.1	34 97.3	14 60.0	13 37.6	17 73.6	5 7.0	2 1.1
	0 0.0	1 2.2	0 0.0	2 4.5	4 25.8	12 30.4	8 42.4	11 32.3	1 1.7	0 0.0
	0 0.0	0 0.0	0 0.0	1 2.3	0 0.0	2 16.7	4 17.5	0 0.0	1 0.8	0 0.0
17° N	0 0.0	0 0.0	0 0.0	1 0.3	1 1.4	0 0.0	0 0.0	0 0.0	3 1.6	0 0.0

102° W 101° W

Figure 4.9 The same as figure 4.8 except that the parameters are calculated for events with a minimum of five readings for P and S arrival times, a root mean square error of time residuals less than or equal to 0.5 seconds, and an error for epicentral distance and focal depth less or equal to 10 km.

18° N

0 0.0	0 0.0	0 0.0	0 0.0	0 0.0	0 0.0	0 0.0	0 0.0	1 2.2	1 15.2
0 0.0	0 0.0	0 0.0	0 0.0	0 0.0	0 0.0	0 0.0	0 0.0	1 7.3	0 0.0
0 0.0	1 0.7	0 0.0	0 0.0	2 2.5	2 1.4	1 0.6	0 0.0	0 0.0	0 0.0
0 0.0	0 0.0	0 0.0	1 0.3	3 29.6	1 0.4	1 0.4	2 2.3	1 0.8	0 0.0
0 0.0	0 0.0	0 0.0	1 0.4	4 3.1	12 20.3	7 10.3	6 2.8	1 0.2	1 1.2
0 0.0	0 0.0	1 0.4	7 18.7	34 142.9	18 45.5	12 40.7	18 23.9	12 5.7	3 2.8
0 0.0	0 0.0	1 3.4	4 67.2	30 86.8	9 48.1	8 11.8	14 64.0	5 7.0	2 1.1
0 0.0	1 2.2	0 0.0	1 1.2	4 25.9	9 28.6	5 41.2	8 24.7	1 1.7	0 0.0
0 0.0	0 0.0	0 0.0	0 0.0	0 0.0	2 16.7	3 17.2	0 0.0	1 0.8	0 0.0
0 0.0	0 0.0	0 0.0	0 0.0	0 0.0	0 0.0	0 0.0	0 0.0	3 1.6	0 0.0

17° N

102° W — 101° W

Figure 4.10 Contour map for number of aftershocks in 0.1^{o} by 0.1^{o} squares. The lower and upper portion of the figure show the results using data of grid in figure 4.8 and figure 4.9 respectively.

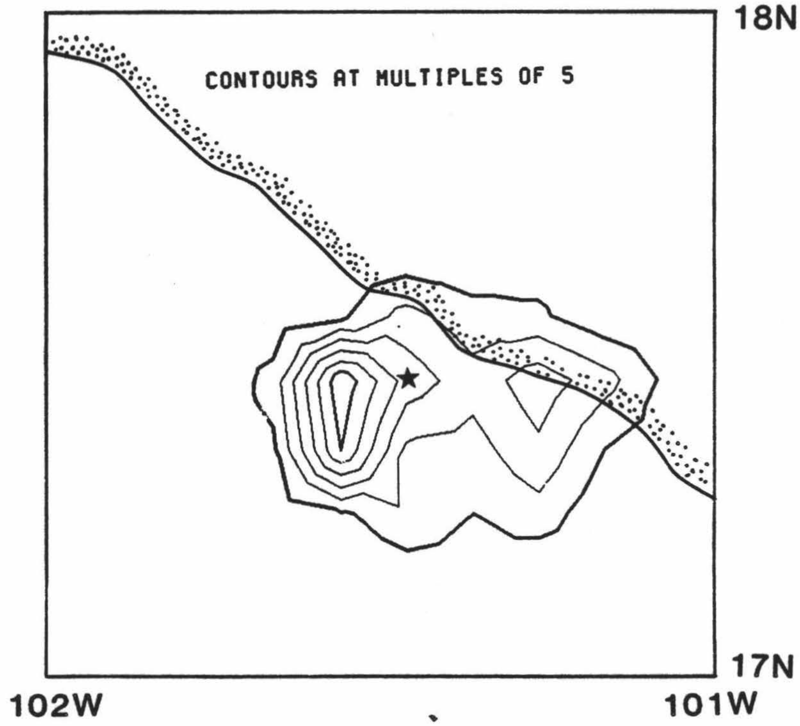
CONTOURS AT MULTIPLES OF 5
18N
17N
102W
101W

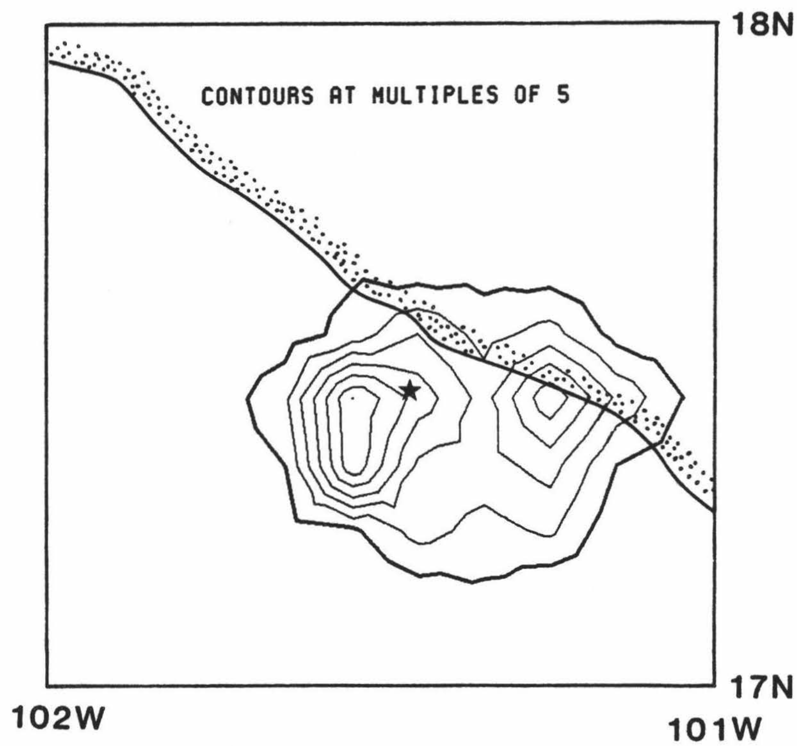
CONTOURS AT MULTIPLES OF 5
18N
17N
102W
101W

Figure 4.11 3-D plot for number of events in 0.1° by 0.1° squares. The lower and upper portion of the figure show the results using data of grid in figure 4.8 and 4.9 respectively.

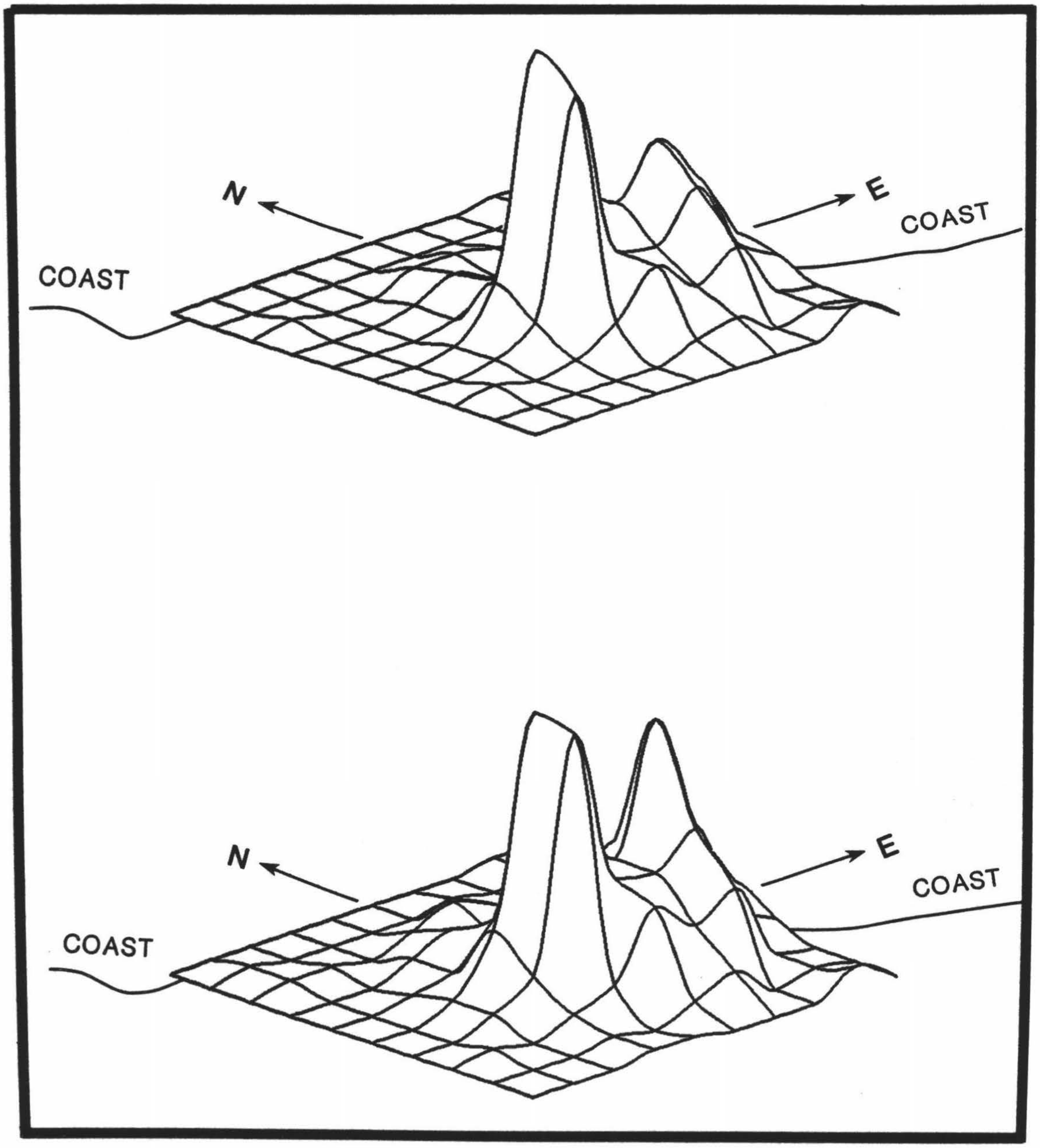
N
E
COAST
COAST
N
E
COAST
COAST

Figure 4.12 3-D plot for energy release in 0.1° by 0.1° squares. The lower and upper portion of the figure show the results using data grid in figure 4.8 and 4.9 respectively.

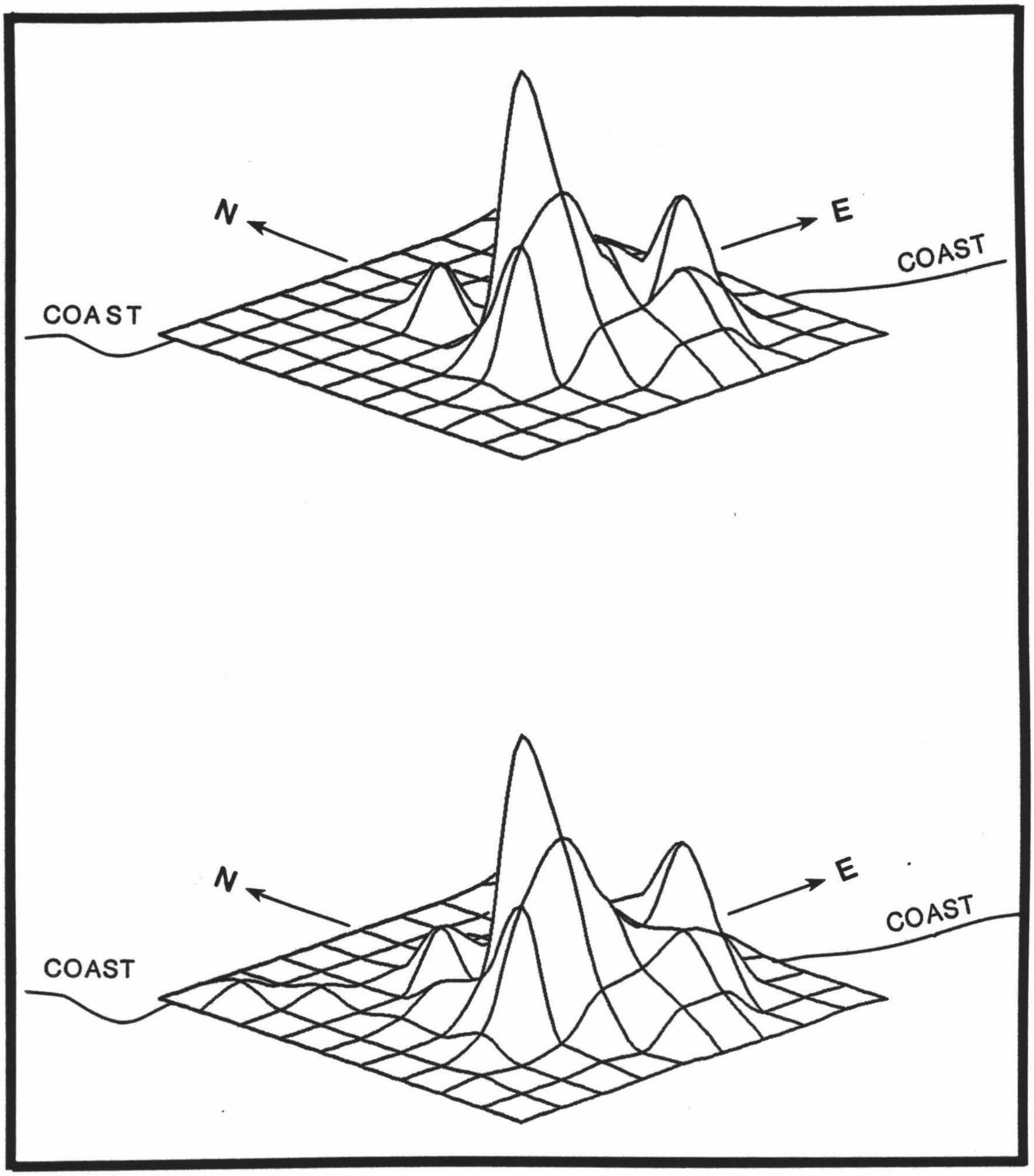
N
E
COAST
COAST
N
E
COAST
COAST

In order to get more evidence to support the existence of two asperities in the aftershock area, the epicenters of the events located between the coordinates 17°N and 18°N latitude, and 101°W and 102°W longitude were projected on the lines A-B and C-D shown in figure 3.4. Figure 4.13 shows the histogram obtained for the projection on line A-B which is parallel to the coast. We still observe the two groups of high concentration of events. Although the two groups are more evident in the E-W projection along line C-D shown in figure 4.14.

Observing figure 4.6 and figure 4.10, and comparing figure 4.13 with figure 4.14, we can see that the asperities are not parallel to the coast, and are in an E-W trend. The same observation was made by Valdes et al. (1982) in the area of concentrated epicenters after their 36 days period of aftershock analysis. This finding again supports Kanamori, that the main features of the aftershock zone are established by the aftershock patterns during the first one or two days.

Other evidence is shown in figure 4.15 where a histogram of S-P times recorded by station 104 for events located between the coordinates described above, has been plotted. The station 104 is located southeast of the epicenter of the Petatlan earthquake (Figure 1.1) and it is approximately in the line that joints the center of the two groups of concentrated aftershocks. We observe that S-P times between 5.5 and 8.5 seconds define one group and the other group is perfectly defined between 9.0 and 11.0 seconds.

Figure 4.13 Number of earthquakes in 5 km wide stripes perpendicular to line A-B in figure 3.4.

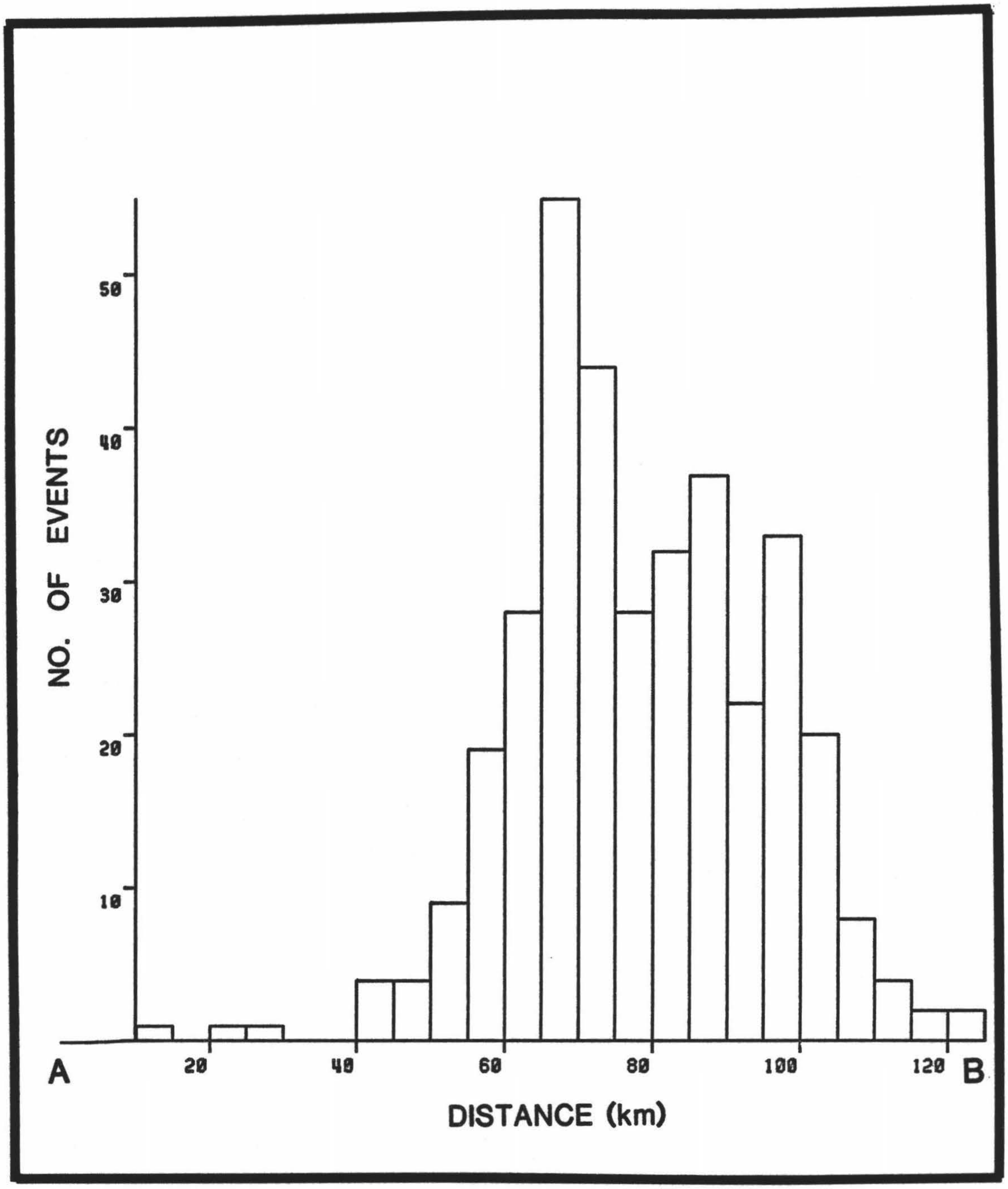

NO. OF EVENTS
50
40
30
20
10
A
20
40
60
80
100
120
B
DISTANCE (km)

Figure 4.14 Number of earthquakes in 5 km wide stripes perpendicular to line C-D in figure 3.4.

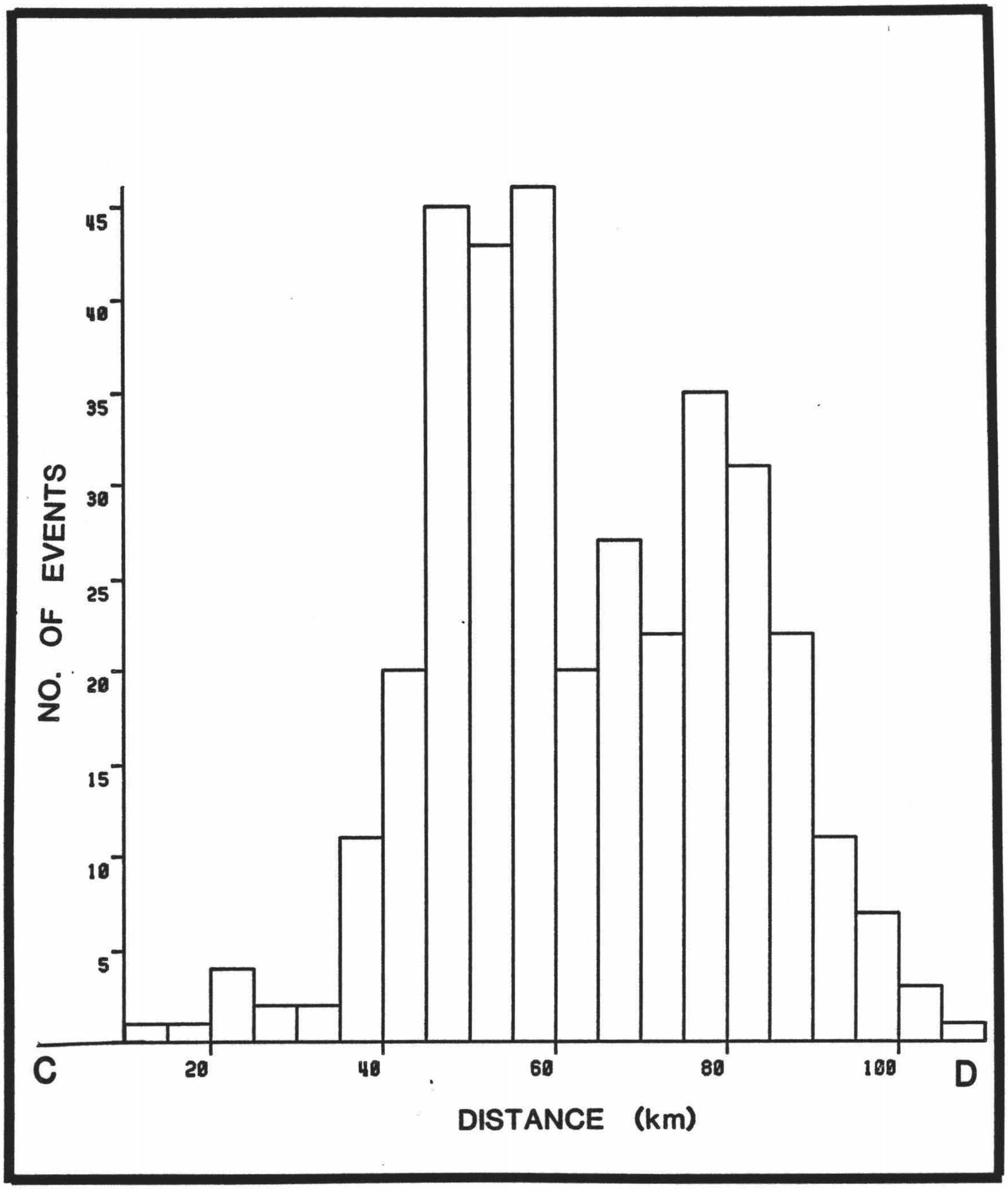
NO. OF EVENTS
45
40
35
30
25
20
15
10
5
C
20
40
60
80
100
D
DISTANCE (km)

Figure 4.15 Number of events versus S-P times recorded by station 104 during the first 54 hours after the Petatlan earthquake within the coordinates 17° N and 18° N latitude, and 101° W and 102° W longitude.

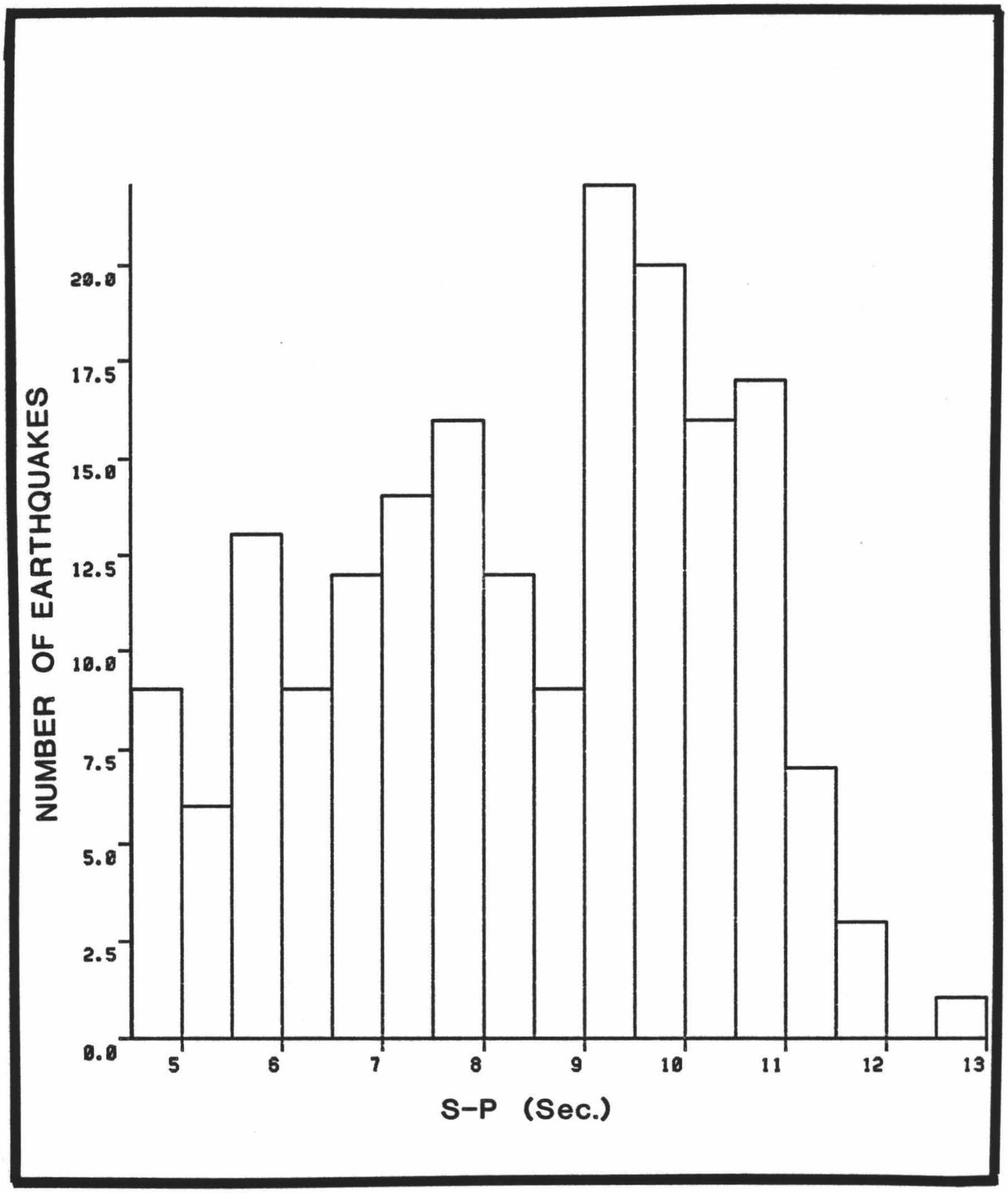

NUMBER OF EARTHQUAKES
20.0
17.5
15.0
12.5
10.0
7.5
5.0
2.5
0.0
5
6
7
8
9
10
11
12
13
S-P (Sec.)

Finally, due to the evidence of two different groups of concentrated aftershocks, it was decided to plot the epicenter locations and focal depths for those aftershocks with error limits very well constrained. The criteria to select these events were: root mean square (RMS) of time residuals less than or equal to 0.35 seconds, an error for epicentral distance (ERH) and focal depth (ERZ) less than or equal to 5 km, and a minimum of 7 readings for P and S arrival times (P and S arrival times for the same station are considered as two readings). With the last restriction we are only considering aftershocks located using four or more stations. The epicenters are shown in figure 4.16. We can still observe two groups of concentrated events in the aftershock area. The focal depths shown in figure 4.17 were projected in a plane approximately perpendicular to the trench. We observe two seismic zones clearly separated, and both dipping at different angles. This result may suggest two different interpretations: there are two rupture planes in the fault plane of the Petatlan earthquake, or the Cocos plate is being subducted at different angles in the region.

From all our analysis, we can say that the clustering of the two groups of aftershocks are real and that they define two asperities.

4.3 More Analysis of the Asperities

In this section we will analyze the sequence of aftershocks that defined each asperity. In figure 4.18 we can see the number of events

Figure 4.16 Epicenter locations with root mean square of time residuals less than or equal to 0.35 seconds, epicentral and vertical error less than or equal to 5 km, and a minimum of seven readings for P and S arrival times.

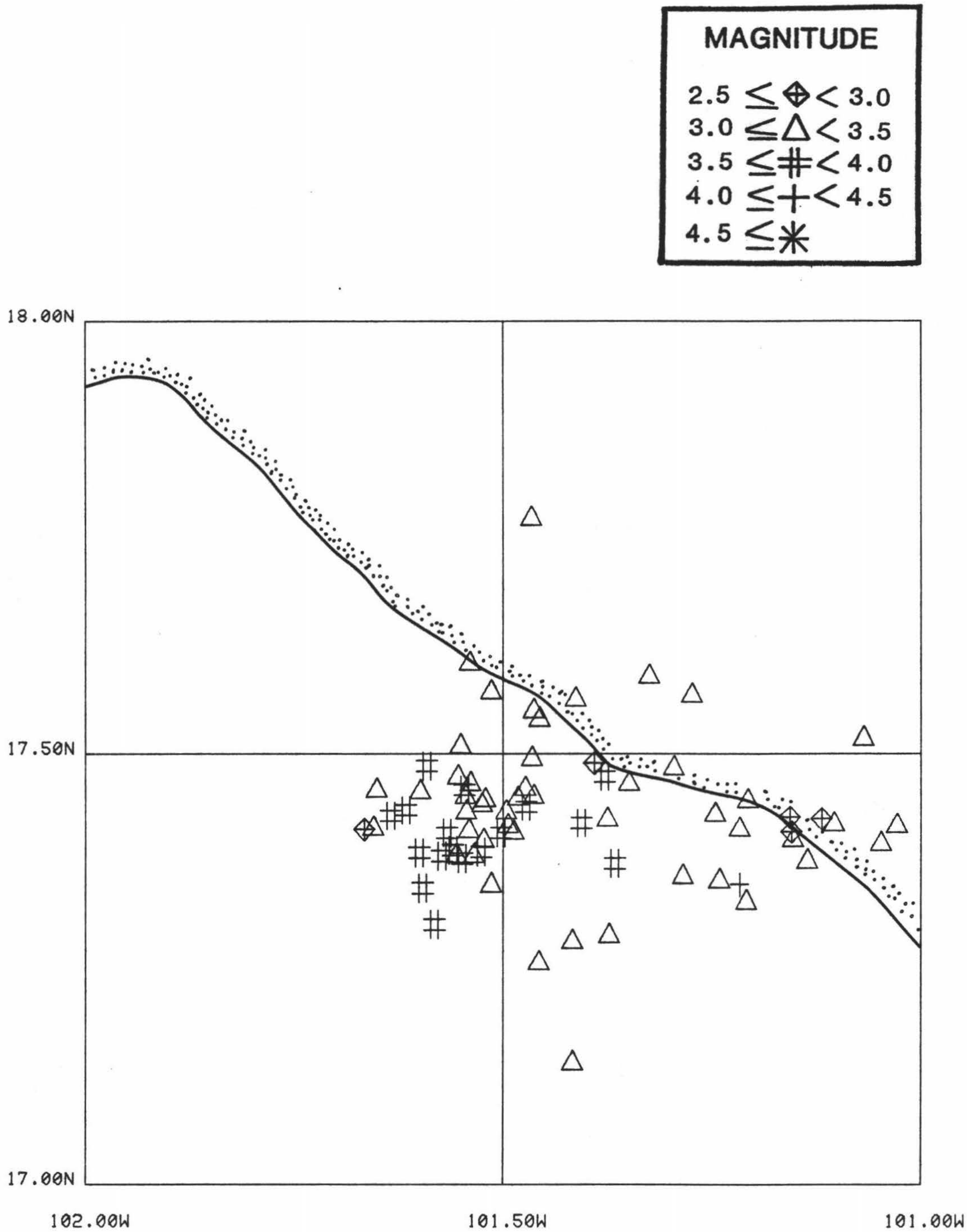
MAGNITUDE
2.5 ≤ ⊕ < 3.0
3.0 ≤ △ < 3.5
3.5 ≤ # < 4.0
4.0 ≤ + < 4.5
4.5 ≤ ✳
18.00N
17.50N
17.00N
102.00W
101.50W
101.00W

Figure 4.17 Focal depths projected in a plane approximately perpendicular to the trench for those aftershocks with the error limits described in figure 4.16.

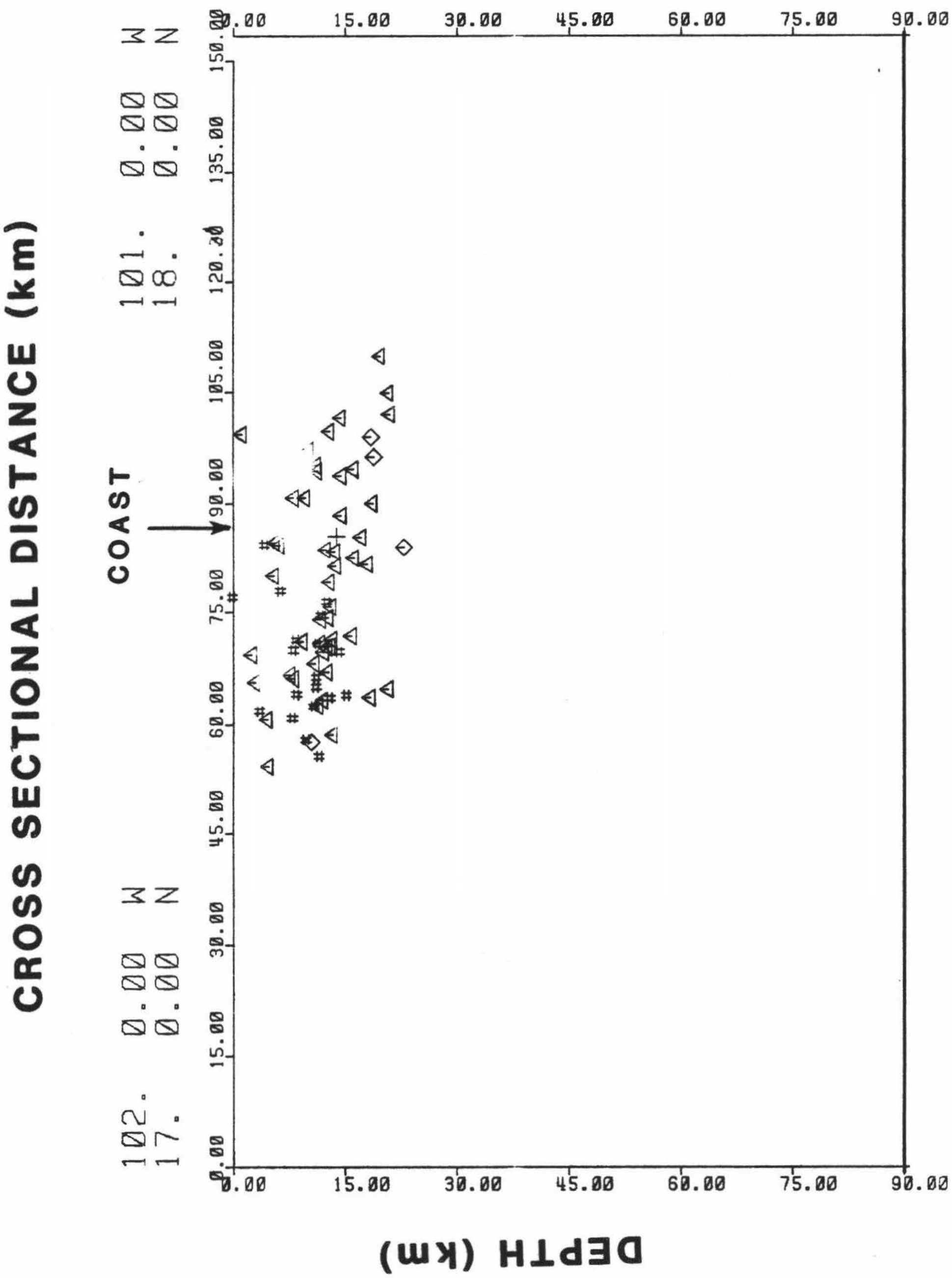
CROSS SECTIONAL DISTANCE (km)
DEPTH (km)
COAST
102. 0.00 W
17. 0.00 N
101. 0.00 W
18. 0.00 N
0.00
15.00
30.00
45.00
60.00
75.00
90.00
105.00
120.00
135.00
150.00

Figure 4.18 Number of aftershocks per two hour intervals. The activity is shown for the entire aftershock area, and the west and east asperity. The numbers in the periods A, B, C, D, E, and F represent the percentage of earthquakes that took place in the asperity during that time. The letters L and H stand for low and high concentration of aftershocks. Note that low release periods in one asperity correspond to high release periods in the other.

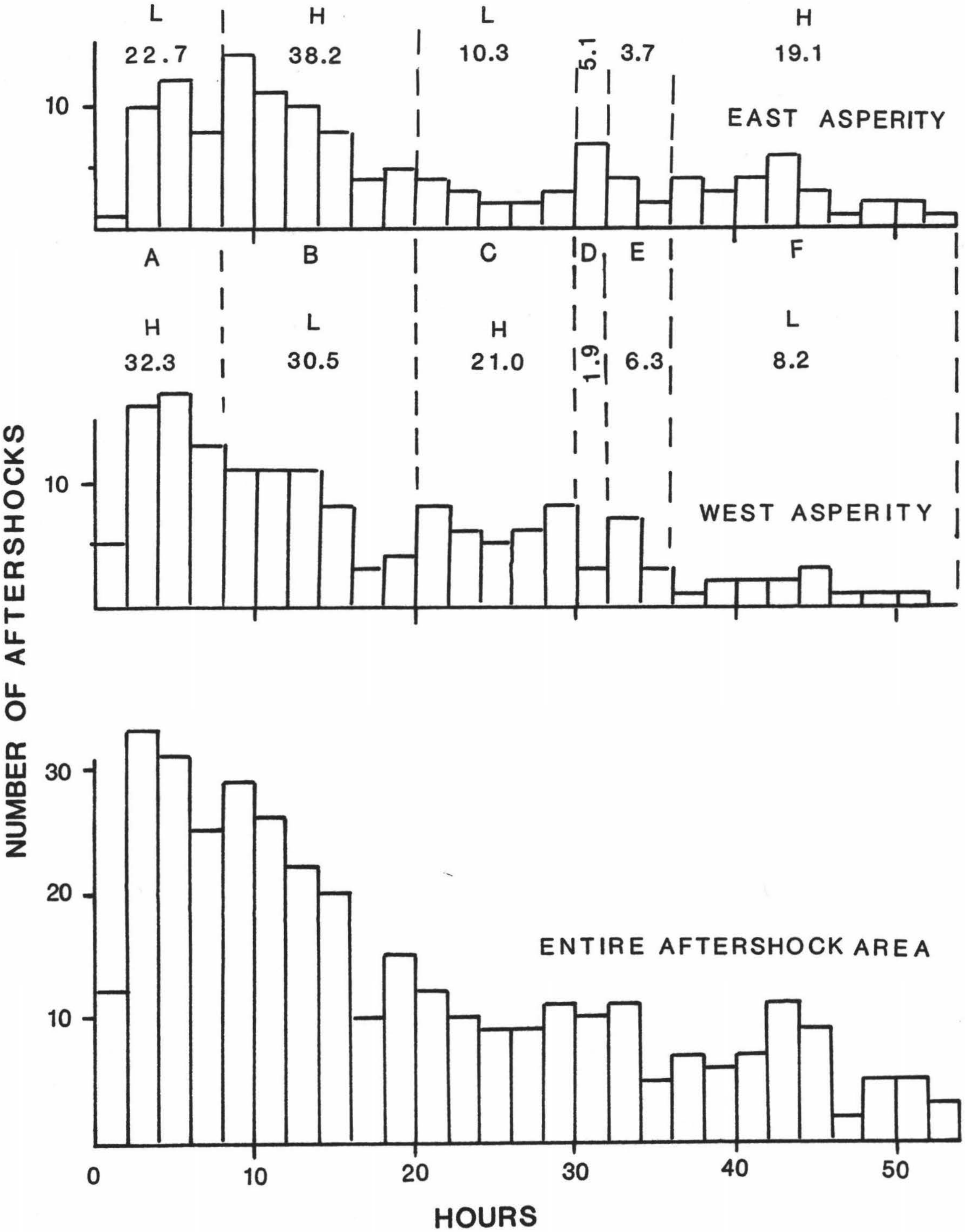
L
22.7
H
38.2
L
10.3
5.1
3.7
H
19.1
EAST ASPERITY
A
B
C
D
E
F
H
32.3
L
30.5
H
21.0
1.9
6.3
L
8.2
WEST ASPERITY
ENTIRE AFTERSHOCK AREA
NUMBER OF AFTERSHOCKS
HOURS
10
20
30
0
40
50

that took place in each two hour interval after the Petatlan earthquake. The figure shows the sequence for all the earthquakes in the aftershock area and for those located in each asperity. Depending on the position of the event with respect to the imaginary line dividing the two asperities (figure 4.6), an event was considered as taking place either in the asperity to the west or in the asperity to the east. The numbers in the periods defined by the letters A, B, C, D, E, and F represent the percentage of the total number of earthquakes that took place in the asperity during that time. The letters L and H stand for low and high concentration of events respectively. The number of earthquakes in the first two hours may not be real because, as was mentionated before, for many of the aftershocks during this time it was not possible to read P and S wave arrival times since their record were obscured by overlaping events. We observe that in the intervals of time A, B, C, D, E, and F, when a high percentage of aftershocks take place in one of the asperities, there is a low percentage occurring in the other. And this high and low concentrations of seismic activity take place alternately in both asperities during all the 54 hour period. If we consider periods D and E as periods of transition or part of period C, we can see that the period for the change of concentration of seismic activity from one asperity to the other increases with time. Based on figure 4.18, figure 4.19 shows the percentage of aftershocks that take place every two hours. The continuous and dashed lines represent the percentage for the western and eastern asperity respectively. We can see clearly the sharp changes of concentration of aftershocks. And the differences between the

Figure 4.19 Percentage of aftershocks that took place in each asperity every two hours. The continuous and dashed lines show the percentage for the asperity to the west and the asperity to the east respectively.

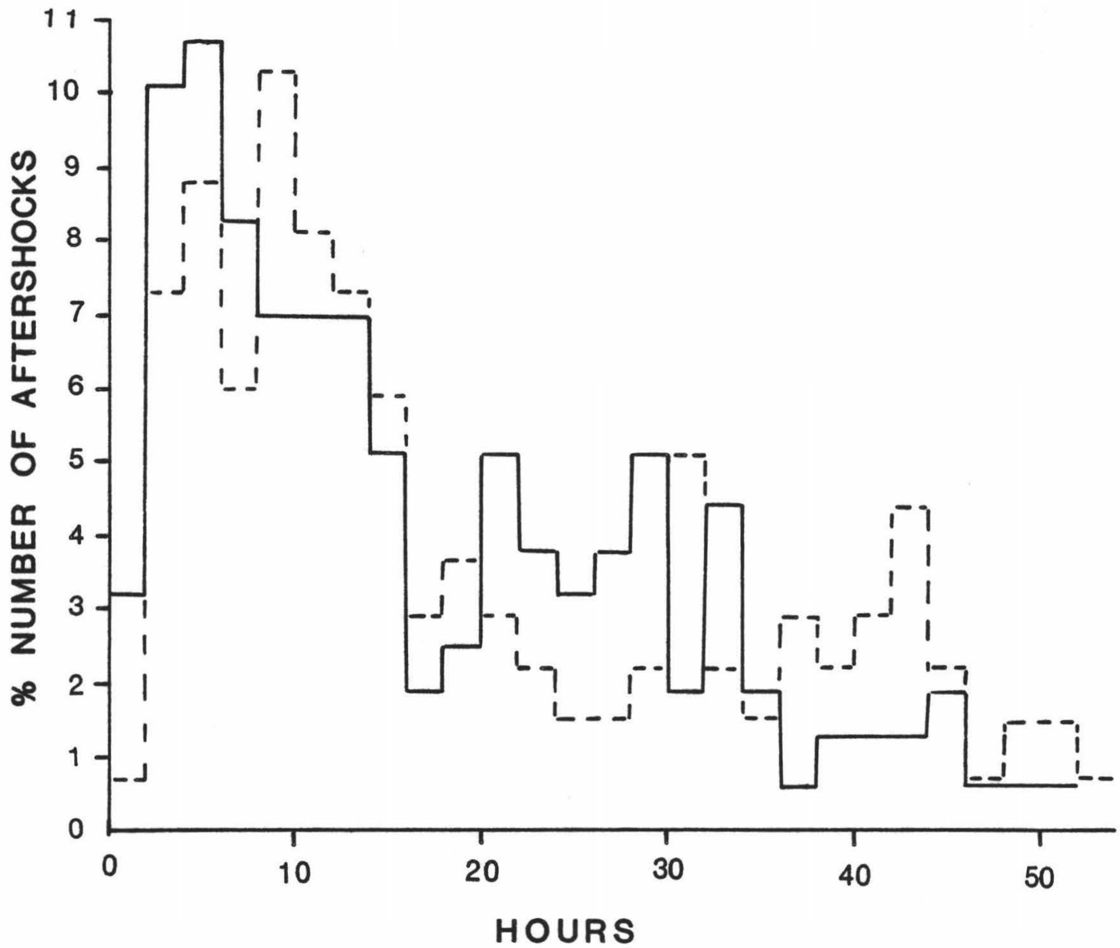

% NUMBER OF AFTERSHOCKS
0
1
2
3
4
5
6
7
8
9
10
11
0
10
20
30
40
50
HOURS

activity in one asperity and the other.

By restricting the following analysis to only those events that ocurred in the squares shown in figure 3.4, we are limiting our analysis to those earthquakes that took place in the zones of maximum energy release inside each asperity (figure 4.12). If we substract the energy released by each aftershock in the eastern asperity from the energy released by the aftershocks in the western asperity. we obtain the cumulative energy release difference with time shown in figure 4.20. We observe a fast increase of cumulative energy difference within 30 hours after the Petatlan earthquake. Then the energy difference is more or less stable, this indicates that by this time there is no remarkable difference between the energy release in both asperities. This result is in agreement with the fact that the aftershock area is well defined during the first 27 hours following the main shock (section 4.1), and with Kanamori´s assumption that the patterns of aftershocks are well defined in the first one or two days of the aftershock sequence. The periods when negative slopes are observed in figure 4.20 indicates the times when the energy release in the eastern asperity was higher than in the western asperity. In general the period of this shift of energy increases with time.

This behavior of concentration of events taking place in the rupture area in one asperity and then the other, and then back again is not well understood. However from our preceding analysis we have seen that the

Figure 4.20 Cumulative energy release difference (x 10^{17} ergs, using the formula shown in page 68) between the western asperity and the eastern asperity. The events considered are limited to locations in the two smaller squares inside the coordinates 17^{o} and 18^{o} N latitude, and 101^{o} and 102^{o} W longitude shown in figure 3.4.

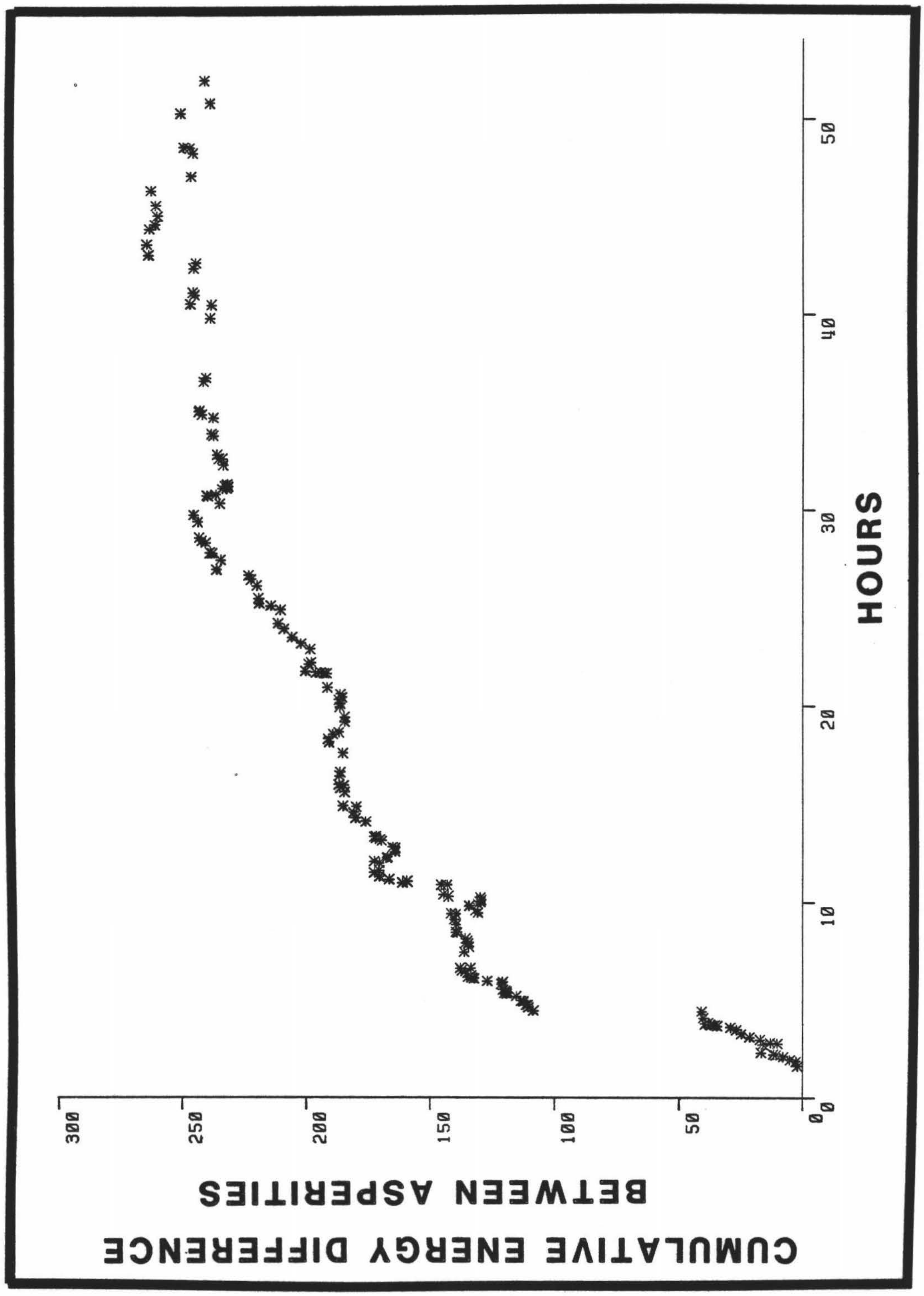
CUMULATIVE ENERGY DIFFERENCE
BETWEEN ASPERITIES
0
50
100
150
200
250
300
HOURS
10
20
30
40
50

highest concentration of aftershocks at the beginning of the sequence took place in the asperity to the west, and because the main shock ocurred in this side, we can consider that this asperity was the first to be broken. This assumption will be more obvious in the next section after comparison with the foreshock data.

4.4 Analysis of Foreshock Data

The foreshocks reported by Hsu et al. (1983) in the aftershock area from March 1, 1979 until the Petatlan earthquake have been plotted in figure 4.21. Figure 4.22 shows the 3-dimensional plot for number of foreshocks (upper portion) and their energy release (lower portion). We can observe a concentration of events and high energy release on the east side of the the aftershock area; in fact, exactly at the same place where the eastern asperity was defined by our aftershock data. The asperity on the west side defined by the number of aftershocks is not so obvious. However it is clearly defined in the energy release plot. We observe two peaks of high energy concentration. Therefore, we conclude that two asperities were detected both before and after the Petatlan earthquake. To our knowledge, this is the first time that a set of data has detected asperities not only after but also before the main shock.

It is interesting to compare the results obtained with the foreshock and the aftershock data. In the foreshock data it was observed that the

Figure 4.21 Foreshocks reported by Hsu et al. (1983) from March 1, 1979, to prior to the Petatlan earthquake.

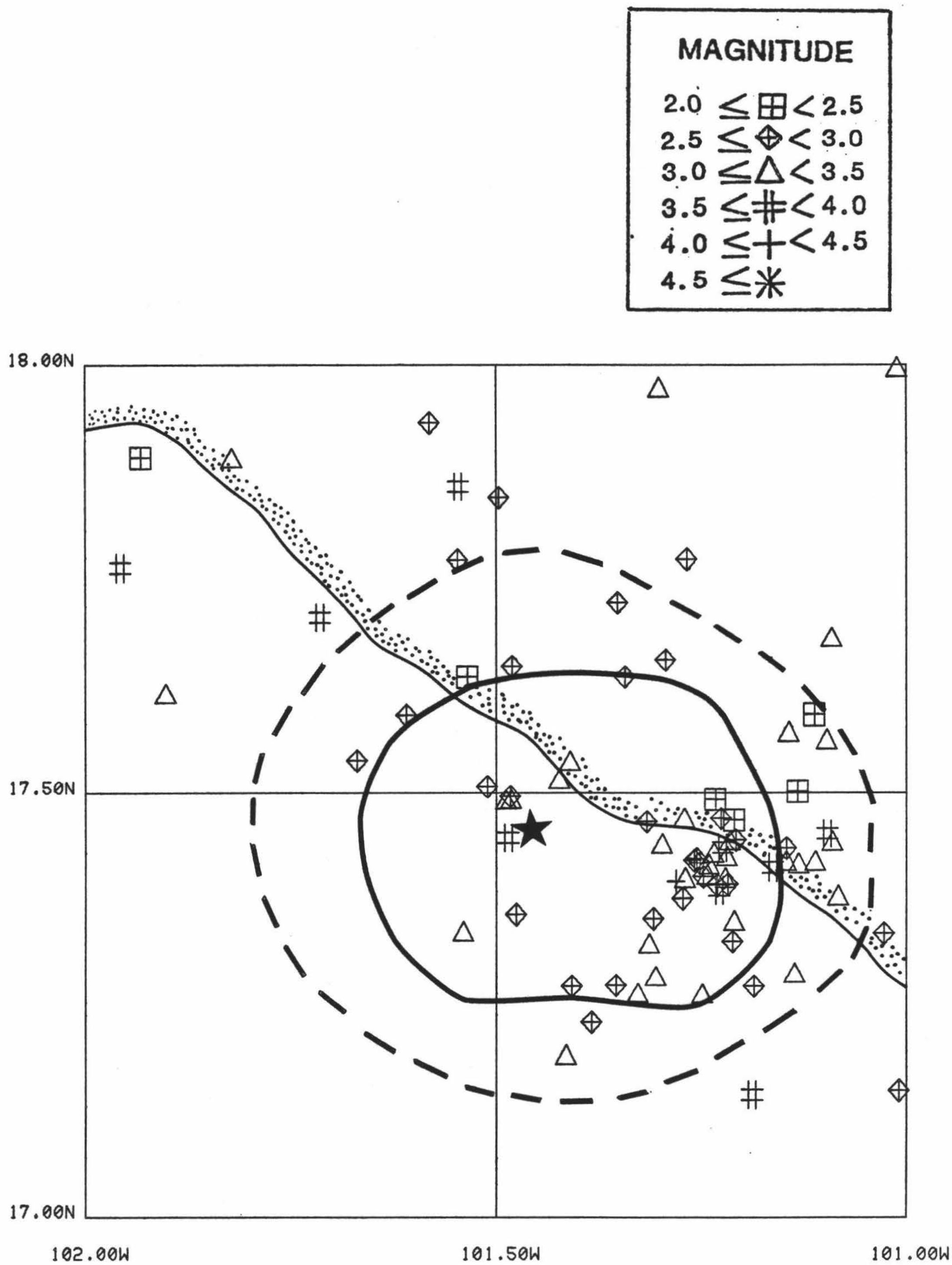
MAGNITUDE
2.0 ≤ ⊞ < 2.5
2.5 ≤ ◈ < 3.0
3.0 ≤ △ < 3.5
3.5 ≤ # < 4.0
4.0 ≤ + < 4.5
4.5 ≤ ✳
18.00N
17.50N
17.00N
102.00W
101.50W
101.00W

Figure 4.22 3-D plot for number of foreshocks (upper figure), and energy release (lower figure) in 0.1° by 0.1° squares. Data comes from foreshocks of figure 4.18.

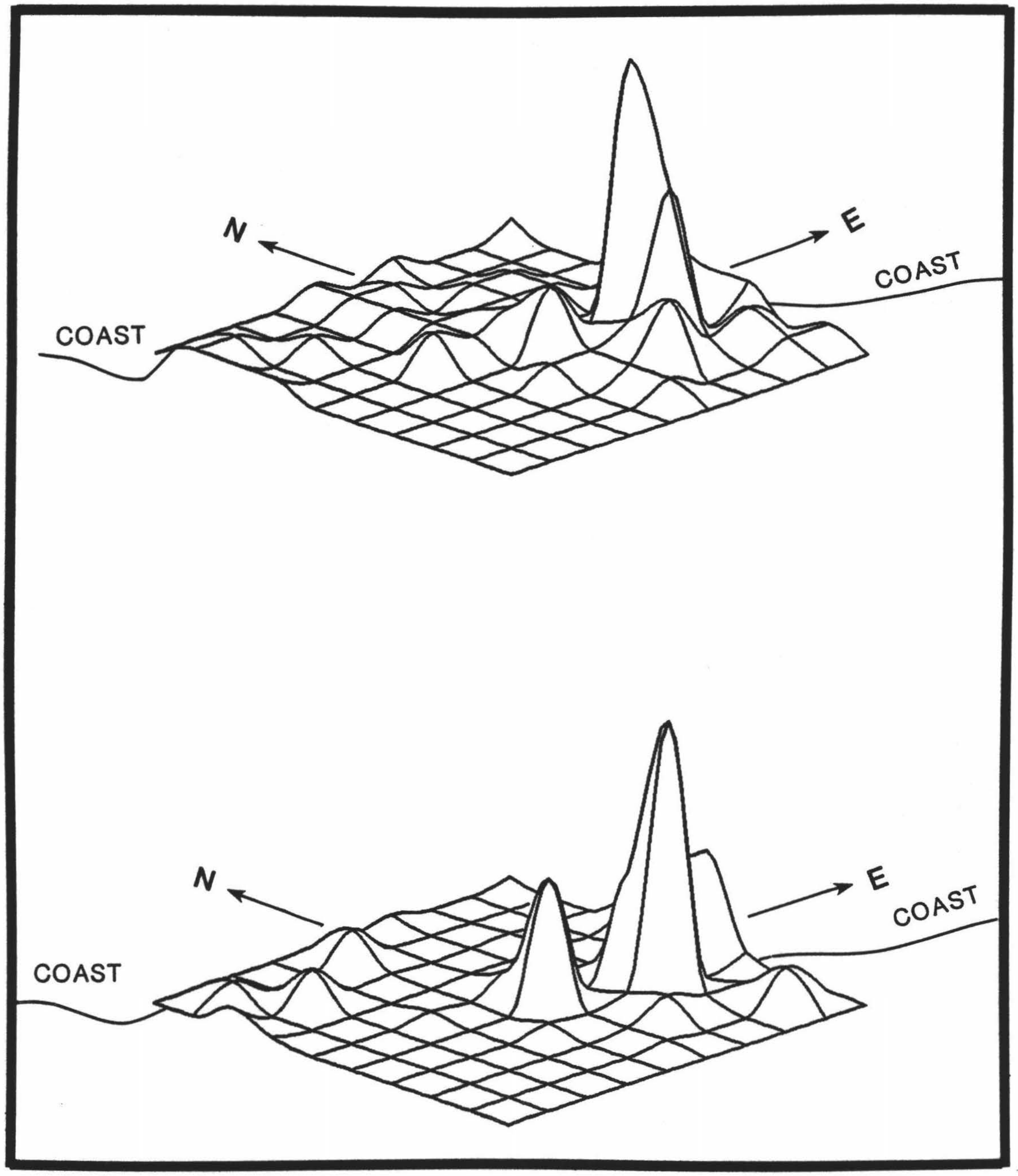
N
E
COAST
COAST
N
E
COAST
COAST

asperity with higher concentration of events and energy release was the one situated to the east (Figure 4.22), but with the aftershock data it was the asperity located to the west that had the most events (Figure 4.10) and energy release (Figure 4.11). This result can be interpreted in the following way: before the main shock, the more active asperity was releasing stress by a number of small events without breaking, while the less active one was accumulating stress until it reached the breaking strength of the asperity, producing the large earthquake.

The lower portion of figure 4.22 (foreshock energy release) also indicates that the length of the zone along the coast line really defines the length of the aftershock zone. Real time analysis would have allowed to speculate on the magnitude of the following mainshock, using a suitable magnitude-length relation.

4.5 b values

The frequency-magnitude relation obeys the Gutenberg-Richter formula (Richter, 1958; Mogi, 1962; Scholz, 1968):

$$\log N = a - bM$$

where N is the cumulative number of events with magnitude $\geq$ M, and a and b are constants for a given area and time interval. The b value is related to the state of stress of the area under study. A higher b value is expected for aftershocks sequences than for foreshock sequences. This indicates a reduced state of stress and high fractured region after the main shock (Scholz, 1968; Suyehiro et al., 1964; Berg 1968).

Figure 4.23 shows the cumulative number of earthquakes versus magnitude plot for determining the b value for the entire aftershock region. Figure 4.24 and figure 4.25 show the plots from which the b values for the western and eastern asperities were obtained. The b values were determined from the slope of the line obtained by the least square method that fit the solid circles shown in each figure. The estimated errors were calculated from the standard deviation of the points to the fitting line.

It is not possible to compare the b value (1.6) obtained by Valdes et al. (1982) and those obtained here due to the discrepancy of our magnitudes (section 3.2, figure 3.10). However, we can compare the b values for foreshocks obtained by Hsu (1981) and Hsu et al. (1983) since we have used the same data set and the same formula to compute magnitudes.

For the aftershock region b=1.49, which is higher than the b=1.07 observed for the foreshock sequence. This result is consistent with the postulate of high and low state of stress before and after the main shock.

Figure 4.23 Cumulative number of earthquakes versus magnitude for the entire aftershock area (first 54 hours). The solid circles were used to calculate the b value, which is $1.49 \pm .02$.

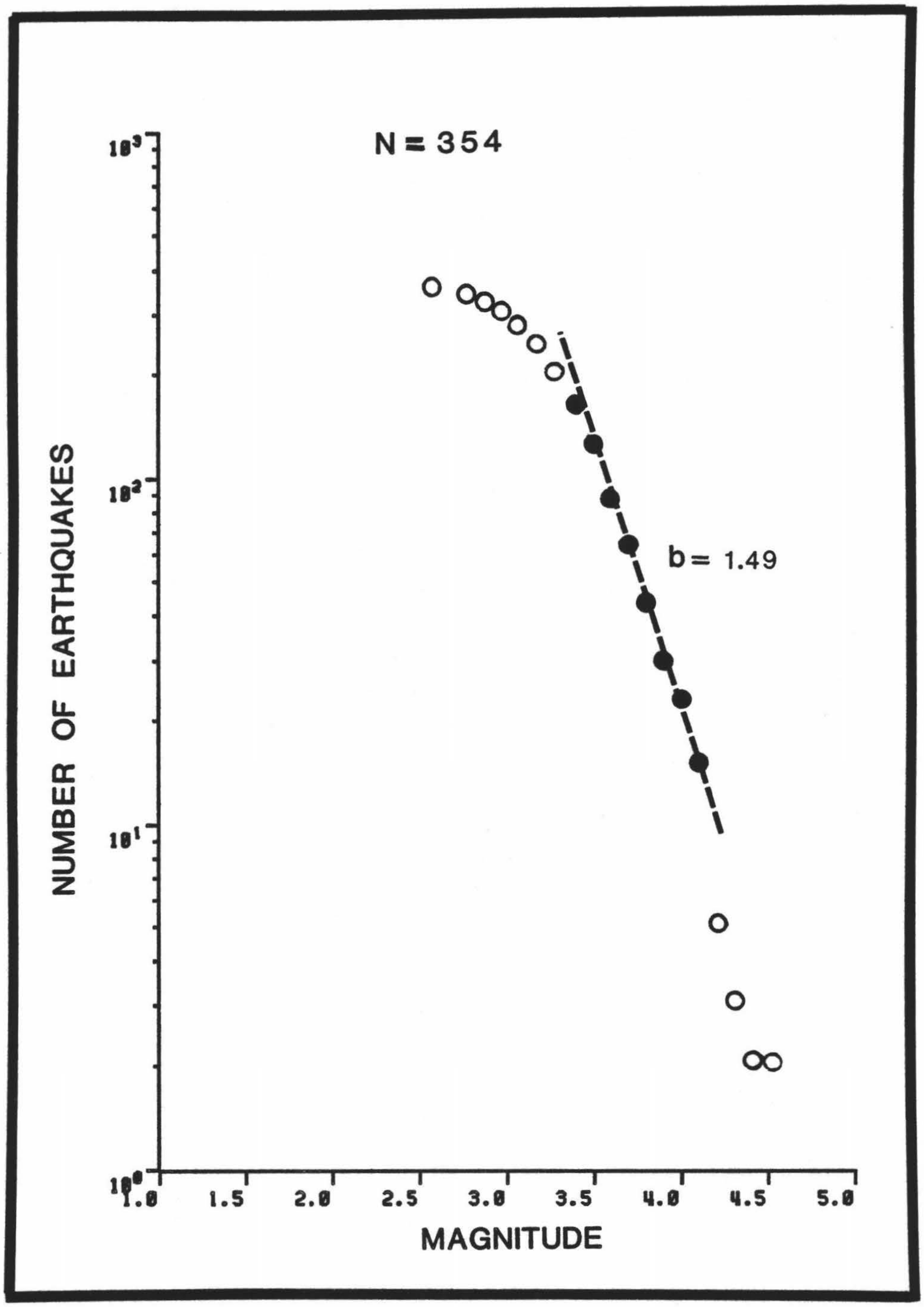
N = 354
b = 1.49
NUMBER OF EARTHQUAKES
10³
10²
10¹
10⁰
1.0
1.5
2.0
2.5
3.0
3.5
4.0
4.5
5.0
MAGNITUDE

Figure 4.24 Cumulative number of aftershocks versus magnitude for the western asperity (first 54 hours). The solid circles were used to calculate the b value, which is 1.77 ± .03.

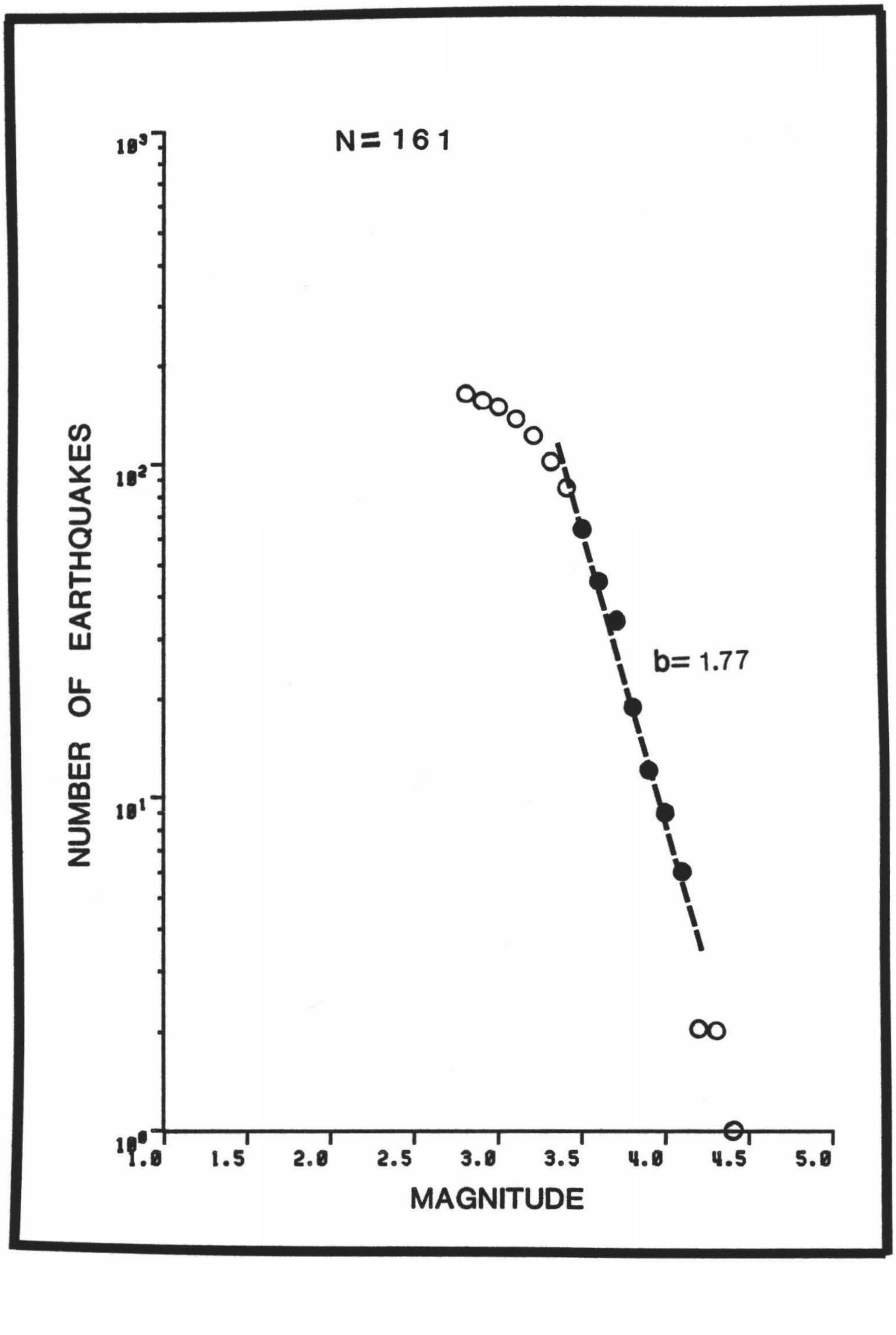

N= 161
b= 1.77
NUMBER OF EARTHQUAKES
10³
10²
10¹
10⁰
1.0
1.5
2.0
2.5
3.0
3.5
4.0
4.5
5.0
MAGNITUDE

Figure 4.25 Cumulative number of aftershocks versus magnitude for the eastern asperity (first 54 hours). The solid circles were used to calculate the b value, which is 1.48 $\pm$.03.

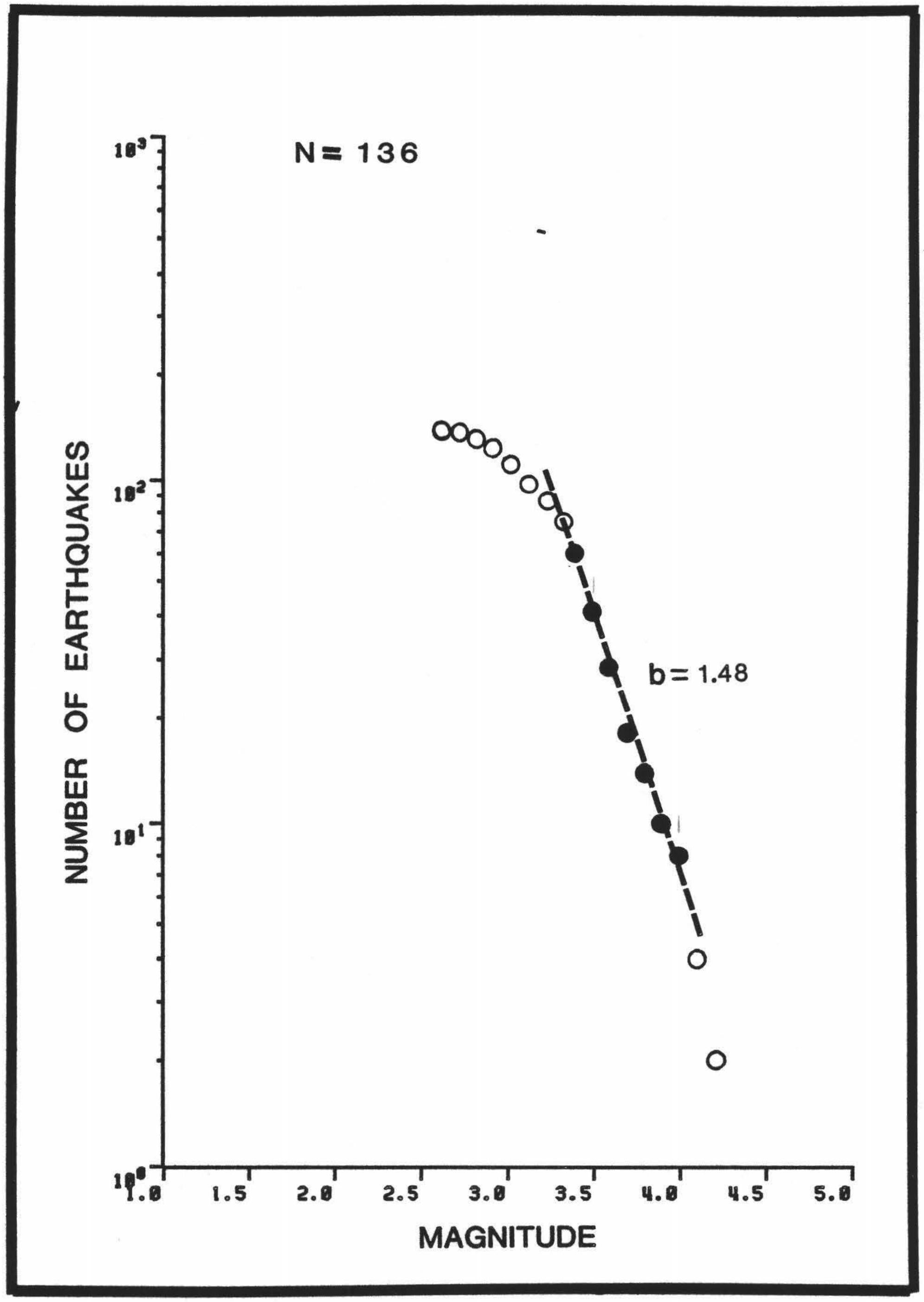

N= 136
b= 1.48
NUMBER OF EARTHQUAKES
MAGNITUDE

For the western asperity b=1.77, and for the eastern asperity b=1.48. This contrast shows that the western asperity was the most fractured region. This is compatible with the fact that the Petatlan earthquake took place at this asperity.

The b value obtained in the eastern asperity for the aftershocks is 1.48. which is higher than b=1.07 obtained for the foreshock sequence . These values are also consistent with the reduced stress after the major event.

4.6 The Rupture Model

To understand the rupture process, we have appealed to the asperity model for large earthquakes extensively discussed in the literature (Kanamori, 1981; Lay and Kanamori, 1981; Rudnicki and Kanamori,1981). The asperities are considered to be regions of the fault rupture where the stress before an earthquake is high relative to the average stress on the entire fault plane. Because these locked segments have high resistance to slip, the earthquake takes place when the local stress reaches the breaking strength of an asperity. In areas without complex tectonics, the spacing and strength of the asperities are considered such that each asperity produces a simple event, without triggering adjacents ones, but would cause an increase in stress of the adjacent asperities. Interactions between adjacent zones of large asperities can induce triggering (Lay and Kanamori, 1981) of large earthquake ruptures or multiple rupture events.

Since the Petatlan earthquake ocurred at a location where the Orozco Fracture Zone is being subducted, it is expected that a complex mechanism was involved in the rupture process. Based on all the preceeding analysis, the rupture process can be interpreted as follows: the main rupture starts near the boundary of the asperity in the west side of the aftershock area (Figure 4.26), then, the asperity ruptures triggering the second asperity.

The rupture model here obtained seems to be the same as for the Playa Azul, Michoacan, Mexico earthquake (Ms=7.3) reported by Havskov et al. (1983). The aftershock area for this earthquake is located NW of our aftershock area, and two groups, one to the east and another to the west were observed. Havskov et al., suggested that the clustering may represent either the edge of the ruptured area or two asperities.

The major tectonic feature in the combined Playa Azul and Petatlan region is the Orozco Fracture Zone (Figure 2.1). We can speculate that this fracture zone influences the subduction of the Cocos plate, separating the two asperities and presenting a zone of relative weakness in the aftershock area. From only two earthquakes showing the same pattern it cannot be generalized that this behavior is characteristic of this tectonic zone. However this observation does provide a good frame of reference to start new studies in order to understand the complex

Figure 4.26 Representation of the fault plane containing the two asperities which broke during the Petatlan earthquake.

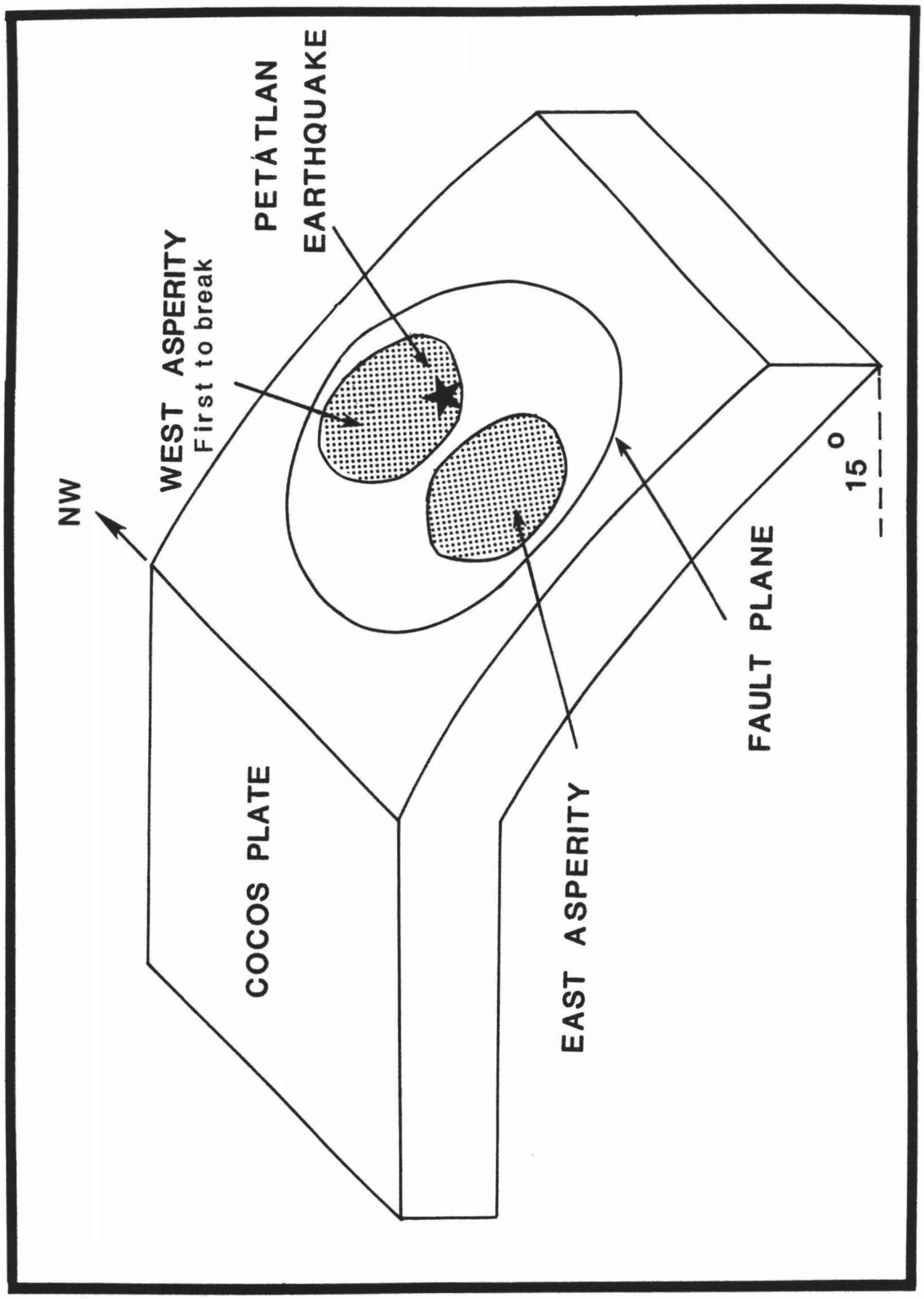
PETATLAN
EARTHQUAKE
WEST ASPERITY
First to break
NW
COCOS PLATE
EAST ASPERITY
FAULT PLANE
15 o

subduction processes in this area.

4.7 Conclusions

From the analysis of the aftershocks recorded during the first 54 hours following the Petatlan earthquake, I conclude that:

1.- The rupture area as indicated by the aftershock epicenters is well defined in the first day of the aftershock sequence.

2.- There is little expansion (about 26%) of the aftershock area between one day and thirty six days following the main shock.

3.- The rupture region contains two asperities which broke when the Petatlan earthquake took place. The first asperity broken (the western one) was the one containing the hypocenter of the main shock.

4.- After the main shock, concentration of aftershocks oscilated from one asperity to another.

5.- Since the two asperities were not located perpendicular to the direction of the subducting Cocos plate, we can consider that the Orozco Fracture Zone plays a major role in the subduction processes that take place in this zone, possibly separating the east and west asperities.

6.- A well constraint subset of hypocenters indicates a dual seismic zone (in depth) of very shallow dip.

7.- Both, the foreshock and aftershock data identify the two asperities.

8.- The high b value of 1.49 obtained for aftershocks is consistent with the low state of stress of the region after the Petatlan earthquake.

9.- It would be interesting to study our aftershock data together with the data from the University of Wisconsin-Madison. The integrated data set would be a unique collection of data from which hypocenter locations would be more accurate.

APPENDIX A

TABLE 3.4 AFTERSHOCKS OF THE PETATLAN EARTHQUAKE LOCATED DURING THE FIRST 54 HOURS

TABLE 3.4 AFTERSHOCKS OF THE PETATLAN EARTHQUAKE
LOCATED DURING THE FIRST 54 HOURS

	ORIGIN		EPICENTER		DEPTH	@	+	ERROR*		-
#	Y/M/D	H/M	LAT(N)	LON(W)	km	MAG	RMS	ERH	ERZ	N
1	790314	1130	18.1265	100.7797	2.19	3.61	0.51	0.0	0.0	4
2	790314	1201	17.3017	101.6985	12.76	4.52	0.02	0.6	0.4	5
3	790314	1206	17.8398	101.1365	11.42	3.90	0.26	3.3	3.4	6
4	790314	1214	17.7060	101.8547	1.72	3.17	0.09	1.0	5.8	5
5	790314	1215	17.5193	100.2318	3.31	3.58	0.44	0.2	0.3	5
6	790314	1220	17.7027	101.7960	9.89	3.86	1.17	0.0	0.0	4
7	790314	1223	16.7398	101.3313	45.29	4.02	1.57	0.0	0.0	4
8	790314	1224	18.1552	101.1367	1.34	3.54	1.01	0.0	0.0	4
9	790314	1226	17.8720	100.9630	33.58	3.72	0.75	0.0	0.0	4
10	790314	1237	18.2887	101.1273	7.23	3.75	0.13	5.4	4.4	5
11	790314	1241	18.0183	101.5730	65.82	2.95	0.80	0.0	0.0	4
12	790314	1243	17.4072	101.6447	13.88	3.54	0.00	0.0	0.0	4
13	790314	1246	17.9613	101.0475	6.32	4.12	0.36	2.2	4.4	7
14	790314	1247	17.2602	101.3102	12.05	4.25	0.17	5.5	3.3	5
15	790314	1250	17.6785	101.4962	15.76	4.08	0.00	0.0	0.0	4
16	790314	1253	19.0308	101.2900	2.50	3.17	0.21	0.0	0.0	4
17	790314	1258	17.3888	101.5637	25.34	3.14	0.38	6.0	4.9	7
18	790314	1300	17.5315	101.4613	11.49	3.36	0.44	7.3	1.0	6
19	790314	1301	17.7660	100.9380	29.19	3.40	0.82	0.0	0.0	4
20	790314	1303	17.3352	101.5952	17.15	3.57	0.48	9.6	1.0	6
21	790314	1305	17.6280	101.5182	20.50	4.30	0.02	1.7	0.4	5
22	790314	1312	17.5908	101.3245	10.21	3.42	0.30	3.8	3.6	7
23	790314	1314	17.5140	101.4520	12.01	3.59	0.49	5.5	4.0	9
24	790314	1318	17.4037	101.5330	12.74	3.62	0.19	4.1	3.5	5
25	790314	1319	17.1682	101.3463	31.10	3.35	0.39	2.2	3.7	6
26	790314	1320	17.4335	101.4960	15.89	3.31	0.35	3.6	4.2	7
27	790314	1325	17.4313	101.4707	6.41	3.78	0.24	2.7	1.9	6
28	790314	1326	17.7258	101.3427	25.33	3.62	0.18	0.0	0.0	4
29	790314	1335	17.4028	101.0112	77.88	3.27	0.01	0.0	0.0	4
30	790314	1335	18.3855	100.8442	6.89	3.40	0.77	0.0	0.0	4
31	790314	1338	17.6812	101.1438	6.88	3.22	0.02	2.8	0.5	5
32	790314	1343	17.5615	101.5238	15.00	3.21	0.21	7.8	4.0	6
33	790314	1344	17.3753	101.3533	16.88	3.39	0.24	1.3	4.7	5
34	790314	1348	17.2515	101.5287	13.92	4.02	0.11	4.0	2.3	5
35	790314	1350	17.5230	101.2500	16.49	3.21	0.09	2.8	3.5	5
36	790314	1352	17.4463	101.2358	10.52	3.83	0.66	0.0	0.0	6
37	790314	1355	17.4443	101.4370	15.69	3.62	0.05	0.0	0.0	4
38	790314	1358	18.1705	100.9312	1.98	3.71	0.56	0.0	0.0	4
39	790314	1404	17.7102	100.4205	80.86	3.41	0.20	5.3	5.4	5
40	790314	1405	17.3912	101.5730	12.07	3.71	0.19	0.0	0.0	4

TABLE 3.4 (Continued) AFTERSHOCKS OF THE PETATLAN EARTHQUAKE LOCATED DURING THE FIRST 54 HOURS

	ORIGIN		EPICENTER		DEPTH	@	+	ERROR*		-
#	Y/M/D	H/M	LAT(N)	LON(W)	km	MAG	RMS	ERH	ERZ	N
41	790314	1405	18.0183	101.1307	15.00	3.83	0.01	0.0	0.0	3
42	790314	1407	17.4692	101.3767	6.37	3.51	0.49	3.5	5.3	8
43	790314	1412	17.4670	101.6228	11.01	3.74	0.49	6.9	5.0	8
44	790314	1423	17.4258	101.5622	9.86	3.67	0.42	2.8	2.8	11
45	790314	1429	17.2880	101.2413	17.23	3.15	0.27	4.8	3.9	6
46	790314	1430	17.2972	101.1960	31.51	3.46	0.42	5.7	4.1	7
47	790314	1432	17.0593	101.5122	20.22	3.39	0.73	4.7	0.9	6
48	790314	1436	17.4608	101.4725	13.49	3.50	0.34	2.4	2.3	9
49	790314	1440	17.5642	101.4133	14.55	3.22	0.30	2.1	3.4	8
50	790314	1443	17.4860	101.5905	15.18	3.56	0.18	2.1	2.6	7
51	790314	1447	17.3785	101.5645	19.05	3.81	0.48	6.6	4.2	8
52	790314	1450	17.4342	101.6158	13.91	3.57	0.28	2.5	2.3	8
53	790314	1450	17.5065	101.2730	25.93	3.46	0.82	6.3	8.3	5
54	790314	1452	17.3837	101.4723	11.46	3.53	0.42	5.3	4.2	8
55	790314	1454	17.3900	101.6022	24.18	3.49	0.08	0.0	0.0	4
56	790314	1457	17.2637	101.6312	12.26	3.36	0.10	1.3	1.3	6
57	790314	1458	17.4200	101.3077	6.49	3.38	0.64	1.8	3.5	6
58	790314	1502	17.9688	101.1418	8.69	3.54	0.22	6.3	3.6	6
59	790314	1503	17.3373	100.9973	43.72	3.45	0.00	0.0	0.0	4
60	790314	1512	17.4383	101.4738	11.45	3.53	0.40	4.7	3.7	9
61	790314	1517	17.4997	101.0992	2.55	3.43	0.18	2.7	2.2	5
62	790314	1519	17.1920	101.3470	11.82	4.13	0.03	1.0	0.9	5
63	790314	1525	17.3183	101.4568	9.17	4.18	0.14	3.4	2.5	6
64	790314	1532	17.5282	101.4630	12.19	3.20	0.37	2.4	2.8	10
65	790314	1535	17.4983	101.5983	13.19	4.57	0.26	5.6	4.1	6
66	790314	1546	17.4718	101.5172	19.27	3.50	0.44	5.3	3.1	9
67	790314	1547	18.2970	101.2282	0.32	3.22	0.60	0.0	0.0	4
68	790314	1549	17.5328	101.1663	1.03	2.91	0.34	0.0	0.0	4
69	790314	1553	17.4172	101.4952	22.77	3.01	0.33	4.4	8.3	6
70	790314	1553	17.5040	101.6052	26.68	3.04	0.46	7.6	8.0	5
71	790314	1557	17.6148	101.3898	12.52	3.04	0.07	6.0	2.3	6
72	790314	1558	17.6015	100.8690	33.58	3.99	0.77	0.0	0.0	4
73	790314	1558	17.3542	101.3558	15.00	4.23	0.06	0.0	0.0	3
74	790314	1603	17.4670	101.5393	13.30	3.34	0.29	2.2	2.0	9
75	790314	1606	17.4730	101.2093	20.32	2.68	0.05	1.1	0.8	6
76	790314	1606	17.4423	101.5248	12.68	3.36	0.29	2.1	1.9	10
77	790314	1613	17.2715	101.3363	25.02	2.86	0.47	8.6	3.5	6
78	790314	1620	17.3563	101.4725	10.56	3.48	0.37	2.6	3.3	10
79	790314	1624	16.9610	101.6257	18.32	3.16	0.56	2.5	2.6	5
80	790314	1626	17.4600	101.0208	6.89	3.37	0.34	3.5	7.7	6

TABLE 3.4 (Continued) AFTERSHOCKS OF THE PETATLAN EARTHQUAKE LOCATED DURING THE FIRST 54 HOURS

#	ORIGIN Y/M/D	H/M	EPICENTER LAT(N)	LON(W)	DEPTH km	@ MAG	+ RMS	ERROR* ERH	ERZ	- N
81	790314	1628	17.3815	101.5305	12.96	3.70	0.00	0.0	0.0	4
82	790314	1630	17.4342	101.4955	10.51	3.22	0.39	2.7	2.8	10
83	790314	1632	17.7555	100.8292	37.97	2.91	0.60	0.0	0.0	4
84	790314	1633	17.3093	101.3233	12.80	3.29	0.04	0.5	4.9	6
85	790314	1634	17.4123	101.2062	15.00	3.24	0.04	0.0	0.0	4
86	790314	1636	18.0872	101.2120	4.90	2.92	0.11	7.7	6.5	5
87	790314	1637	17.3828	101.5555	12.10	3.19	0.18	1.4	1.4	9
88	790314	1640	17.3332	101.3815	0.95	3.04	0.48	3.3	2.8	10
89	790314	1641	17.4958	101.4648	12.97	3.30	0.33	2.2	2.1	10
90	790314	1644	17.2570	101.2862	18.00	3.43	0.40	2.9	7.8	5
91	790314	1646	18.4470	101.3917	0.84	3.47	1.20	0.0	0.0	4
92	790314	1656	17.5993	101.2507	7.03	2.86	0.31	1.3	2.4	6
93	790314	1657	17.3727	101.5200	10.18	3.15	0.37	2.5	2.5	10
94	790314	1658	17.4535	100.9815	77.37	3.18	0.06	1.2	1.5	6
95	790314	1701	17.4280	101.1822	11.00	3.00	0.23	2.9	2.7	6
96	790314	1705	17.4255	101.1565	18.89	2.97	0.12	1.3	2.2	8
97	790314	1707	17.3687	101.5045	8.25	3.85	0.43	6.5	4.5	7
98	790314	1716	17.3907	101.5507	2.36	3.80	0.27	4.4	4.0	6
99	790314	1718	17.3983	101.5368	12.09	3.29	0.40	3.0	2.4	10
100	790314	1720	17.5712	101.5562	15.05	2.86	0.49	8.5	5.7	7
101	790314	1720	17.4142	101.6553	13.34	3.41	0.35	4.4	2.7	8
102	790314	1724	17.4408	101.2698	19.24	3.34	0.54	5.1	5.6	8
103	790314	1725	17.6110	101.1955	35.13	2.82	0.19	0.0	0.0	4
104	790314	1729	17.7308	101.5247	22.19	3.52	0.45	4.2	4.6	8
105	790314	1732	17.3918	101.5313	3.58	3.43	0.31	0.0	0.0	5
106	790314	1738	17.4765	101.5337	10.38	3.16	0.39	2.6	2.7	10
107	790314	1739	17.4570	101.5985	8.24	3.45	0.27	2.6	3.2	8
108	790314	1746	17.7637	100.8292	15.00	3.00	3.43	2.0	1.8	5
109	790314	1747	17.4992	101.4833	25.56	3.10	0.13	0.2	0.4	5
110	790314	1747	17.3912	101.2098	8.74	3.74	0.34	5.6	3.5	7
111	790314	1751	17.7733	101.4660	14.45	3.11	0.32	2.4	3.4	7
112	790314	1754	17.2687	101.5503	19.30	3.60	0.47	5.5	5.4	9
113	790314	1809	17.6058	101.5395	16.24	3.24	0.27	3.2	2.1	9
114	790314	1812	17.2780	101.3013	12.79	4.01	0.48	6.8	3.1	9
115	790314	1815	17.4192	101.4062	7.27	3.87	0.31	3.3	1.7	9
116	790314	1818	18.1208	101.2650	18.70	3.08	0.15	3.1	2.5	6
117	790314	1827	17.2838	101.3220	2.01	3.67	0.36	5.9	3.9	8
118	790314	1837	17.3873	101.5603	16.11	3.60	0.27	2.2	1.6	9
119	790314	1842	18.0753	100.8783	10.82	3.04	0.52	0.0	0.0	4
120	790314	1844	17.7180	101.4988	22.80	3.25	0.23	7.9	1.8	8

TABLE 3.4 (Continued) AFTERSHOCKS OF THE PETATLAN EARTHQUAKE LOCATED DURING THE FIRST 54 HOURS

	ORIGIN		EPICENTER		DEPTH	@	+	ERROR*		-
#	Y/M/D	H/M	LAT(N)	LON(W)	km	MAG	RMS	ERH	ERZ	N
121	790314	1853	17.4902	101.2527	18.46	3.48	0.44	2.9	3.3	9
122	790314	1856	17.4738	101.3785	5.12	3.91	0.35	4.4	4.5	8
123	790314	1903	17.4243	101.4893	25.90	2.87	0.05	1.7	2.6	5
124	790314	1904	17.7587	100.2913	71.63	3.36	0.47	7.1	8.9	6
125	790314	1905	17.4788	101.5382	12.23	3.31	0.26	3.0	7.8	6
126	790314	1908	17.6855	101.6253	18.86	2.77	0.46	9.9	6.5	6
127	790314	1909	17.2628	101.4683	21.42	2.85	0.40	0.1	5.1	6
128	790314	1910	17.3512	101.2743	24.20	3.24	0.32	3.3	7.3	8
129	790314	1917	17.4242	101.4890	11.22	3.24	0.40	2.8	3.6	9
130	790314	1922	17.5613	101.4013	13.89	3.05	0.41	2.6	2.5	10
131	790314	1936	17.3445	101.5963	10.72	3.67	0.29	3.7	2.9	8
132	790314	1937	17.4113	101.5413	7.68	3.17	0.22	3.1	2.7	7
133	790314	1939	17.2598	101.4568	4.58	3.25	0.34	2.3	3.0	10
134	790314	1942	17.6280	101.2240	1.61	2.87	0.09	5.7	4.4	5
135	790314	1951	17.5158	101.3552	7.34	3.38	0.40	3.2	1.9	7
136	790314	1952	17.5783	101.2335	16.23	2.88	0.21	3.5	3.8	6
137	790314	1956	17.3727	101.3813	18.14	2.79	0.16	2.0	3.6	6
138	790314	1958	17.4228	101.2983	20.47	2.78	0.19	2.9	2.8	5
139	790314	2004	17.2832	101.2053	4.42	3.67	0.31	7.9	4.7	6
140	790314	2006	17.5878	101.6335	26.07	4.13	0.55	7.8	3.9	5
141	790314	2013	17.2725	101.2908	21.93	3.67	0.48	7.1	4.0	9
142	790314	2014	17.4700	101.5307	10.31	3.15	0.40	4.6	8.8	8
143	790314	2017	17.1465	101.6337	17.77	3.55	0.55	1.0	5.9	5
144	790314	2022	17.3965	101.0472	21.04	3.24	0.26	3.0	3.8	8
145	790314	2031	17.4195	101.2708	27.43	3.16	0.47	1.0	2.1	7
146	790314	2032	17.3780	101.5488	9.39	3.53	0.32	4.1	2.5	8
147	790314	2034	17.3480	101.2163	13.89	4.02	0.23	3.8	2.2	7
148	790314	2037	17.4822	101.3858	78.20	3.27	0.21	0.5	1.0	5
149	790314	2043	17.4090	101.4868	13.04	3.28	0.20	1.5	1.2	10
150	790314	2051	17.5725	101.5142	18.06	3.45	0.29	4.2	4.4	7
151	790314	2055	17.3953	101.5908	26.55	3.60	0.50	7.7	4.9	8
152	790314	2056	17.3737	101.1693	20.77	2.98	0.11	2.2	1.4	6
153	790314	2101	17.4765	101.2585	23.76	3.66	0.39	4.7	5.8	8
154	790314	2107	17.3535	101.2395	6.24	3.27	0.29	1.9	1.9	10
155	790314	2108	17.4452	101.2998	28.69	2.84	0.43	6.7	5.4	6
156	790314	2113	17.4748	101.2788	16.51	2.77	0.21	8.0	5.8	5
157	790314	2121	17.4830	101.5768	13.07	2.95	0.30	7.7	6.0	6
158	790314	2124	17.4983	101.5160	18.82	4.07	0.44	7.8	5.4	6
159	790314	2130	17.4480	101.5208	9.35	3.47	0.35	2.2	2.0	11
160	790314	2134	17.3037	101.2932	14.55	4.17	0.23	5.7	3.7	6

TABLE 3.4 (Continued) AFTERSHOCKS OF THE PETATLAN EARTHQUAKE LOCATED DURING THE FIRST 54 HOURS

	ORIGIN		EPICENTER		DEPTH	@	+	ERROR*		-
#	Y/M/D	H/M	LAT(N)	LON(W)	km	MAG	RMS	ERH	ERZ	N
161	790314	2137	17.3295	101.2083	5.62	3.42	0.31	4.1	3.2	7
162	790314	2140	17.8667	101.8413	27.24	3.96	0.58	1.7	5.5	6
163	790314	2159	17.3493	101.5137	18.39	3.33	0.23	2.9	3.9	7
164	790314	2159	17.4050	101.2418	7.89	3.56	0.37	2.9	2.6	8
165	790314	2203	17.2378	101.2717	17.45	2.91	0.05	0.8	0.7	6
166	790314	2204	17.1725	101.3452	30.56	2.85	0.39	2.1	3.6	6
167	790314	2205	17.3398	101.4495	12.79	4.16	0.20	5.2	3.5	5
168	790314	2209	17.4922	101.2053	16.65	3.50	0.54	3.8	5.4	8
169	790314	2213	17.3172	101.2823	4.95	3.72	0.51	6.3	4.3	9
170	790314	2215	17.3880	101.5340	10.78	3.89	0.43	6.2	5.3	7
171	790314	2220	17.2927	101.5417	1.71	3.83	0.46	5.8	3.5	8
172	790314	2223	17.3847	101.5995	8.90	3.73	0.34	3.8	2.4	9
173	790314	2234	17.2725	101.4182	1.12	3.71	0.49	5.0	2.7	10
174	790314	2236	17.3342	101.5543	7.08	3.50	0.49	3.4	3.3	10
175	790314	2239	17.5412	101.4562	13.64	3.09	0.35	3.3	4.5	7
176	790314	2242	17.3588	101.2840	13.77	3.47	0.23	2.9	4.0	7
177	790314	2246	17.7118	101.5575	16.12	3.03	0.03	0.5	0.3	6
178	790314	2248	17.2252	101.2137	25.43	3.29	0.32	3.4	0.1	5
179	790314	2305	17.4302	101.1342	8.57	2.96	0.08	1.2	5.4	6
180	790314	2307	17.4083	101.3465	7.67	3.88	0.42	4.5	3.1	8
181	790314	2309	17.4752	101.5297	13.14	3.52	0.40	2.9	3.0	10
182	790314	2319	17.3882	101.3793	2.03	3.55	0.45	6.6	2.5	9
183	790314	2321	17.3360	101.2867	6.09	3.70	0.36	6.2	2.0	8
184	790314	2323	17.4468	101.1967	20.49	3.04	0.36	7.1	5.1	6
185	790314	2339	17.3455	101.2055	5.47	3.63	0.38	3.8	2.3	10
186	790314	2346	17.5098	101.5508	11.75	3.06	0.16	2.4	1.8	8
187	790314	2351	17.3417	101.2122	48.49	2.98	0.11	2.1	3.7	6
188	790314	2353	17.4598	101.6512	11.41	3.26	0.27	3.5	3.3	8
189	790314	2355	17.5187	101.0683	19.71	3.36	0.33	2.1	2.2	9
190	790315	3	17.2762	101.4648	16.40	4.11	0.48	8.9	4.4	8
191	790315	13	17.2443	101.4917	19.48	3.25	0.54	0.0	0.0	4
192	790315	13	17.3905	101.5585	9.74	3.75	0.07	1.5	1.0	6
193	790315	17	17.4750	101.5538	11.73	3.17	0.18	2.6	2.5	7
194	790315	20	17.3335	101.5742	20.13	3.46	0.46	6.3	3.4	8
195	790315	21	17.5593	101.4352	13.26	3.10	0.24	6.0	2.6	7
196	790315	25	17.4798	101.5780	12.24	3.07	0.40	2.7	2.9	11
197	790315	28	17.4012	101.1515	16.15	3.13	0.18	2.1	3.6	8
198	790315	35	17.3843	101.3400	7.05	3.54	0.42	5.3	2.8	8
199	790315	41	17.2593	101.3355	14.34	3.12	0.18	7.8	1.2	6
200	790315	55	17.2913	101.3733	2.53	3.33	0.25	2.5	2.2	9

TABLE 3.4 (Continued) AFTERSHOCKS LOCATED DURING THE FIRST 54 HOURS FOLLOWING THE PETATLAN EARTHQUAKE

	ORIGIN		EPICENTER		DEPTH	@	+	ERROR*		-
#	Y/M/D	H/M	LAT(N)	LON(W)	km	MAG	RMS	ERH	ERZ	N
201	790315	57	17.3247	101.4868	7.54	3.42	0.39	6.4	3.6	7
202	790315	58	17.3865	101.3260	19.42	3.07	0.34	9.0	1.2	5
203	790315	59	18.3068	100.6467	28.35	3.04	0.34	0.0	0.0	4
204	790315	108	17.8187	101.3713	1.45	2.87	0.47	2.3	1.2	6
205	790315	111	17.4195	101.1032	12.99	3.23	0.31	2.6	3.2	9
206	790315	114	17.2277	101.8143	25.79	3.54	0.29	5.8	4.7	5
207	790315	114	17.4747	101.6495	19.82	3.73	0.15	0.0	0.0	4
208	790315	116	17.6720	101.3738	0.64	3.01	0.59	4.7	4.2	6
209	790315	117	17.5920	101.3602	22.95	3.02	0.37	2.7	5.3	8
210	790315	123	17.5422	101.2483	18.09	2.70	0.30	9.0	4.6	6
211	790315	123	17.4277	101.6335	4.49	3.57	0.29	3.0	3.5	8
212	790315	127	17.5910	101.3002	14.79	3.54	0.42	9.2	2.1	8
213	790315	140	17.4425	101.5150	8.64	3.22	0.48	3.1	2.8	11
214	790315	143	17.2557	101.2980	1.13	3.79	0.59	5.7	3.2	11
215	790315	158	17.3655	101.1732	9.51	3.33	0.38	3.0	3.3	7
216	790315	159	17.3865	101.7412	19.20	3.67	0.46	5.7	4.0	8
217	790315	201	17.4557	101.6243	15.99	3.80	0.37	4.9	3.1	8
218	790315	244	17.4643	101.2458	24.02	3.09	0.22	3.8	0.7	6
219	790315	256	17.4513	101.5445	12.17	3.48	0.32	2.9	3.4	8
220	790315	300	17.5690	101.2728	1.16	3.02	0.23	2.4	2.1	8
221	790315	302	17.1245	101.1975	4.05	3.22	0.07	6.6	1.7	5
222	790315	303	17.3810	101.2033	12.84	3.41	0.36	3.7	6.0	8
223	790315	306	17.3487	101.5492	8.93	3.50	0.37	2.4	2.0	10
224	790315	308	17.5320	101.4347	13.29	3.46	0.17	1.0	3.6	5
225	790315	312	17.3172	101.7817	8.88	3.85	0.55	3.7	2.4	8
226	790315	332	17.4163	101.1413	19.48	2.96	0.08	2.3	3.3	6
227	790315	340	17.4675	101.3490	17.18	3.06	0.25	1.9	2.1	8
228	790315	342	17.4133	101.7067	16.30	3.01	0.30	4.4	3.5	6
229	790315	343	17.3968	101.1670	19.97	2.80	0.15	4.0	5.8	6
230	790315	349	17.5833	101.1103	6.58	2.76	0.40	5.9	7.6	6
231	790315	417	17.2735	101.4187	1.07	3.23	0.52	4.3	4.0	8
232	790315	423	17.3077	101.4832	59.45	2.88	0.28	4.8	0.5	6
233	790315	440	17.4668	101.2668	12.94	3.31	0.49	3.5	4.8	9
234	790315	509	17.1543	101.4857	14.04	4.13	0.11	5.2	2.5	5
235	790315	514	17.3412	101.4648	2.71	3.81	0.53	5.8	4.2	9
236	790315	523	17.3313	101.5383	21.72	2.94	0.35	1.2	2.2	6
237	790315	537	17.4658	101.2642	11.21	3.48	0.42	2.3	2.3	11
238	790315	539	17.3668	101.3912	24.53	3.15	0.36	2.5	1.7	6
239	790315	543	17.4080	101.2737	5.98	3.57	0.57	4.0	6.2	9
240	790315	546	17.2862	101.4630	62.33	3.22	0.16	2.7	5.3	6

TABLE 3.4 (Continued) AFTERSHOCKS OF THE PETATLAN EARTHQUAKE LOCATED DURING THE FIRST 54 HOURS

#	ORIGIN Y/M/D	H/M	EPICENTER LAT(N)	LON(W)	DEPTH km	@ MAG	+ RMS	ERROR* ERH	ERZ	- N
241	790315	601	17.6575	101.5453	28.98	3.08	0.49	0.0	0.0	4
242	790315	615	17.5063	101.2357	7.51	3.56	0.39	4.9	5.7	7
243	790315	618	17.4713	101.7673	20.73	3.33	0.50	0.0	0.0	4
244	790315	629	17.5067	101.4463	11.06	2.90	0.19	5.6	3.9	6
245	790315	638	17.3250	101.0880	22.04	2.96	0.10	3.5	2.1	5
246	790315	639	17.2253	101.2268	19.67	3.81	0.47	3.7	3.1	11
247	790315	651	17.5407	101.2463	1.05	2.92	0.21	0.1	5.4	5
248	790315	701	17.4265	101.4805	7.39	3.47	0.43	7.2	4.3	8
249	790315	711	17.4118	101.1748	16.61	2.98	0.05	0.9	0.8	6
250	790315	723	17.5142	101.5053	11.21	3.24	0.14	7.8	7.4	6
251	790315	730	17.4067	101.1950	9.01	3.41	0.58	3.4	3.7	10
252	790315	741	17.3605	101.4838	18.23	3.23	0.36	3.7	4.9	8
253	790315	749	17.4250	101.3753	5.39	3.44	0.31	2.0	2.0	10
254	790315	801	17.4077	101.5015	9.03	3.80	0.18	2.0	1.1	8
255	790315	810	16.8927	100.6212	26.87	3.79	0.15	3.2	3.1	6
256	790315	827	17.4235	101.1183	18.44	2.95	0.32	3.0	4.3	8
257	790315	844	17.4827	101.5635	12.33	2.92	0.12	5.8	2.4	6
258	790315	845	17.4938	101.4432	17.24	3.31	0.53	4.3	2.9	9
259	790315	847	17.3617	101.5625	24.23	3.35	0.45	3.7	3.5	8
260	790315	848	17.4587	101.5455	12.30	3.54	0.30	2.2	2.5	10
261	790315	852	17.3708	101.5770	27.09	3.72	0.46	8.7	5.8	7
262	790315	914	17.4640	101.2687	7.03	3.32	0.39	2.7	2.2	9
263	790315	920	17.4468	101.2058	11.33	3.35	0.35	2.1	2.3	9
264	790315	929	17.3243	101.3995	22.15	3.41	0.29	0.9	4.2	6
265	790315	948	17.0712	101.1948	7.47	3.08	0.11	3.0	1.3	6
266	790315	952	17.2845	101.4167	2.98	3.30	0.33	2.3	2.0	9
267	790315	1000	17.3345	101.5120	64.39	3.11	0.14	2.3	4.8	6
268	790315	1018	17.4385	101.4723	12.70	3.69	0.29	2.1	1.9	9
269	790315	1024	17.2982	101.5027	23.43	3.59	0.38	5.0	6.7	8
270	790315	1037	17.3323	101.5243	24.82	3.68	0.43	4.0	4.2	10
271	790315	1103	17.3570	101.4837	25.63	3.64	0.38	3.4	3.8	8
272	790315	1108	17.5312	101.7580	15.00	3.72	0.63	7.7	4.3	5
273	790315	1113	17.2895	101.6618	18.69	3.66	0.54	7.4	5.1	8
274	790315	1120	17.3855	101.5258	12.10	3.58	0.30	2.6	2.5	8
275	790315	1138	17.5235	101.3443	0.78	2.82	0.04	2.0	7.3	5
276	790315	1156	16.9502	101.6050	43.87	3.46	0.39	0.0	0.0	4
277	790315	1200	17.4730	101.2428	7.02	3.29	0.53	3.2	3.4	10
278	790315	1203	18.0983	101.1622	8.26	3.27	0.30	6.0	4.4	6
279	790315	1212	17.3803	101.5725	11.78	3.71	0.29	2.5	3.0	8
280	790315	1219	17.5980	101.3795	23.77	3.29	0.49	3.2	6.3	10

TABLE 3.4 (Continued) AFTERSHOCKS OF THE PETATLAN EARTHQUAKE LOCATED DURING THE FIRST 54 HOURS

	ORIGIN		EPICENTER		DEPTH	@	+	ERROR*		-
#	Y/M/D	H/M	LAT(N)	LON(W)	km	MAG	RMS	ERH	ERZ	N
281	790315	1220	17.3607	101.4605	4.16	3.76	0.60	7.9	6.5	8
282	790315	1228	18.1458	100.5110	32.09	3.54	0.07	0.0	0.0	4
283	790315	1235	17.3293	101.4807	18.11	2.85	0.19	7.0	3.7	6
284	790315	1312	17.4167	101.4778	12.34	3.25	0.38	3.4	3.5	8
285	790315	1325	18.2610	101.1975	14.02	3.34	0.13	2.3	1.9	6
286	790315	1327	17.0785	101.6292	33.45	2.96	0.14	0.0	0.0	4
287	790315	1330	17.4058	101.5127	24.99	3.54	0.40	4.2	5.0	8
288	790315	1343	17.3260	101.4850	0.98	3.30	0.47	7.1	7.1	5
289	790315	1400	17.4147	101.5203	11.56	4.07	0.15	6.5	8.3	5
290	790315	1421	17.5070	101.3788	15.82	2.94	0.10	0.8	0.7	5
291	790315	1429	17.5125	101.2792	3.22	3.44	0.44	5.3	3.9	8
292	790315	1449	17.3392	101.6370	17.69	3.67	0.41	3.4	3.7	9
293	790315	1451	17.4270	101.5193	7.35	3.23	0.46	3.0	2.7	10
294	790315	1512	17.2785	101.2797	7.01	3.67	0.49	3.2	2.5	11
295	790315	1522	17.3272	101.6090	11.54	3.48	0.37	3.1	3.3	9
296	790315	1526	17.2838	101.4653	18.52	2.97	0.28	8.3	4.5	6
297	790315	1528	17.3977	101.5438	5.39	3.47	0.49	3.0	3.4	12
298	790315	1537	17.4520	101.4628	13.15	3.29	0.35	2.4	2.2	10
299	790315	1556	17.5455	101.4142	21.07	3.11	0.21	1.5	3.4	6
300	790315	1558	17.4397	101.3285	20.14	3.35	0.35	8.1	2.6	8
301	790315	1600	17.3480	101.3675	3.62	3.44	0.46	2.8	2.5	12
302	790315	1626	17.4003	101.5230	12.74	3.10	0.25	3.9	2.0	8
303	790315	1646	17.3993	101.5443	16.73	3.44	0.48	4.1	3.5	8
304	790315	1647	17.4120	101.5320	32.05	2.82	0.45	9.8	0.3	6
305	790315	1723	17.3512	101.2212	11.42	4.01	0.22	4.0	3.3	6
306	790315	1745	17.3907	101.6262	18.73	3.76	0.50	4.1	3.5	9
307	790315	1746	17.5043	101.5112	6.28	3.07	0.37	3.9	7.8	6
308	790315	1750	17.5188	101.3117	17.27	3.68	0.40	3.1	2.9	9
309	790315	1807	17.3827	101.2292	10.84	3.61	0.48	5.1	2.9	10
310	790315	1811	17.4678	101.2447	18.23	3.44	0.43	3.3	3.8	8
311	790315	1815	17.4305	101.2452	18.73	3.18	0.13	1.1	1.4	8
312	790315	1816	17.4450	101.5867	10.49	3.36	0.40	6.1	4.2	7
313	790315	1820	17.3553	101.2038	7.99	3.09	0.14	7.2	5.6	6
314	790315	1822	17.4087	101.1538	11.18	3.00	0.09	1.3	0.9	7
315	790315	1920	17.5185	101.4370	10.93	3.46	0.40	2.5	2.8	10
316	790315	1937	17.4793	101.3625	9.79	3.23	0.49	3.0	2.8	10
317	790315	1939	17.4318	101.5037	12.69	3.08	0.42	3.0	2.8	10
318	790315	1940	17.4933	101.5343	18.36	3.38	0.49	4.2	4.6	8
319	790315	1942	17.3223	101.4373	12.92	3.49	0.39	3.7	3.7	8
320	790315	1945	17.1285	99.7347	36.61	3.22	0.42	3.0	4.8	6

TABLE 3.4 (Continued) AFTERSHOCKS OF THE PETATLAN EARTHQUAKE LOCATED DURING THE FIRST 54 HOURS

#	ORIGIN Y/M/D	H/M	EPICENTER LAT(N)	LON(W)	DEPTH km	@ MAG	+ RMS	ERROR* ERH	ERZ	- N
321	790315	1951	17.3795	101.4270	12.00	3.17	0.14	5.8	5.4	6
322	790315	1952	17.6077	101.4550	23.62	3.03	0.47	3.4	5.6	9
323	790315	2043	17.5578	101.2223	2.18	3.25	0.34	9.1	5.5	6
324	790315	2049	17.3830	101.5353	20.80	3.41	0.35	3.8	2.3	8
325	790315	2056	17.4798	101.4218	20.33	3.22	0.58	0.7	3.8	8
326	790315	2058	17.5502	101.4627	12.47	3.12	0.20	4.2	1.7	8
327	790315	2144	17.4550	101.1933	17.72	3.15	0.13	2.3	2.1	6
328	790315	2154	17.4072	101.5667	12.05	3.75	0.25	2.0	1.9	9
329	790315	2203	17.4660	101.5045	14.46	3.38	0.42	3.1	2.2	10
330	790315	2206	17.4493	101.2238	19.72	2.95	0.33	0.2	1.3	6
331	790315	2237	17.2587	101.4833	56.52	3.37	0.27	3.9	9.2	7
332	790315	2301	18.0017	101.0398	0.02	2.92	0.41	7.2	4.6	6
333	790315	2309	17.2835	101.4178	22.82	3.71	0.31	5.0	5.8	9
334	790315	2338	17.4465	101.2700	6.11	3.40	0.49	2.8	2.5	11
335	790315	2349	17.3755	101.1352	14.53	3.35	0.34	2.2	2.0	10
336	790316	5	17.4710	101.0620	11.45	3.22	0.42	2.6	2.7	9
337	790316	8	17.0952	101.1638	6.39	2.94	0.19	5.0	2.3	6
338	790316	53	17.4237	101.3372	5.43	3.54	0.45	7.1	3.1	9
339	790316	102	17.4893	101.3908	22.93	2.91	0.25	3.0	3.8	8
340	790316	128	17.3605	100.9707	14.43	3.31	0.21	1.4	1.1	9
341	790316	138	17.2475	101.2667	19.35	3.35	0.22	2.9	3.3	6
342	790316	205	17.3928	101.1033	20.28	3.73	0.49	6.9	3.8	9
343	790316	224	17.1420	101.4172	4.69	3.28	0.35	3.9	4.0	9
344	790316	248	17.3043	101.5692	10.35	3.66	0.37	3.1	3.3	9
345	790316	254	17.4848	101.2950	9.69	3.47	0.19	1.4	1.6	8
346	790316	306	17.3033	101.5823	12.50	3.93	0.25	2.4	2.5	8
347	790316	334	17.4510	101.2548	20.48	3.04	0.26	8.0	2.2	6
348	790316	335	17.3003	101.2987	8.97	3.59	0.50	3.4	3.7	10
349	790316	338	17.5293	101.4927	22.64	3.95	0.50	4.3	3.7	8
350	790316	402	17.7312	101.4078	26.93	3.14	0.40	9.3	4.9	5
351	790316	404	17.4212	101.2297	15.68	3.48	0.40	2.6	2.1	10
352	790316	411	17.5073	101.5613	43.52	3.20	0.56	4.6	8.4	5
353	790316	453	17.4208	101.3647	20.62	3.06	0.17	7.2	2.3	6
354	790316	508	17.3195	101.3873	4.28	3.13	0.39	5.8	3.8	8
355	790316	524	17.3697	101.2493	26.01	3.04	0.46	5.6	0.8	8
356	790316	540	17.4735	101.1622	10.40	3.26	0.42	2.4	2.6	10
357	790316	601	17.7198	101.3843	11.06	3.12	0.45	9.7	4.5	6
358	790316	604	17.4867	101.4735	11.15	4.19	0.34	4.8	8.0	7
359	790316	614	17.2770	101.3252	15.68	3.06	0.53	8.0	9.2	6
360	790316	618	17.1743	101.3972	13.18	2.97	0.42	1.7	3.1	6

TABLE 3.4 (Continued) AFTERSHOCKS OF THE PETATLAN EARTHQUAKE LOCATED DURING THE FIRST 54 HOURS

#	ORIGIN Y/M/D	H/M	EPICENTER LAT(N)	LON(W)	DEPTH km	@ MAG	+ RMS	ERROR* ERH	ERZ	- N
361	790316	621	17.6545	101.6307	18.59	2.96	0.13	4.2	2.4	6
362	790316	636	17.4502	101.4817	12.77	3.15	0.25	2.3	2.6	8
363	790316	646	17.2405	101.3088	4.60	3.59	0.48	3.1	2.7	11
364	790316	655	17.2797	101.2622	20.18	3.88	0.42	3.6	3.4	10
365	790316	724	17.5063	101.2327	10.58	3.30	0.17	4.0	0.6	6
366	790316	735	17.4110	101.6658	10.52	2.90	0.25	3.2	4.1	8
367	790316	737	17.4988	101.2457	8.80	3.56	0.48	2.9	3.1	10
368	790316	747	17.6475	101.5863	17.32	3.34	0.36	7.3	2.7	8
369	790316	803	17.2048	101.4208	4.76	3.47	0.35	4.9	7.5	6
370	790316	805	17.4802	101.2610	22.47	3.21	0.37	6.5	9.7	6
371	790316	833	17.6112	101.3963	17.68	2.86	0.36	3.3	5.1	6
372	790316	837	17.4707	101.4388	29.84	3.13	0.69	3.1	0.8	5
373	790316	907	17.4173	101.0283	20.87	3.11	0.29	3.0	3.9	8
374	790316	924	17.4175	101.4940	9.34	3.50	0.34	2.2	2.2	11
375	790316	1010	17.4183	101.3182	18.75	4.14	0.08	0.9	1.2	6
376	790316	1101	17.1963	100.8783	20.16	2.67	0.08	3.2	0.8	6
377	790316	1121	17.4128	101.2160	8.18	3.16	0.33	2.0	2.0	10
378	790316	1130	17.5712	101.2272	5.64	3.02	0.18	8.8	9.8	5
379	790316	1137	17.4333	101.5443	10.97	3.36	0.22	3.0	2.4	8
380	790316	1140	17.4183	101.5397	9.04	3.58	0.48	3.1	2.7	12
381	790316	1229	17.7998	101.2557	2.18	3.03	0.85	4.9	6.5	6
382	790316	1321	17.5013	101.4403	0.59	3.34	0.33	5.8	3.4	8
383	790316	1324	17.3722	101.3660	0.81	3.68	0.23	2.9	1.5	7
384	790316	1352	17.4618	101.1843	15.00	4.05	0.09	0.0	0.0	4
385	790316	1418	17.7722	101.4438	17.19	3.33	0.29	0.0	0.0	4
386	790316	1500	17.5223	101.4620	11.02	3.56	0.14	6.3	4.6	5
387	790316	1515	17.0870	101.1822	7.28	3.23	0.06	1.8	0.8	6
388	790316	1607	17.6287	101.2615	0.19	3.51	0.27	5.1	2.9	8
389	790316	1645	17.5628	101.1098	1.91	3.50	0.33	3.6	8.4	6

@MAG : Magnitude obtained using the formula MAG= - 0.87 + 2.0 LOG T + 0.0035D, where T is coda length in seconds, and D is epicentral distance in km (see text).

+RMS : Root mean square error of time residuals in seconds.

*ERROR: Standard error, ERH= epicenter location error in km, ERZ= focal depth error in km.

-N : Number of stations readings.

APPENDIX B

COMPUTER PROGRAMS

```
C  *****************************************************************  C
C                          ----------------                           C
C                           PROGRAM CEPES                             C
C                          ----------------                           C
C                                                                     C
C  THIS PROGRAM SORTS A LIST OF HYPO71 OUTPUTS INTO ANY SIZE          C
C  SQUARES BETWEEN ANY SPECIFIED GEOGRAPHICAL COORDINATES. THE        C
C  NUMBER OF EVENTS, THE ENERGY RELEASED BY EACH EVENT, AND THE       C
C  TOTAL ENERGY IN EACH SQUARE ARE COMPUTED. CONSIDERING AN AREA      C
C  OF ONE BY ONE DEGREE DIVIDED INTO SQUARES OF 0.1 DEGREE ON A SIDE C
C  THE FIRST ELEMENT IN THE ARRAY A(1,1)(A(COLUMN,ROW)), CONTAINS     C
C  THE PARAMETER FROM THE SOUTHEAST CORNER OF THE AREA. THE COLUMNS   C
C  OF THE ARRAY ARE FILLED FROM SOUTH TO NORTH, AND THE ROWS FROM     C
C  EAST TO WEST. THUS THE LAST ELEMENT IN THE ARRAY IS THE ONE        C
C  LOCATED AT THE NORTHWEST CORNER, A(10,10).                         C
C                                                                     C
C                         ------------------                          C
C                                                                     C
C         OUTPUT LFN ASSIGNMENTS:                                     C
C                                                                     C
C                   AS 13 = FILE WITH NUMBER OF EARTHQUAKES IN EACH   C
C                           SQUARE.                                   C
C                   AS 14 = FILE WITH ENERGY INSIDE EACH SQUARE.      C
C                   AS 16 = LIST THAT INCLUDES THE EVENTS AND THEIR   C
C                           ENERGY IN EACH SQUARE.                    C
C                                                                     C
C         INPUT LFN ASSIGNMENTS:                                      C
C                                                                     C
C                   AS 15 = FILE CONTAINING A LIST OF HYPO71 OUTPUTS  C
C                   AS 17 = DATSQC1 (SEE FILE AT THE END OF THIS      C
C                           PROGRAM)                                  C
C NOTES:                                                              C
C                                                                     C
C  1)  THERE IS THE OPTION TO GET A CONTOUR MAP AND/OR A FIGURE IN    C
C      THREE DIMENSIONS (FIGURES 4.10 AND 4.11 IN THIS THESIS).       C
C      FOR DETAILS SEE INPUT PARAMETERS IN LFN 17 AT THE END OF THE   C
C      PROGRAM.                                                       C
C  2)  THE OUTPUTS IN LFN 13 AND 14 CAN BE USED TO GET CONTOUR MAPS   C
C      AND 3-D PLOTS FOR NUMBER OF EVENTS AND ENERGY USING THE        C
C      PROGRAM PLOTEN .                                               C
C  3)  ENERGY RELEASE (E, in ergs) IS COMPUTED USING THE FORMULA      C
C      GIVEN BY BATH (1979): Log E=1.44M+12.25 WHERE M=MAGNITUDE.     C
C  4)  THE PLOTS ARE OBTAINED USING THE SIMPLE PLOT LIBRARY FROM THE C
C      HAWAII INSTITUTE OF GEOPHYSICS. THE LIBRARY SPECIFICATIONS     C
C      ARE:                                                           C
C    LIB 1512APX*SIMPLE 1512APX*VERLIB XPLT*SAUVPL *SAUL77 *LIBERY    C
C                                                                     C
C  *****************************************************************  C
```

```
      DIMENSION ET(10,10),NEPS(10,10),ETA(10,10)
      INTEGER DX,DY
      INTEGER AB(30)
      INTEGER UDATE,DATE,UN
      REAL ILAT,ILON,NEPS
      REAL LLAT,LAT,LLON,LDEP,LMAG,LGAP,LDMIN,LRMS,LERH,LERZ,LON,MAG
      READ(17,-)LDATE,UDATE,FPLOT
      READ(17,-)LLAT,ULAT,ILAT
      READ(17,-)LLON,ULON,ILON
      READ(17,-)LDEP,UDEP
      READ(17,-)LMAG,UMAG
      READ(17,-)LN,UN
      READ(17,-)LGAP,UGAP
      READ(17,-)LDMIN,UDMIN
      READ(17,-)LRMS,URMS
      READ(17,-)LERH,UERH
      READ(17,-)LERZ,UERZ
      DY=IFIX((ULAT-LLAT)/ILAT)
      DX=IFIX((ULON-LLON)/ILON)
      FLON=LLON
      FLAT=LLAT
      I=1
112   J=1
      LLAT=FLAT
      ULAT1=LLAT
      ULAT1=ULAT1+ILAT
      ULON1=LLON+ILON
      IF(ULON1.GT.ULON)GO TO 100
110   WRITE(16,22)LLAT,ULAT1,LLON,ULON1
22    FORMAT(//,3X,'LOW LAT :',F5.2,3X,'UP LAT :',F5.2,5X,'LOW LON :
     *',F6.2,3X,'UP LON :',F6.2,/)
      NEPS(I,J)=0.0
      ET(I,J)=0.0
      REWIND 15
111   READ(15,28,END=99)AB
28    FORMAT(30A3)
      IF(AB(1).EQ.' DA')GO TO 111
      DECODE(90,11,AB,ERR=111)DATE,A,B,C,D,DEP,MAG,N,GAP,DMIN,RMS,
     *ERH,ERZ
      LAT=A+(B/60.0)
      LON=C+(D/60.0)
11    FORMAT(2X,I4,12X,F2.0,1X,F5.2,1X,F3.0,1X,F5.2,1X,F6.2,3X,F4.2,
     *1X,I2,1X,F3.0,F5.1,1X,F4.2,F5.1,F5.1)
      IF(DATE .LE.  UDATE .AND.  DATE .GE.  LDATE)GO TO 12
      GO TO 111
12    IF( LAT .LE.  ULAT1 .AND.  LAT  .GE.  LLAT) GO TO 13
      GO TO 111
13    IF(LON  .LE. ULON1   .AND. LON   .GE. LLON) GO TO 14
      GO TO 111
```

```
14    IF(DEP .LE. UDEP   .AND.  DEP   .GE.  LDEP) GO TO 15
      GO TO 111
15    IF(MAG .LE. UMAG  .AND.  MAG   .GE.   LMAG) GO TO 16
      GO TO 111
16    IF(N    .LE. UN     .AND.  N     .GE. LN  ) GO TO 17
      GO TO 111
17    IF(GAP  .LE. UGAP   .AND.  GAP   .GE. LGAP) GO TO 18
      GO TO 111
18    IF(DMIN .LE. UDMIN  .AND. DMIN  .GE. LDMIN) GO TO 19
      GO TO 111
19    IF(RMS  .LE. URMS   .AND. RMS   .GE.  LRMS) GO TO 20
      GO TO 111
20    IF(ERH .LE. UERH .AND. ERH   .GE.   LERH) GO TO 1119
      GO TO 111
1119  IF( ERZ .LE. UERZ  .AND.  ERZ .GE.  LERZ) GO TO 1129
      GO TO 111
1129  CONTINUE
      WRITE(16,28)AB
      E=10.**(1.44*MAG+12.25)/10.**17.0
      WRITE(16,40)E
40    FORMAT(3X,'ENERGY=',F10.5)
      NEPS(I,J)=NEPS(I,J)+1.0
      ET(I,J)=ET(I,J)+E
32    GO TO 111
99    CONTINUE
      LLAT=ULAT1
      ULAT1=ULAT1+ILAT
      WRITE(16,41)I,J,ET(I,J),NEPS(I,J)
41    FORMAT(/,3X,'TOTAL ENERGY (',I2,',',I2,')=',F12.6,/,3X,
     *'# OF EVENTS=',F3.0)
      J=J+1
      NY=J-1
      IF(ULAT1.GT.ULAT)GO TO 21
      GO TO 110
21    LLON=ULON1
      I=I+1
      GO TO 112
100   CONTINUE
      NX=I-1
      Y1=FLAT+ILAT/2.0
      X1=-(FLON+ILON/2.0)
      WRITE(14, )NX,NY,DX,DY
      WRITE(14, )X1,Y1,ILON,ILAT
      WRITE(13, )NX,NY,DX,DY
      WRITE(13, )X1,Y1,ILON,ILAT
      DO 93 N=1,NX
      WRITE(13, )(NEPS(N,K),K=1,NY)
93    WRITE(14, )(ET(N,K),K=1,NY)
      IF(FPLOT.EQ.0.0)GO TO 95
```

```
      IF(FPLOT.EQ.1.0.OR.FPLOT.EQ. 3.0)GO TO 94
80    DO 60 I=1,NX
      DO 61 J=1,NY
61    ETA(I,J)=ET(I,J)
60    CONTINUE
      NP1=NY+1
      DO 65 K=1,NX
      DO 66 N=1,NY
66    ET(K,N)=ETA(K,NP1-N)
65    CONTINUE
      CALL SOLIDO(ET,NX,NY,DX,DY)
      IF(FPLOT.EQ.2.0.OR.FPLOT.EQ.3.0)GO TO 95
94    CALL CONTOR(ET,X1,ILON,NX,Y1,ILAT,NY,DX,DY,FPLOT)
      IF(FPLOT.EQ.3.0)GO TO 80
95    STOP
      END
C
C
      SUBROUTINE SOLIDO(ETS,NXS,NYS,IXS,IYS)
      DIMENSION ETS(IXS,IYS)
      CALL SOLID(ETS,-NXS,-NYS,20.0,25.0)
      CALL END PLT
      RETURN
      END
C
C
      SUBROUTINE CONTOR(ETP,X1P,ILONP,NXP,Y1P,ILATP,NYP,IX,IY,PLOT1)
      DIMENSION ETP(IX,IY)
      REAL ILATP,ILONP
      CALL CONTR(ETP,X1P,-ILONP,NXP,20.0,9HLONGITUDE,9,Y1P,ILATP,NYP,
     *20.0,8HLATITUDE,8)
      IF(PLOT1.NE.1.0)GO TO 10
      CALL END PLT
10    RETURN
      END
C
C
```

LFN 17 SORT CRITERIA INPUT TO PROGRAM CEPES

---

			*
0101	1231	2.0	DATE (ONLY WITHIN THE YEAR) AND FPLOT
17.	18.	.1	LOW & UPP LATITUDE AND INCREMENT OF LATITUDE
101.	102.	.1	LOW & UPP LONGITUDE & INCREMENT OF LONGITUDE
0.0		1000.0	DEPTH
0.0		10.0	MAGNITUDE
5		100	# OF ARRIVALS
0.0		1000.0	GAP (km)
0.0		1000.0	DMIN (DISTANCE TO CLOSEST STN.)
0.0		0.5	RMS
0.0		10.0	ERH (ERROR OF EPICENTER)
0.0		10.0	ERZ (ERROR OF DEPTH)

---

*FPLOT : THE FOLLOWING RESULTS CAN BE OBTAINED GIVEN DIFFERENTS VALUES TO FPLOT

FPLOT = 0.0 ONLY LIST OF EVENTS, TOTAL ENERGY, AND NUMBER OF EVENTS IN EACH SQUARE.

FPLOT = 1.0 LIST AND CONTOUR MAP FOR ENERGY.

FPLOT = 2.0 LIST AND 3-D PLOT FOR ENERGY.

FPLOT = 3.0 LIST ,CONTOUR MAP, AND 3-D PLOT.

Appendix B.2

```
C ****************************************************************** C
C                                                                    C
C                      ------------------                            C
C                       PROGRAM: PLOTEN                              C
C                      ------------------                            C
C                                                                    C
C THIS PROGRAM PLOTS THE RESULTS OBTAINED FROM CEPES PROGRAM WHICH   C
C COME FROM LFN 13 AND LFN 14. BEFORE RUNNING THIS PROGRAM THE       C
C INPUT FILE MUST BE EDITED GIVEN IN THE FIRST LINE ANY OF THE       C
C NUMBERS 1.0, 2.0, OR 3.0 TO OBTAIN  A CONTOUR MAP, A 3-D PLOT,OR   C
C BOTH RESPECTIVELY. IN THIS LINE MUST BE ALSO INCLUDED THE ANGLE    C
C OF VIEW OF THE 3-D PLOT AND THE SIZE OF THE FIGURE. FOR DETAILS    C
C ABOUT THE ANGLE OF VIEW, SEE THE SIMPLE PLOT MANUAL. ALL THESE     C
C PARAMETERS ARE REAL NUMBERS. THE LIBRARY SPECIFICATIONS ARE :      C
C                                                                    C
C LIB 1512APX*SIMPLE 1512APX*VERLIB XPLT*SAUVPL *SAUL77 *LIBERY      C
C                                                                    C
C                    -----------------------                         C
C                                                                    C
C LFN ASSIGNMENT 14 = INPUT DATA                                     C
C                                                                    C
C ****************************************************************** C
      DIMENSION ET(10,10),ETA(10,10)
      INTEGER DX,DY
      REAL ILAT,ILON
      READ(14,-)PLOT,AV,SP
      READ(14,-)NX,NY,DX,DY
      READ(14,-)X1,Y1,ILON,ILAT
      DO 93 N=1,NX
93    READ(14,-)(ET(N,K),K=1,NY)
      IF(PLOT.EQ.1.0.OR.PLOT.EQ. 3.0)GO TO 94
80    DO 60 I=1,NX
      DO 61 J=1,NY
61    ETA(I,J)=ET(I,J)
60    CONTINUE
      NP1=NY+1
      DO 65 K=1,NX
      DO 66 N=1,NY
66    ET(K,N)=ETA(K,NP1-N)
65    CONTINUE
      CALL SOLIDO(ET,NX,NY,DX,DY,AV,SP)
      IF(PLOT.EQ.2.0.OR.PLOT.EQ.3.0)GO TO 95
94    CALL CONTOR(ET,X1,ILON,NX,Y1,ILAT,NY,DX,DY,PLOT,SP)
      IF(PLOT.EQ.3.0)GO TO 80
95    STOP
      END
C
```

```
C
      SUBROUTINE SOLIDO(ETS,NXS,NYS,IXS,IYS,AV1,SP1)
      DIMENSION ETS(IXS,IYS)
      CALL SOLID(ETS,-NXS,-NYS,SP1,AV1)
      CALL END PLT
      RETURN
      END
C
C
      SUBROUTINE CONTOR(ETP,X1P,ILONP,NXP,Y1P,ILATP,NYP,IX,IY,PLOT1,
     *SP1)
      DIMENSION ETP(IX,IY)
      REAL ILATP,ILONP
      CALL CONTR(ETP,X1P,-ILONP,NXP,SP1,9HLONGITUDE,9,Y1P,ILATP,NYP,
     *SP1,8HLATITUDE,8)
      IF(PLOT1.NE.1.0)GO TO 10
      CALL END PLT
10    RETURN
      END
C
C
```

BIBLIOGRAPHY

Bath, M., Introduction to Seismology, Birkhauser Verlag, Boston, 428p., 1979.

Berg, E., Relation between earthquake foreshocks, stress and mainshocks, Nature, 219, 1141-1143, 1968.

Chael, E. P., and G. S. Stewart, Recent large earthquakes along the Middle American trench and their implications for the subduction process, J. Geophys. Res., 87, 329-338, 1982.

Couch, R., and S. Woodcock, Gravity and structure of the continental margins of southwestern Mexico and northwestern Guatemala, J. Geophys. Res., 86, 1829-1840, 1981.

Dean, B. W., and C. L. Drake, Focal mechanism solutions and tectonics of the Middle America arc, J. Geol., 86, 111-128, 1978.

Ewing, J. I., and R. P. Meyer, Rivera Ocean Seismic Experiment (ROSE) overview, J. Geophys. Res., 87, 8345-8357, 1982.

Gettrust, J. F., V. Hsu, C. E. Helsley, E. Herrero, and T. Jordan, Patterns of local seismicity preceding the Petatlan earthquake of 14 March 1979, Bull. Seismol. Soc. Am., 71, 761-769, 1981.

Havskov, J., S.K. Singh, E. Nava, T. Dominguez, and M. Rodriguez, Playa Azul, Michoacan, Mexico earthquake of 25 October 1981 (Ms=7.3), Bull. Seismol. Soc. Am., 73, 449-457, 1983.

Hsu, V., A breaking seismic gap: microearthquake seismicity of the Petatlan region, Mexico, preceding the March 14, 1979 earthquake (Ms=7.6), Ph.D. thesis, University of Hawaii, August,1981.

Hsu, V., J. F. Gettrust, C. E. Helsley, and E. Berg, Local seismicity preceding the March 14, 1979, Petatlan, Mexico earthquake, J. Geophys. Res., 88, 4247-4262, 1983.

Kanamori, H., The energy release in great earthquakes, J. Geophys. Res., 20, 2981-2987, 1977.

Kanamori, H., The nature of seismicity patterns before large earthquakes in D. W. Simpson and P. G. Richards (Eds.), Earthquake Prediction: An International Review, M. Ewing Series 4, American Geophysical Union, Washington, D. C., 1-19, 1981.

Kelleher, J., L. Sykes, and J. Oliver, Possible criteria for predicting earthquake locations and their application to major plate boundaries of the Pacific and the Caribbean, J. Geophys. Res., 78, 2547-2585, 1973.

Kennett, J. M., Marine Geology, Prentice-Hall Inc., Englewood Cliffs, N. J., 813 p., 1982.

Klitgord, K.D., and J. Mammerickx, Northern East Pacific Rise: Magnetic anomaly and bathymetric framework, J. Geophys. Res., 87, 6725-6759, 1982.

Lay, T., and H. Kanamori, An asperity model of large earthquake sequences, in D. W. Simpson and P. G. Richards (Eds.), Earthquake Prediction: An International Review, M. Ewing Series 4, American Geophysical Union, Washington D.C., 579-592, 1981.

Lee, W. H. K., R. E. Bennet, and K. L. Meaghar, A method of estimating magnitude of local earthquakes from signal duration, U. S. Geol. Surv., Open File Rep., 1972.

Lee, W. H. K., and J. C. Lahr, HYPO71 (revised): A computer program for determining hypocenter, magnitude and first motion pattern of local earthquakes, U. S. Geol. Surv. Open File Rep. 75-311, 113p., 1975.

Lienert, B. R., and L. N. Frazer, An improved earthquake location algorithm (abstract), EOS, Trans. Am. Geophys. Union, 64, 267, 1983.

Lienert, B. R., and L. N. Frazer, Evaluation of seismometer arrays for earthquake location (submitted for publication), 1983a.

McCann, W., S. Nishenko, L. Sykes and J. Krause, Seismic gaps and plate tectonics: seismic potential for major plate boundaries, U.S. Geol. Surv. Open File Rep., 78-943, 1978.

McNally, K. C., Plate subduction and prediction of earthquakes along the Middle America trench, in D. W. Simpson and P. G. Richards (Eds.), Earthquake Prediction : An International Review, M. Ewing Series 4, American Geophysical Union, Washington, D. C., 63-72, 1981.

McNutt, M., and R. Batiza, Paleomagnetism of northern Cocos seamounts: constraints on absolute plate motion, Geology, 9, 148-154, 1981.

Meyer, R. P., W. D. Pennington, L. A. Powell, W. L. Unger, M. Guzman, J. Havskov, S. K. Singh, C. Valdes, and J. Yamamoto, A first report on the Petatlan, Guerrero, Mexico earthquake of 14 March 1979, Geophys. Res. Lett., 7, 97-100, 1980.

Minster, J. B., and T. H. Jordan, Present-day plate motions, J. Geophys. Res., 83, 5331-5354, 1978.

Mogi, K., Study of elastic shocks caused by the facture of heterogeneous materials and its relations to earthquake phenomena, Bull. Earthquake Res. Inst., Tokio Univ., 40, 125-173, 1962.

Molnar, P., and L. Sykes, Tectonics of the Caribbean and Middle America regions from focal mechanisms and seismicity, Bull. Geol. Soc. Am., 80, 1639-1684, 1969.

Richter, C. F., Elementary Seismology, W. H. Freeman and Co., San Francisco, Calif., 768 pp. 1958.

Rudnicki, J. W., and H. Kanamori, Effects of fault interaction on moment, stress drop, and strain energy release, J. Geophys. Res., 86, 1785-1793, 1981.

Scholz, C. H., The frecuency-magnitud relation of microfracturing in rock and its relation to earthquakes, Bull. Seism. Soc. Am., 58, 399-415, 1968.

Singh, S. K., L. Astiz, and J. Havskov, Seismic gaps, and recurrence periods of large earthquakes along the Mexican subduction zone : a reexamination, Bull. Seism. Soc. Am., 71, 827-843, 1981.

Suyehiro, S., T. Asada, and M. Otake, Foreshock and aftershock accompanying a perceptible earthquake in Central Japan, Papers Meteorol., Geophysics, 15, 71-88, 1964.

Valdes, C., R. Meyer, R. Zuniga, J. Havskov, and S. K. Singh, Analysis of Petatlan aftershocks: numbers, energy release, and asperities, J. Geophys. Res., 87, 8519-8527, 1982.

Vogt, P. R., A. Lowrie, D. Bracey, and R. Hey, Subduction of aseismic oceanic ridges: effects on shape, seismicity and other characteristics of consuming plates boundaries, Spec. Pap. Geol. Soc. Am., 172, 59pp., 1976.

Zuniga, F. R., C. M. Valdes, R. P. Meyer, J. Havskov, and S. K. Singh, Aftershocks of the Petatlan, Mexico, earthquake of 14 March 1979 (Ms=7.6)(abstract), EOS, Trans. Am. Geophys. Union 61, 289, 1980.